

**Application of Viability Real-time PCR in Detecting Shiga Toxin-producing *Escherichia coli* From Clinical Stool Samples**

by

Taryn Erika Stokowski

A thesis submitted in partial fulfillment of the requirements for the degree of  
Master of Science

Department of Laboratory Medicine and Pathology  
University of Alberta

© Taryn Erika Stokowski, 2023

## Abstract

Shiga toxin-producing *Escherichia coli* (STEC) is a food-borne pathogen that causes acute gastroenteritis. It has a low infectious dose and children have an elevated risk of developing severe complications (e.g., hemolytic uremic syndrome). To prevent secondary spread, Alberta's microbiological clearance exclusion protocols prohibit patients with active STEC infections from working in healthcare, handling food, or attending daycare. Such patients submit specimens until they produce two consecutively culture negative stools at least 24 hours apart. This testing is typically conducted using CHROMagar™ STEC. However, some non-O157 STEC strains are unable to grow on the media so samples are instead enriched in tryptic soy broth before being tested by real-time PCR (RT-PCR) for the *stx* genes. This thesis investigates whether a novel direct-from-stool viability RT-PCR assay can serve as an alternative testing method. This involves applying a membrane-impermeable dye which, when photoactivated, irreversibly binds DNA and prevents amplification. If successful, this assay will determine with high sensitivity if a sample contains live STEC without an overnight growth period. Currently, few studies have attempted viability RT-PCR in stool, none of which have used STEC as the target organism.

Viability RT-PCR conditions were first optimized using cell suspensions in phosphate buffered saline (PBS). The multiplexed *stx*<sub>1</sub> and *stx*<sub>2</sub> primer-probe sets had a limit of detection of 10<sup>3</sup> CFU/mL, did not cross-react with DNA from other organisms (including four *Shigella* strains), and detected all of the *stx* subtypes tested except for *stx*<sub>2f</sub>. The final viability RT-PCR protocol involved treating samples with 100 μM PMAxx™ and 1% dimethyl sulfoxide (DMSO), a 15 min photoactivation, and transferring the suspension to a new tube prior to DNA extraction. While this protocol successfully eliminated the detection of a high concentration of heat-killed cells (10<sup>9</sup> CFU/mL), its performance was inconsistent and produced some false negative results at a low concentration (10<sup>4</sup> CFU/mL) of live cells.

The conditions above were used to develop viability RT-PCR assays for direct-from-stool (DFS) and rectal swab (RS) applications. The major modification made when applied to stool was the elimination of the tube transfer step because it did not improve the detection of live cells. Both the DFS and RS viability RT-PCR protocols successfully eliminated the detection of heat-killed cells spiked into stool at a high concentration, but consistently produced false negative results when live STEC cells were spiked at a low concentration ( $10^5$  CFU/mL stool). The DFS protocol was tested using clinical microbiological clearance specimens from four patients, and was found to perform inconsistently and to produce false negative results. That is, despite being positive by post-enrichment RT-PCR, several stool samples were negative by DFS viability RT-PCR.

In conclusion, all of the viability RT-PCR protocols developed in this thesis were successful at selectively detecting live cells at high bacterial loads when found alongside a high concentration of heat-killed STEC. This suggests that PMAxx™ was successfully activated in stool and bound DNA from heat-killed STEC. However the protocols were not consistently successful at detecting live cells at low bacterial loads. Thus, the hypothesis that viability RT-PCR would be as sensitive as conventional RT-PCR was not supported. This means that the DFS viability RT-PCR assay is unsuitable for microbiological clearance testing because such specimens often have a low load of live bacteria. Instead, the results of this study endorse the use of post-enrichment RT-PCR because it was the most sensitive assay tested and was suitable for strains which did not grow on CHROMagar™ STEC.

## **Preface**

This thesis is an original work of Taryn Erika Stokowski. No part of this thesis has been previously published.

## **Acknowledgments**

Firstly, I would like to extend my sincerest gratitude to my supervisor Dr. Linda Chui for her mentorship and friendship. You have helped me grow as a researcher and as a person, and I feel very fortunate to have had this experience with you.

To my lab mates Dr. Surangi Thilakarathna, Colin Lloyd, Dr. Michael Bording-Jorgensen, Dr. Angela Ma, and Hannah Tyrrell, thank you for your insight, patience, and encouragement. Thank you also to my other colleagues Alexa Thompson, Dr. Ashley Williams, Dr. Ran Zhuo, and Thomas Corsiatto for your positivity and wisdom.

Thank you to the staff from ProvLab for their support and willingness to share their technical expertise. A special thanks is owed to Christina Ferrato who sent all of the clinical samples. Thank you also to the staff at the National Microbiology Laboratory who completed the serotyping on the clinical isolates, and to Dr. Alexander Gill from Health Canada for supplying DNA extracts for the subtype coverage experiments.

To Dr. Monika Keelan and Dr. Gregory Tyrrell, thank you for serving as supervisory committee members and thesis examiners. It has been a pleasure working with both of you. I would also like to thank Dr. Stephanie Yanow for serving as a thesis examiner and Dr. Jelena Holovati for serving as chair for the thesis examination.

I am grateful to have received funding from the Canadian Institute of Health Research through the Fredrick Banting and Charles Best Canada Graduate Scholarship, the Province of Alberta through the Alberta Graduate Excellence Scholarship, and the department of Laboratory Medicine and Pathology through the Bell McLeod Educational Fund Graduate Entrance Scholarship.

Finally, thank you to my friends and family for supporting me throughout this journey. I could not have done it without you.

# Table of contents

## Chapter 1: Introduction

<b>1.1 Shiga toxin-producing Escherichia coli (STEC) infection</b>	<b>1</b>
1.1.1 STEC characteristics	1
1.1.2 Consequences of STEC infection	2
1.1.3 Public health concerns	3
<b>1.2 STEC diagnostics</b>	<b>5</b>
1.2.1 Overview of the Canadian diagnostic guidelines for STEC	5
1.2.2 Specimen types	6
1.2.3 Culture	7
1.2.4 Enzyme immunoassays (EIA)	9
1.2.5 Nucleic Acid [Amplification] Tests (NAT / NAATs)	11
1.2.6 The “culture-independent” era	14
1.2.7 Microbiological clearance testing	15
<b>1.3 Viability PCR</b>	<b>15</b>
1.3.1 Defining viability	15
1.3.2 Premise of viability RT-PCR	17
1.3.3 Interpreting viability RT-PCR results	19
1.3.4 Viability RT-PCR with complex sample types	21
<b>1.4 Research rationale</b>	<b>23</b>
1.4.1 Background	23
1.4.2 Hypothesis	24
1.4.3 Objectives	24
<b>1.5 References</b>	<b>25</b>
<b>Chapter 2: Optimizing viability real-time PCR for STEC cell suspensions</b>	<b>37</b>
<b>2.1 Introduction</b>	<b>37</b>
<b>2.2 Methods and Materials</b>	<b>39</b>
2.2.1 Cell suspensions	39
2.2.1.1 Reference strain	39
2.2.1.2 Dilution series and preparation of heat-killed cells	39
2.2.2 DNA extraction	40
2.2.3 Real-time PCR	41
2.2.3.1 Primers-probe sets and reaction conditions	41
2.2.3.2 Primer-probe sensitivity	43
2.2.3.3 Primer-probe subtype coverage	43

2.2.3.4	Primer-probe specificity	43
2.2.4	PMAxx™ Optimization	44
2.2.4.1	PMAxx™ stock solution and photolysis device	44
2.2.4.2	Assessment of PMAxx™ binding irreversibility	45
2.2.4.3	Buffer suitability for PMAxx™ treatment	46
2.2.4.4	Photoactivation time and PMAxx™ Concentration	47
2.2.4.5	Effect of DMSO on viability RT-PCR and cell viability	48
2.2.4.6	PMAxx™ residual activity and resuspension of live cells	49
2.2.4.7	PMAxx™ interactions with microcentrifuge tubes	50
2.2.4.8	PMAxx™ pre-photoactivation	52
2.2.5	Final viability RT-PCR protocol for pure culture	52
2.2.6	Statistical analyses	54
<b>2.3</b>	<b>Results</b>	<b>55</b>
2.3.1	Primer performance	55
2.3.1.1	Sensitivity	55
2.3.1.2	Subtype coverage	57
2.3.1.3	Specificity	58
2.3.2	PMAxx™ irreversibility	58
2.3.3	Buffer suitability for PMAxx™ treatment	58
2.3.4	Photoactivation time and PMAxx™ Concentration	59
2.3.5	PMAxx™ and 1% DMSO	61
2.3.6	Effects of resuspension on live cells	62
2.3.7	PMAxx™ interactions with microcentrifuge tubes	63
2.3.8	PMAxx™ Pre-photoactivation	64
2.3.9	Final viability RT-PCR protocol performance	65
<b>2.4</b>	<b>Discussion</b>	<b>68</b>
2.4.1	Primer set performance	68
2.4.2	PMAxx™ performance and treatment conditions	69
2.4.3	Viability RT-PCR protocol performance with mixes of live and heat-killed culture	72
<b>2.5</b>	<b>Conclusion</b>	<b>72</b>
<b>2.6</b>	<b>References</b>	<b>74</b>
<b>Chapter 3: Development and application of a direct-from-stool viability real-time PCR assay for STEC detection</b>		<b>78</b>
<b>3.1</b>	<b>Introduction</b>	<b>78</b>
<b>3.2</b>	<b>Methods and Materials</b>	<b>80</b>
3.2.1	Artificially spiked stool	80



3.2.1.1 Reference strain	80
3.2.1.2 STEC-free stool used for spiking experiments	80
3.2.1.3 Stool spiking	81
3.2.1.4 Growth on CHROMagar™ STEC	82
3.2.2 Real-time PCR analysis of stool and rectal swabs	83
3.2.2.1 Sample preparation for direct-from-stool (DFS) detection	83
3.2.2.2 Sample preparation for rectal swab (RS) detection	84
3.2.2.3 Comparison of rapid lysis buffer and MagaZorb® DNA Mini-Prep Kit	84
3.2.2.4 RT-PCR Reaction conditions	87
3.2.2.5 Comparison of DNA extracted from the liquid phase of a settled 10% stool suspension versus that of the total sample	87
3.2.2.6 Baseline performance of DFS and RS RT-PCR protocol using live and HK cells	90
3.2.3 Spiked stool and rectal swab viability RT-PCR	90
3.2.3.1 Effect of tube transfer on cells treated with PMAxx™	90
3.2.3.2 PMAxx™ interactions with substances in the liquid phase	91
3.2.3.3 Final viability RT-PCR protocol for spiked stool and rectal swab specimens	93
3.2.4 Microbiological clearance samples	95
3.2.4.1 Specimens and inclusion criteria	95
3.2.4.2 Microbiological clearance specimen testing	96
3.2.5 Statistical analyses	99
<b>3.3 Results</b>	<b>99</b>
3.3.1 DNA extraction optimization for DFS and RS specimens	99
3.3.1.1 Rapid lysis buffer versus MagaZorb® DNA Mini-Prep Kit	99
3.3.1.2 Liquid phase versus total stool sample DNA extraction	101
3.3.2 DFS and RS RT-PCR sensitivity for live cells	101
3.3.3 DFS and RS PMAxx™ treatment optimization using spiked samples	102
3.3.3.1 Tube transfer to improve live cell detection	102
3.3.3.2 PMAxx™ interactions with substances found in the liquid phase	103
3.3.4 DFS and RS viability RT-PCR performance for stools spiked with mixes of live and HK cells	104
3.3.5 Analysis of microbiological clearance samples	106
3.3.5.1 Patient A (O121:H19)	106
3.3.5.2 Patient B (Mixed infection)	110
3.3.5.3 Patient C (O157:H7)	114
3.3.5.4 Patient D (O117:H7)	118
3.3.5.5 Summary of positive stool samples by microbiological clearance detection method.	122

<b>3.4 Discussion</b>	<b>123</b>
3.4.1 Direct-from-stool and Rectal Swab sample preparation	123
3.4.2 DNA Extraction	124
3.4.3 PMAxx™ and spiked stool	125
3.4.4 Microbiological clearance testing methods: detection rate, sensitivity, and limitations	126
3.4.4.1 Post-enrichment (PE) RT-PCR	126
3.4.4.2 Direct-from-stool viability RT-PCR	127
3.4.4.3 CHROMagar™ STEC	128
3.4.4.4 SHIGA TOXIN QUIK CHEK™ (STQC)	129
3.4.4.5 Duration of microbiological clearance	130
<b>3.5 Conclusion</b>	<b>131</b>
<b>3.6 References</b>	<b>132</b>
<b>Chapter 4: General Discussion</b>	<b>137</b>
<b>4.1 Significance</b>	<b>137</b>
<b>4.2 Limitations</b>	<b>140</b>
<b>4.3 Future directions</b>	<b>142</b>
<b>4.4 Final conclusions</b>	<b>143</b>
<b>4.5 References</b>	<b>144</b>
<b>Bibliography</b>	<b>148</b>
<b>Appendix</b>	<b>168</b>

## List of Tables

<b>Table 1.1.</b> Summary of viability PCR results anticipated for STEC cells across the viability spectrum.	<b>20</b>
<b>Table 1.2.</b> Studies which have conducted viability PCR for STEC in complex samples.	<b>22</b>
<b>Table 2.1.</b> Primers and probes used for the multiplexed detection of <i>stx</i> <sub>1</sub> and <i>stx</i> <sub>2</sub> by real-time PCR.	<b>42</b>
<b>Table 2.2.</b> Performance of the multiplexed RT-PCR <i>stx</i> <sub>1</sub> and <i>stx</i> <sub>2</sub> primer sets.	<b>55</b>
<b>Table 2.3A.</b> Subtypes amplified by the <i>stx</i> <sub>1</sub> primer set.	<b>57</b>
<b>Table 2.3B.</b> Subtypes amplified by the <i>stx</i> <sub>2</sub> primer set.	<b>57</b>
<b>Table 2.4.</b> Colony forming units counted after PMAxx™ treatment in different buffers.	<b>59</b>
<b>Table 2.5.</b> Effect of PMAxx™ concentration and photoactivation time on the mean <i>stx</i> <sub>1</sub> cycle threshold values associated with an extract of 1 ng/μL STEC DNA.	<b>59</b>
<b>Table 2.6.</b> The effect of increasing PMAxx™ concentrations on the cycle threshold values of heat-killed cells.	<b>60</b>
<b>Table 2.7.</b> Cycle threshold values of heat-killed cells treated with 1% DMSO, 100 μM PMAxx™, or 100 μM PMAxx™ + 1% DMSO.	<b>61</b>
<b>Table 2.8.</b> Effect of treatment with 100 μM PMAxx™, 100 μM PMAxx™ + 1% DMSO, or 1% DMSO on live cell survival.	<b>62</b>
<b>Table 2.9.</b> Effect of resuspending live cells versus remaining in the original supernatant (with or without PMAxx™) during boiling.	<b>63</b>
<b>Table 2.10.</b> Effect of 100 μM PMAxx™ + 1% DMSO residue in microcentrifuge tubes on the cycle threshold value of heat-killed cells.	<b>64</b>
<b>Table 2.11.</b> Effect of “pre-photoactivation” compared to standard photoactivation on the cycle threshold value of heat-killed cells treated with 100 μM PMAxx™ + 1% DMSO.	<b>65</b>
<b>Table 2.12A.</b> Impact of 100 μM PMAxx™ + 1% DMSO treatment on the <i>stx</i> <sub>1</sub> cycle threshold values of live and mixed cell suspensions.	<b>66</b>
<b>Table 2.12B.</b> Impact of 100 μM PMAxx™ + 1% DMSO treatment on the <i>stx</i> <sub>2</sub> cycle threshold values of live and mixed cell suspensions.	<b>66</b>
<b>Table 2.13A.</b> Estimated CFU/mL by plate count and by <i>stx</i> <sub>1</sub> cycle threshold value for live and mixed cell suspensions treated with 100 μM PMAxx™ + 1% DMSO.	<b>67</b>

<b>Table 2.13B.</b> Estimated CFU/mL by plate count and by <i>stx</i> <sub>2</sub> cycle threshold value for live and mixed cell suspensions treated with 100 µM PMAxx™ + 1% DMSO.	<b>68</b>
<b>Table 3.1.</b> Characteristics of the STEC microbiological clearance specimens used in this study.	<b>95</b>
<b>Table 3.2.</b> Rapid lysis buffer (RLB) compared to MagaZorb® DNA Mini-Prep Kit and KingFisher™ mL Purification System (MZ-KF) for DNA extraction.	<b>100</b>
<b>Table 3.3.</b> Sensitivity of the direct-from-stool (DFS) and rectal swab (RS) protocols in detecting live cells spiked into liquid stool.	<b>102</b>
<b>Table 3.4.</b> Effect of exposing direct-from-stool liquid phase to PMAxx™ prior to adding live and HK cells.	<b>104</b>
<b>Table 3.5.</b> Mean <i>stx</i> <sub>1</sub> Ct value for live and mixed cell suspensions spiked into stool and analyzed using the direct-from-stool and rectal swab RT-PCR and viability RT-PCR protocols.	<b>105</b>
<b>Table 3.6.</b> Shiga toxin assay results for Patient A stool submissions.	<b>107</b>
<b>Table 3.7.</b> Growth on CHROMagar™ STEC compared to RT-PCR Ct for Patient A 10% and TSB-enriched stool specimens.	<b>109</b>
<b>Table 3.8.</b> Shiga toxin assay results for Patient B stool submissions.	<b>111</b>
<b>Table 3.9.</b> Growth on CHROMagar™ STEC compared to RT-PCR Ct for Patient B 10% and TSB-enriched stool specimens.	<b>113</b>
<b>Table 3.10.</b> Shiga toxin assay results for Patient C stool submissions.	<b>115</b>
<b>Table 3.11.</b> Growth on CHROMagar™ STEC compared to RT-PCR Ct for Patient C 10% and TSB-enriched stool specimens.	<b>117</b>
<b>Table 3.12.</b> Shiga toxin assay results for Patient D stool submissions.	<b>119</b>
<b>Table 3.13.</b> Growth on CHROMagar™ STEC compared to RT-PCR Ct for Patient D 10% and TSB-enriched stool specimens.	<b>121</b>
<b>Table 3.14.</b> Summary of STEC positive microbiological clearance stool samples by testing method.	<b>122</b>

## List of Figures

<b>Figure 1.1.</b> Canadian Public Health Laboratory Network recommendations for the detection of Shiga toxin-producing <i>Escherichia coli</i> in stool specimens.	<b>6</b>
<b>Figure 1.2.</b> Mechanism of TaqMan probe-based real-time PCR.	<b>12</b>
<b>Figure 1.3.</b> Molecular structure of propidium monoazide compared to ethidium monoazide bromide.	<b>19</b>
<b>Figure 2.1.</b> Procedure used to prepare dilution series of live and heat-killed cells.	<b>40</b>
<b>Figure 2.2.</b> Procedure used to determine whether PMAxx™ binds DNA irreversibly.	<b>46</b>
<b>Figure 2.3.</b> Procedure used to determine whether PMAxx™ remains active following photoactivation.	<b>50</b>
<b>Figure 2.4.</b> Procedure used to determine whether PMAxx™ interacts with microcentrifuge tubes.	<b>51</b>
<b>Figure 2.5.</b> Procedure used to test the final viability RT-PCR protocol for STEC cell suspensions.	<b>53</b>
<b>Figure 2.6A.</b> Standard curve relating Log CFU/mL to <i>stx</i> <sub>1</sub> cycle threshold value.	<b>56</b>
<b>Figure 2.6B.</b> Standard curve relating Log CFU/mL to <i>stx</i> <sub>2</sub> cycle threshold value.	<b>56</b>
<b>Figure 3.1.</b> Workflow used to prepare dilution series of live and heat-killed STEC and spike STEC-negative liquid stool.	<b>82</b>
<b>Figure 3.2.</b> Illustration of the quadrant streaking method used for CHROMagar™ STEC.	<b>83</b>
<b>Figure 3.3</b> Flow chart describing the MagaZorb® DNA Mini-Prep Kit and KingFisher™ mL Purification System DNA extraction protocol.	<b>86</b>
<b>Figure 3.4.</b> Flow chart describing the experiment used to determine whether the liquid phase DNA extract of a 10% stool suspension approximates the DNA found in the undiluted sample.	<b>89</b>
<b>Figure 3.5.</b> Workflow used to determine whether PMAxx™ adheres to substances found in the liquid phase of a settled 10% stool suspension.	<b>92</b>
<b>Figure 3.6.</b> Flow chart describing how the final direct-from-stool and rectal swab real-time viability PCR protocols were tested using spiked stool.	<b>94</b>
<b>Figure 3.7.</b> Workflow used to analyze clinical microbiological clearance stool specimens in this study.	<b>97</b>

<b>Figure 3.8.</b> Diagram of a SHIGA TOXIN QUIK CHEK™ membrane device.	<b>99</b>
<b>Figure 3.9.</b> Supernatant color of original liquid phase compared to liquid phase exposed to PMAxx™ after tube transfer and the addition of cells in PBS.	<b>103</b>
<b>Figure 3.10.</b> RT-PCR <i>stx</i> <sub>2</sub> Ct values of Patient A 10% and enriched specimens.	<b>108</b>
<b>Figure 3.11.</b> RT-PCR <i>stx</i> <sub>2</sub> Ct values of Patient B 10% and enriched specimens.	<b>112</b>
<b>Figure 3.12.</b> RT-PCR <i>stx</i> <sub>2</sub> Ct values of Patient C 10% and enriched specimens.	<b>116</b>
<b>Figure 3.13.</b> RT-PCR <i>stx</i> <sub>1</sub> Ct values of Patient D 10% and enriched specimens.	<b>120</b>

## List of abbreviations

<b>°C</b>	Degree Celsius
<b>AGE</b>	Acute gastroenteritis
<b>BAP</b>	Blood agar plate
<b>BD-EBP</b>	BD MAX™ Enteric Bacterial Panel
<b>CFU</b>	Colony forming units
<b>CIDT</b>	Culture independent diagnostic test
<b>CPHLN</b>	Canadian Public Health Laboratory Network
<b>Ct</b>	Cycle threshold
<b>DFS</b>	Direct from stool
<b>DMSO</b>	Dimethyl sulfoxide
<b>DNA</b>	Deoxyribonucleic acid
<b>EHEC</b>	Enterohemorrhagic <i>E. coli</i>
<b>EIA</b>	Enzyme Immunoassay
<b>EIEC</b>	Enteroinvasive <i>E. coli</i>
<b>EPEC</b>	Enteropathogenic <i>E. coli</i>
<b>GI</b>	Gastrointestinal
<b>HUS</b>	Hemolytic uremic syndrome
<b>LoD</b>	Limit of detection
<b>LP</b>	Liquid phase
<b>MAC</b>	MacConkey agar
<b>PBS</b>	Phosphate-buffered saline
<b>PE RT-PCR</b>	Post-enrichment real-time polymerase chain reaction
<b>PMA</b>	Propidium monoazide
<b>PMAxx™</b>	A proprietary form of PMA
<b>ProvLab</b>	Alberta's Provincial Laboratory for Public Health
<b>RS</b>	Rectal swab

<b>RT-PCR</b>	Real-time polymerase chain reaction (also known as quantitative PCR)
<b>stx</b>	Shiga toxin (gene)
<b>Stx</b>	Shiga toxin (protein)
<b>Stx phage</b>	Shiga toxin-converting bacteriophage
<b>STEC</b>	Shiga toxin-producing <i>Escherichia Coli</i>
<b>STQC</b>	SHIGA TOXIN QUIK CHEK™
<b>TSB</b>	Tryptic soy broth
<b>VBNC</b>	Viable but non-culturable



# Chapter 1: Introduction

## 1.1 Shiga toxin-producing *Escherichia coli* (STEC) infection

### 1.1.1 STEC characteristics

*Escherichia coli* are diverse organisms in the Enterobacteriaceae family. These Gram-negative facultative anaerobes can naturally be found in the environment and commensally in the gastrointestinal tract of warm-blooded animals, but some strains have acquired genes which allow them to cause disease (1). Of the pathogenic strains that cause diarrhea, Shiga toxin-producing *E. coli* (STEC) are considered the most virulent because of the potency of their phage-encoded toxin (2). Shiga toxin is also referred to as “verotoxin” because of the cytotoxic effect it was found to have on Vero cells, a monkey kidney epithelial cell line (2). The toxin is encoded by the *stx* genes located in the late-phase region of the phage (3,4). Although STEC may carry virulence factors that overlap with other diarrheagenic *E. coli* such as the *eae* gene, which encodes a protein used to adhere to the interior of the intestine, and is also found in enteropathogenic *E. coli* (EPEC), they are defined by the carriage of at least one Shiga toxin-converting phage (Stx Phage). STEC that cause hemorrhagic colitis are additionally referred to as enterohemorrhagic *E. coli* (EHEC).

All *E. coli* are categorized into serotypes according to the characteristics of two cell surface components: the somatic (O) and flagellar (H) antigens. The O-antigen refers to a lipopolysaccharide embedded in the outer cell membrane, whereas the H-antigen refers to the protein that constitutes the organism's flagella. There are reported to be 186 different O-antigens and 56 unique H-antigens (5). STEC of the O157:H7 serotype are considered prototypical; historically such bacteria have been associated with severe disease and large-scale outbreaks. However, so-called “non-O157” serotypes have garnered increasing attention as testing methods have improved and more is understood about STEC diversity.

Recent estimates now suggest that non-O157 infections account for about half of all STEC cases (6). Further, the world's second-largest documented STEC outbreak (3,000 cases, 53 deaths) occurred in Germany in 2011 and was caused by an O104:H4 strain, highlighting the clinical significance of non-O157 bacteria (7). In North America the most commonly detected non-O157 serotypes are referred to as the "top-6" and include O26, O45, O103, O111, O121, and O145 (8).

### **1.1.2 Consequences of STEC infection**

STEC is a major cause of bacterial acute gastroenteritis (AGE). Patients typically experience loose stools and abdominal cramping for 5 - 7 days (9,10). Bloody diarrhea is considered a hallmark of STEC infection as it is present in approximately 70 - 80% of cases (10,11).

During infection, STEC adhere to the colon epithelium and secrete Shiga toxin, which interferes with epithelial cells' ability to produce proteins and causes apoptosis as well as inflammation (12). Shiga toxin is also able to cross the intestinal epithelium and enter systemic circulation (13). When this occurs, it can affect cells in the kidneys and central nervous system which express the Stx receptor, globotriaosylceramide (Gb3) (14). Between 5 - 10% of STEC patients develop hemolytic uremic syndrome (HUS), a condition characterized by renal microvascular damage which can lead to fatal kidney failure (10,15). Neurological involvement is a less common feature of STEC infection, but is suspected to contribute to HUS fatalities (16).

There are two types of Shiga toxin (Stx-1 and Stx-2) found in STEC, and a bacterium can carry both toxin types, or may have either alone. Over time, the sequences of both types have diverged to produce several subtypes (1a, 1c, 1d, and 2a - 2j, 2o) which can be distinguished by using specifically designed RT-PCR primer sets (14). Studies have reported that Stx-2 is up to

1,000 times more toxic (i.e., has a lower lethal dose) than Stx-1 (17), so it follows that Stx-2 (especially subtypes 2a and 2c) is often associated with more severe disease (i.e., bloody diarrhea and HUS) (1,11,18). Compared to O157 isolates, non-O157 STEC are more likely to only produce Stx-1 and cause watery diarrhea (12). However, there continue to be HUS cases associated with such strains (19,20).

In addition to toxin type, patient age is considered a major factor that contributes to disease severity. Children below the age of 10 and adults above the age of 60 are considered to be at an increased risk of STEC complications because of their immune deficiencies (13). In Alberta, children (<10) are consistently reported as having the highest proportion of STEC cases and incidence of HUS (8,21).

Current Canadian guidelines recommend against treating STEC infections with antibiotics (22). Instead, clinicians are advised to utilize intravenous therapy to manage symptoms and prevent sequelae (23). Such recommendations are based on the potential for antibiotics to induce the lytic phase of the Shiga toxin-converting bacteriophage, which could result in an increase in Shiga toxin production (12,24). This conclusion has been supported by some studies which have documented a positive relationship between antibiotic treatment and the development of HUS (25). Since antibiotic use is indicated for other enteric pathogens, it is important that STEC infections be diagnosed quickly and accurately so that antibiotics are not wrongfully prescribed and that intravenous fluids can be started early if necessary.

### **1.1.3 Public health concerns**

According to the National Enteric Surveillance Program, the average rate of STEC illness in Canada ranges between 1 - 2 cases per 100,000 (26). As a zoonotic pathogen, STEC can be

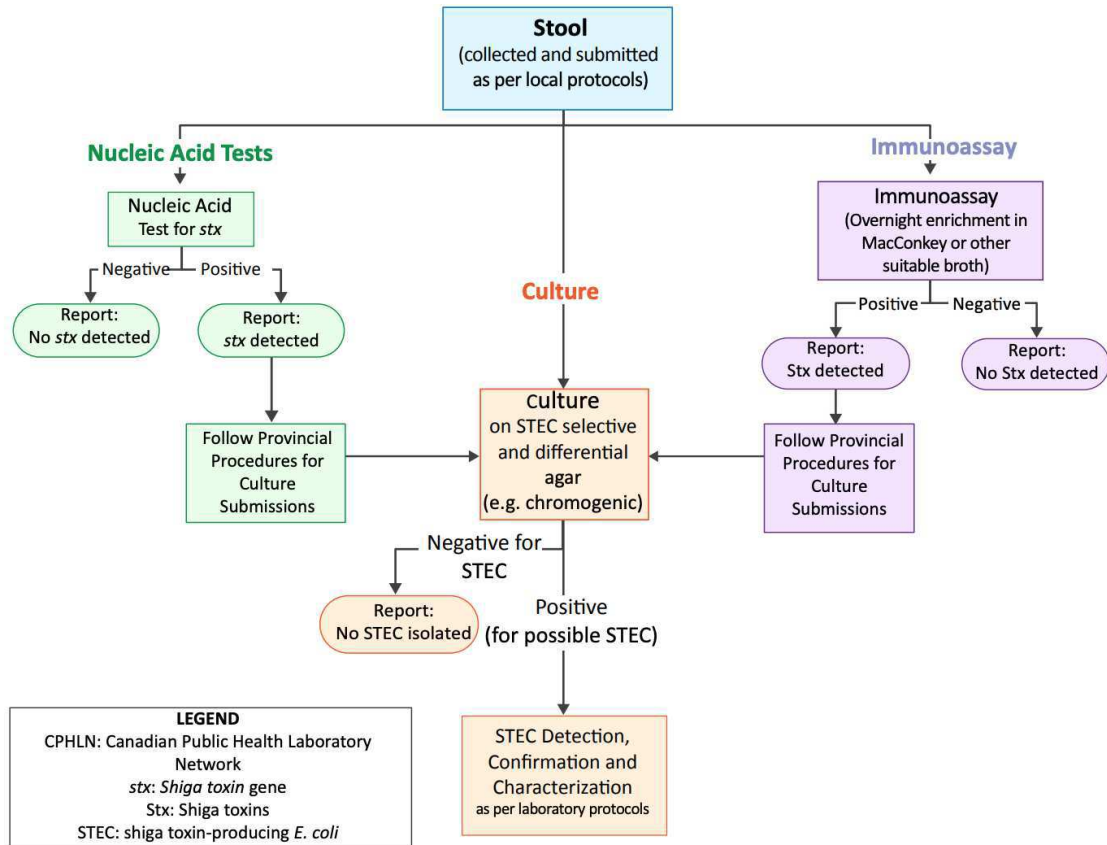
naturally found in ruminants (i.e., cattle and sheep) and water (27). Contaminated food products—especially meat, dairy, and leafy vegetables grown with manure-based fertilizers—are considered the primary mode of transmission for STEC infection (27). Troublingly, STEC are highly acid-resistant which allows them to more easily survive in certain foods and pass through the stomach to establish infection (28,29). This feature means that the infectious dose for STEC is low, with some estimates suggesting that less than one hundred live bacteria are needed for infection (13). It follows that STEC has caused many large-scale foodborne outbreaks. The largest documented outbreaks in Canada have all been attributed to O157, with the top 3 occurring in Ontario (2008, 235 cases associated with onions), Nova Scotia (1998, 182 cases associated with salad) and Quebec (2000, 176 cases associated with ground beef) (30). Product recalls are initiated once the source of an outbreak is identified; these waste considerable amounts of product, are costly, laborious, and generate distrust amongst consumers (27). Canada's largest beef recall (2012), which was linked to an O157 STEC strain, led to the recall of 4,000 tons of beef products (31). In many countries, STEC is a closely monitored notifiable disease because of its infectivity and potential to cause outbreaks.

Secondary transmission via the fecal-oral route has also been cited as a significant source of STEC spread in the community (32). Person-to-person transmission is of greatest concern within families, as well as in childcare and food-handling industries (27). For this reason, public health authorities establish “microbiological clearance” guidelines that require infected individuals to exclude themselves from these work settings until they are confirmed to have fully cleared their infection (See **1.3.7**).

## 1.2 STEC diagnostics

### 1.2.1 Overview of the Canadian diagnostic guidelines for STEC

Since 2001, the Canadian Public Health Laboratory Network (CPHLN) has served as a forum for provincial and federal experts to develop and implement systems for pathogen detection and surveillance (33). In 2018, the CPHLN outlined updated guidelines for STEC detection from stool specimens, which are summarized in **Figure 1.1** (34). Briefly, they endorse screening for STEC via any one of the following three methods: chromogenic agar, nucleic acid test (NAT), or enzyme immunoassay (EIA). The latter two methods test for STEC indirectly by, respectively, determining whether *stx* DNA or expressed Shiga toxin are present in the specimen. However, the CPHLN states that all NAT and EIA positive results should be followed-up with culture, which remains the gold standard. Growth on media confirms the presence of live STEC and allows for the strain(s) to be isolated and characterized for surveillance and cluster analysis.



**Figure 1.1. Canadian Public Health Laboratory Network recommendations for the detection of Shiga toxin-producing *Escherichia coli* in stool specimens.**

Image reproduced from reference (34) under Creative Commons Attribution CC BY 4.0 license

### 1.2.2 Specimen types

Diagnostic testing is usually conducted on unpreserved stool self-collected by the patient, as is recommended by the CPHLN. Stools are transferred to sterile containers and can be stored at 4°C following collection. Although there are several transport media available, STEC samples stored for 7 days without transport media have been found to maintain culture positivity equally as well as those kept in FecalSwab™ Transport or Preservation Medium and modified Cary-Blair (35). Bulk stool provides a representative look at the patient’s bowel contents, and usually provides a sufficient amount of sample for several tests to be conducted.

When stool is liquid it may be difficult to collect, particularly from children. For this reason, rectal swabs have garnered interest as an alternative specimen type. Some major Canadian hospitals have begun implementing rectal swab testing for pediatric patients as it allows more flexibility and is an easier workflow for healthcare practitioners (36). Rectal swabs are compatible with all three methods described above, and have shown comparable sensitivity. One study found an overall agreement of 93% by culture between rectal swabs and bulk stool specimens (37). Another study found that although the bacterial load of rectal swabs is less than one tenth of feces, there was no significant difference in detection rates when an NAT was used (38). Since STEC cells adhere to the colon mucosa, swabs are able to sample these populations of cells (39). However, unlike bulk stool samples which are usually of sufficient quantity for multiple tests, the amount of sample on a swab can be limiting.

### **1.2.3 Culture**

Despite being the gold standard, STEC culture suffers from several challenges. Microfloral *E. coli* may out-compete pathogenic organisms on media, making STEC isolation difficult in some circumstances. This necessitates using media which are selective (i.e., chemical additives are used to inhibit the growth of some organisms) and/or differential (i.e., compounds are added that allow colonies of one type to be visually distinguished from others). Historically, the formulation of such media has focused on the unique biochemical characteristics of O157 strains. For example, the widely-used Sorbitol-MacConkey (SMAC) agar was developed to distinguish STEC based on most O157 organisms' inability to ferment sorbitol (40). On SMAC agar, commensal organisms (which are generally sorbitol-fermenting) appear pink in colour whereas non-sorbitol-fermenters appear colourless (41). However, it is now recognized that this O157-driven approach may have contributed to an under-detection of non-O157 organisms in the past. Non-O157 STEC exhibit great metabolic diversity and some strains evade detection

because they are metabolically similar to commensal *E. coli*. To illustrate this point, Fan et al. grew 476 non-O157 organisms on SMAC agar, and found that only 80 isolates (16.8%) produced the colourless colonies expected of O157 STEC while the remaining 396 (83.2%) grew pink colonies (42).

A newer solid media, CHROMagar™ STEC (CHROMagar™, Paris, France), has begun to replace SMAC in diagnostic laboratories. Its proprietary formulation has both selective and chromogenic additives. According to the manufacturer, most STEC will appear mauve coloured, other Enterobacteriaceae will appear blue / colourless, and Gram-positive organisms will be inhibited (6). Several studies have suggested that potassium tellurite ( $K_2TeO_3$ ; an oxidizer which is toxic to most bacteria) is one of the compounds added to the medium (6,42). Tellurite resistance is considered a characteristic of O157 STEC, and is also often found in Top-6 non-O157 isolates (43). One study found CHROMagar™ STEC to inhibit the growth of 25% (93 / 365) of the isolates tested, and to have a detection frequency between 85 - 100% for O157, O26, O111, O121, and O145 (44). However, another study with 476 non-O157 strains found that only 23% were resistant to tellurite and more than half could not be grown on CHROMagar™ STEC (42). Some STEC strains that fail to grow when stool is directly plated onto CHROMagar™ STEC have been found to grow successfully when first isolated on MacConkey agar then subcultured on CHROMagar™ STEC (43). This suggests that bacterial load and interactions with commensal bacteria might further contribute to the inability of some strains to grow on solid media. Regardless, the variability seen throughout the literature pertaining to CHROMagar™ STEC's performance, especially with non-O157 bacteria, suggests that it may not be a suitable way of initially screening for STEC, but may be useful for isolating some organisms once identified (45).



For all plating media, stool consistency can affect recovery. Mucoïd stools are especially challenging because of the difficulty in acquiring a homogenized inoculum (6). A low bacterial load (as seen near the end of the infection) or cell death during specimen transport may also contribute to the difficulties in culturing STEC from patient samples. Specimens with a low bacterial load are prone to sampling errors: if an aliquot of stool happens to contain too few (or no) organisms, then no STEC will be isolated. Finally, although antibiotics should not be used for STEC infections, they may still be prescribed and can interfere with culturability.

#### **1.2.4 Enzyme immunoassays (EIA)**

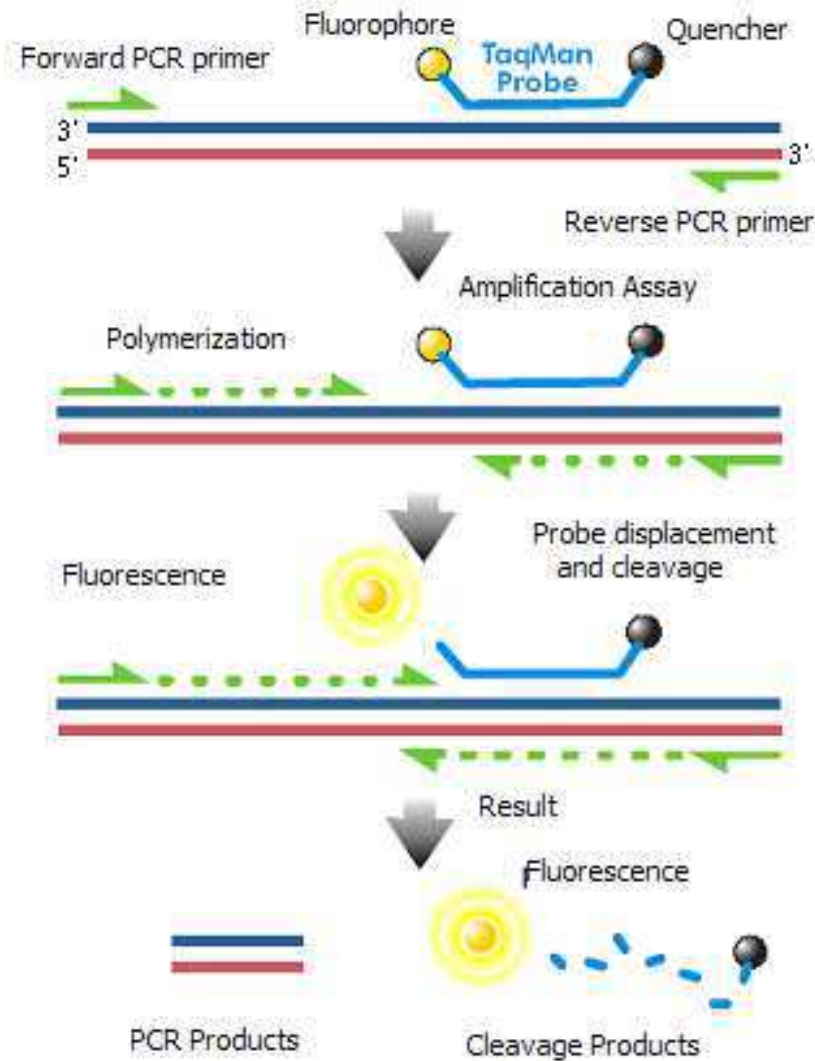
Lateral flow enzyme immunoassays (EIAs) indirectly detect STEC by identifying the presence of Shiga toxin in patient stool samples. Shiga toxin is a protein, so antibodies can be designed to detect specific antigens on its surface (4). However, the structures of Stx-1 and Stx-2 differ significantly enough (~55% amino acid similarity) that two sets of antibodies are required (4,46). Many frontline laboratories use a commercially-available EIA called SHIGA TOXIN QUIK CHEK™ (STQC) (Techlab®, Blacksburg, Virginia, US). The test takes approximately 30 minutes to qualitatively detect and differentiate between Stx-1 and Stx-2 toxins (47). Stool samples can be tested directly or first enriched overnight in broth. The STQC cassette has monoclonal antibodies specific to Stx-1 and Stx-2 which are immobilized in different locations (two lines) on a porous membrane (48). When a diluted specimen is applied to the membrane, Shiga toxin proteins will be bound by their corresponding antibodies as the sample migrates across the membrane via capillary flow. A second set of Stx-1 and Stx-2 antibodies (which are conjugated to horseradish peroxidase) are then applied to the membrane and will bind the Shiga toxin kept in place by the first set. When tetramethylbenzidine is subsequently added, the horseradish peroxidase attached to the second set of antibodies will act on it to produce a colour change

(making the line(s) of antibodies observable on the cassette membrane). In the absence of Shiga toxin, the second set of antibodies will be washed away and no colour change will occur.

In clinical practice, STQC suffers from a few limitations. First, Stx-1 and the toxin expressed by *Shigella dysenteriae* differ by only one amino acid (4). This antigenic similarity means that *S. dysenteriae* can give false-positive STQC results. Second, one study found that direct fecal testing was only 46.7% sensitive and that, depending on the strain and toxin subtype, STQC's limit of detection (LoD) ranged from  $10^8$  -  $10^4$  CFU/mL (47). Another study found STQC's direct fecal sensitivity to be better (~70%) but nonetheless showed that enrichment could increase sensitivity by ~15% (i.e., 85% sensitivity when the sample was grown overnight in broth) (49). For this reason, the CPHLN recommends that samples be enriched prior to being tested by EIA (34). The choice of enrichment broth can likely affect STEC growth and/or Stx production, and thus may affect STQC positivity (47). The necessity of an overnight incubation period increases the turnaround time for STQC results. Third, some studies that compared STQC with real time-PCR (RT-PCR) have suggested that STQC might have difficulty detecting the Stx-2f form of the toxin (50). Similar detection difficulties have been reported for some (but not all) STEC with other "rare" toxin subtypes (i.e., 1c, 2b, 2e, and 2g) (47,49). However, it might not be appropriate to compare RT-PCR with STQC performance. A more robust study instead compared STQC with a Vero cell cytotoxicity assay and found that STQC could detect all of the subtypes when they were expressed (51). These findings suggest that the issue lies not in the STQC antibodies, but in the low expression levels of certain subtypes (e.g. 2f). It is also reasonable to assume that *in vitro* toxin expression may not accurately resemble how an organism behaves during infection. Ultimately STQC can offer useful diagnostic insight, but negative results do not necessarily rule out the possibility of STEC being present in a patient specimen.

### 1.2.5 Nucleic Acid [Amplification] Tests (NAT / NAATs)

Nucleic acid amplification tests (NAATs), which are sometimes just referred to as nucleic acid tests (NATs), are primarily RT-PCR-based assays that target specific pathogen-associated genes. Both commercial and laboratory-developed RT-PCR assays utilize TaqMan probe-based technology. Probes are specific to the gene of interest and contain both a fluorophore, which emits fluorescence, and a quencher, which absorbs fluorescence (**Figure 1.2**). When in close proximity to each other, the quencher absorbs the fluorescence from the fluorophore. When the gene of interest is amplified by a set of specific forward and reverse primers, the probe is cleaved and the fluorophore is physically separated from the quencher. This allows for the fluorescent signal to be detected by a RT-PCR system. For STEC, the *stx<sub>1</sub>* and *stx<sub>2</sub>* genes are often chosen as targets because of their specificity for the pathogen, but other targets like *92\*uidA* have also been used to detect a single nucleotide polymorphism in the beta-glucuronidase gene which is common to most O157 strains (52,53).



**Figure 1.2. Mechanism of TaqMan probe-based real-time PCR.** Image is part of the public domain (54).

Recently frontline laboratories have begun adopting multiplex syndromic panels. These RT-PCR-based systems are optimized to simultaneously identify different bacterial species from a single sample. One such commercially available assay is the BD MAX™ Enteric Bacterial Panel (BD-EBP), which can detect *Salmonella* spp., *Shigella* spp., Enteroinvasive *Escherichia coli* (EIEC), *Campylobacter* spp. (*jejuni* and *coli*) and Shiga toxin-producing organisms (STEC, *Shigella dysenteriae*) (55). This system can test up to 24 stool specimens simultaneously, and offers a turnaround time of approximately 3 hours (56). The panel has been found to detect STEC at bacterial loads lower (10 to 100x less) than what is required for a positive culture result

(55). The limit of detection for bulk stool is estimated to be between 10 - 1,000 CFU/mL (56). Although all multiplex panels show an increased sensitivity compared to culture methods (56), the BD-EBP has been found to outperform other systems (RIDA®GENE Bacterial Stool Panel, Fast Track Diagnostics Bacterial Gastroenteritis Assay, Prodesse® ProGastro™ SSCS Assay) when it comes to STEC detection (57). The BD-EBP has also been successfully used with rectal swabs, which were found to have a limit of detection of 10<sup>3</sup> CFU/mL for STEC (58).

All NATs are subject to similar limitations. First, NATs do not indicate viability or whether the organism is capable of expressing the target gene. DNA from both dead and live organisms can be amplified. Second, polymorphisms in the target sequence may interfere with detection. This is especially pertinent given the diversity seen in the sequence of *stx*<sub>2</sub> (14). Although some primer-probe sets utilize degenerate sites to accommodate for known single nucleotide polymorphisms, there is always the possibility that an organism may have a new mutation that is incompatible with a given primer-probe set. The sequences of the primers and probes developed by companies like BD MAX™ are considered proprietary information, so it is not possible to know to what extent polymorphisms are accommodated. However, it has been reported that the BD-EBP cannot detect *stx*<sub>2f</sub> (57). Finally, certain chemical substances can interfere with RT-PCR. Although a patient's diet affects specimens, most stools contain the following PCR-inhibitors: complex polysaccharides, bile, salts, lipids, and urate (59).

Commercial assays attempt to minimize the effects of these compounds by diluting and removing particulates during DNA extraction. It is also possible that other interfering substances may be added to specimens during the collection process. For example, stools contaminated with nystatin cream, spermicidal lubricant, hydrocortisone cream, or Vagisil were found to interfere with the BD-EBP's performance (60).

### 1.2.6 The “culture-independent” era

Increasingly frontline laboratories are turning towards culture-independent diagnostic tests (CIDTs, like EIAs and NATs) because they include higher throughput assays, require less technical labor, and offer faster turnaround times than traditional culture (61). Overall, this trend has been associated with an increased detection of STEC infections, especially for non-O157 organisms (62).

At the same time, there is concern that an overemphasis on CIDTs could lead to a loss of public health data. In the US, infections are increasingly being diagnosed based on CIDT results alone, and culture is being performed less often (63,64). In such cases, an isolate is not obtained and further characterization (i.e., serotyping, sequencing, susceptibility testing) is limited. This information is necessary for public health surveillance and cluster analysis, which are used to detect and investigate outbreaks (65). Crucially, there may be discordance when reflex culture is performed on CIDT-positive samples. One study (which did not specify the type(s) of agar used) found that the pathogen recovery was only 50% (109 / 219) for RT-PCR-positive samples, and 62% (196 / 315) for EIA-positive STEC samples (66). They also found that, for all of the enteric pathogens tested, transit time negatively impacted pathogen recovery (66). When discordance between culture and RT-PCR-positivity was investigated by another study, dead cells were the primary driver of discordance (67). Although free phage could also theoretically contribute to this issue, this phenomenon was rare (67). Ultimately, the challenges associated with this new era of diagnostics are calling into question how a “real” infection ought to be defined.

### **1.2.7 Microbiological clearance testing**

In Alberta, to prevent the secondary spread of STEC in sensitive settings (e.g. childcare, healthcare, and food handling), public health orders require that any employee (or child in daycare) with a confirmed STEC case be excluded from these contexts until they have fully cleared their infection (68). Such individuals must submit stool specimens until there are two consecutive culture-negative samples taken at least 24 hours apart (68,69). It takes a median 2.5 weeks from symptom onset for a patient to clear a STEC infection; however, some patients can remain positive for several months (70,71). Asymptomatic cases tend to clear faster, while symptomatic young patients tend to shed for a longer period of time (72).

At present, this testing is primarily conducted using CHROMagar™ STEC. However this media's sensitivity challenges and tendency to suppress the growth of some organisms means that it may not accurately reflect the presence of STEC at low bacterial loads. This is especially true for non-O157 organisms which are more sensitive to the media's additives. A study previously conducted in our laboratory using microbiological clearance samples found that except for one patient (of fourteen), samples were RT-PCR positive for as long as (if not longer) than they were culture positive (68).

## **1.3 Viability PCR**

### **1.3.1 Defining viability**

In order for an active infection to be diagnosed, the causative agent must be found to be capable of life (i.e., be viable). It is generally accepted that for something to be considered "alive", it must undergo biological processes such as those involved in replication, protein synthesis, and maintaining organization.

Culture remains the simplest way of determining viability for most bacteria: growth on traditional media confirms that the organism is alive and capable of replicating. However, some bacteria, including STEC, can enter a quiescent state referred to as “viable but non-culturable” (VBNC) where they are not undergoing active replication (73). VBNC organisms are still considered capable of replication (and thus alive) because they can be “resuscitated” under specific conditions to replicate again (74). Since this quiescence is thought to be triggered by stress (e.g., low temperature and/or limited nutrients), it is possible that an organism might readily replicate *in vivo* despite its apparent VBNC behavior *in vitro* (73,75). Further, VBNC cells have been found to retain their ability to produce active Shiga toxin (76). Although it still remains unclear to what extent VBNC cells play a role in human disease, these qualities suggest that the detection of VBNC should still be considered indicative of an active infection (77). As noted in **Section 1.3.3** the selection of media and growth conditions can also interfere with a replicating bacterium’s ability to grow properly. Ultimately, these limitations mean that [apparent] replicability in culture may not be sufficient to detect every active STEC infection.

The production of Shiga toxin is often used to indicate that a bacterium is capable of protein synthesis, and is thus alive. Protein synthesis can be measured directly through enzyme immunoassays (EIAs) and cytotoxicity assays, and indirectly using reverse transcriptase PCR. One example of an EIA, SHIGA TOXIN QUIK CHEK™, is discussed in **Section 1.3.4**; however, more sophisticated EIAs are capable of quantifying the protein of interest (78). Similarly, cytotoxicity assays can be used to identify the effects of Shiga toxin, and also quantify the amount expressed (76). Reverse transcriptase PCR involves detecting specific messenger RNA sequences, a precursor to protein synthesis (79). Both culturable and VBNC cells have been shown to produce detectable amounts of Shiga toxin by these methods (76,79). However, like other proteins, Shiga toxin is not produced in all circumstances. Although a cell may be



biologically active and capable of protein synthesis, it may not produce and export [detectable] amounts of Shiga toxin at the time of testing. It may be possible to alternatively monitor the levels of certain constitutively expressed proteins, however selecting a protein other than Shiga toxin might reduce an assay's specificity for STEC.

Unlike replication and the synthesis of Shiga toxin, which can fluctuate at times, cell membrane integrity is a fundamental requirement for and indicator of bacterial life. Without the homeostasis that it provides, all other cellular processes would be disrupted. This is why many antibiotics are designed to perforate the membrane or interfere with enzymes involved in membrane maintenance (e.g., transpeptidases) (80). Gram-negative organisms, like STEC, have a double phospholipid bilayer that maintains the equilibrium of the cytosol by acting as a semi-permeable barrier. Maintaining this cellular organization is an active process; the phospholipids, peptidoglycan, and membrane proteins must be regularly replaced in order for the barrier to remain functional and the cell to survive. Cell death occurs if the membrane is sufficiently disrupted by chemicals, heat, or pressure (81). Further, in the absence of metabolic activity, the cell membrane will accumulate unfixable damage and naturally degrade over time. Immediately after death (in the metabolic sense) so-called "ghost cells" may remain intact temporarily, but the exact amount of time is unknown (81). Regardless, in almost all cases cell membrane integrity serves as a valid marker of cell viability.

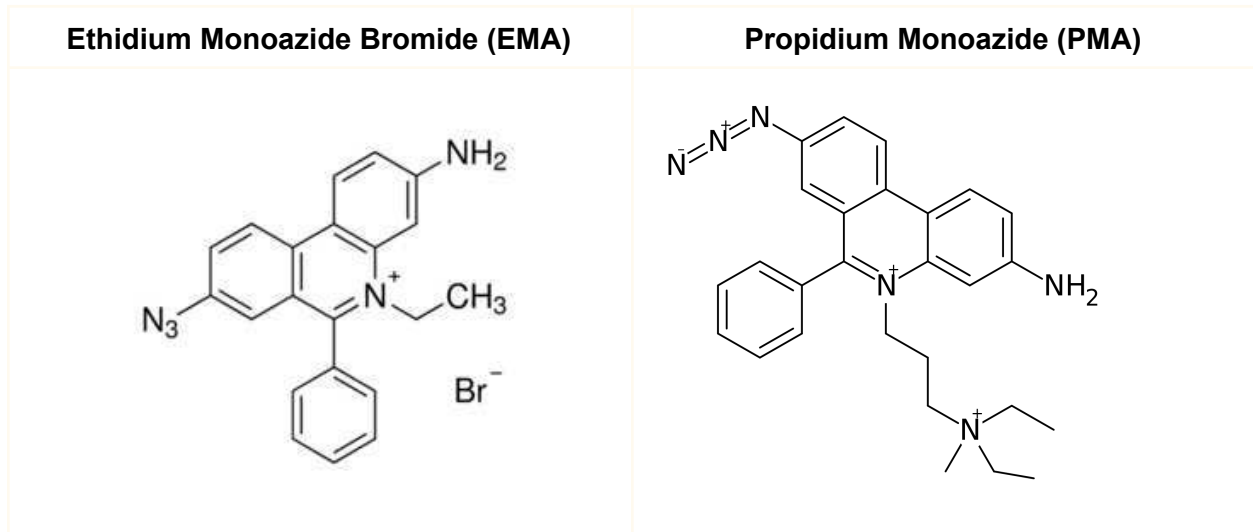
### **1.3.2 Premise of viability RT-PCR**

Viability RT-PCR exploits differences in cell membrane integrity to allow for the exclusive amplification of DNA from intact cells. This "molecular enrichment" is achieved by applying a photoreactive dye that covalently binds double stranded DNA (81). Crucially, viability dyes carry a positive charge which prevents them from passively crossing the cellular membrane. This

means that only freely available DNA (e.g., in the solution or inside damaged cells) will be bound.

Treatment with viability dye first involves a dark incubation period, which allows time for the dye to penetrate damaged cells and associate (via electrostatic forces) with DNA before being activated (82). A subsequent exposure to bright light (465–475 nm) activates the dye (83). When a dye molecule undergoes photoactivation, its azide group (N<sub>3</sub>) becomes a reactive nitrene intermediate (NH) that then covalently binds to carbon (C-H bond) in the DNA backbone (82,84). The exact mechanism by which this prevents RT-PCR amplification remains unclear. Some sources suggest that DNA bound by a viability dye is removed from solution, but it is also possible that the dye's binding location physically prevents DNA polymerase from replicating the strand (82). Excess dye reacts with water to form an inert complex (hydroxylamine), so it should not negatively impact live cell DNA during subsequent extraction (82).

Ethidium monoazide (EMA) is a popular first generation viability dye. However, it has been found to penetrate live cell membranes to an undesirable degree (85). Its successor, propidium monoazide (PMA), is larger in size and has an additional positive charge (**Figure 1.3**) which together make it less membrane-permeable than EMA (85). An enhanced form of PMA, PMAxx™ (Biotium, San Francisco Bay, California, USA) is speculated of being more hydrophobic, but its exact modifications are not known because of its proprietary nature (86). Finally, dye combinations like PEMAX™ (which contains a low amount of EMA and a higher amount of PMA) have also begun to be used for viability RT-PCR (87). Live cells are able to actively expel the low amount of EMA, which can help eliminate the detection of ghost cells (87).



**Figure 1.3. Molecular structure of propidium monoazide compared to ethidium monoazide bromide.**

Images are part of the public domain. PMA reference (88); EMA reference (89).

### 1.3.3 Interpreting viability RT-PCR results

When targeting *stx*, a RT-PCR-positive result can indicate the presence of: [1] live (culturable) STEC, [2] viable but non-culturable STEC, [3] dead STEC, and/or [4] free Stx phage (**Table 1.1**). In theory, viability dyes should only affect the DNA of membrane compromised cells (e.g. [3]). As such, a “true positive” result means that if RT-PCR amplification occurs after the dye is applied, then intact cells ([1] or [2]) and/or free Stx phage ([4]) are present. It is expected that intact cells have detectable metabolic activity and might also express toxin. On the other hand, a “true negative” is defined by the absence of amplification when no intact cells are present. Such a result should concord with the absence of colony forming units, detectable metabolic activity, and/or toxin expression.

**Table 1.1. Summary of viability PCR results anticipated for STEC cells across the viability spectrum.**

	STEC cells			Free Stx phage
	Culturable	VBNC	Dead	
<b>Description</b>	Metabolically active, actively replicating	Low metabolic activity, not actively replicating	No metabolic activity, no replication	May be found alone or alongside bacteria
<b>Capacity to cause disease</b>	Infectious	Potentially infectious**	Not infectious	Can convert commensal <i>E. coli</i> into toxigenic
<b>Incubation on conventional media</b>	Growth expected*	No growth	No growth	No growth
<b>Membrane</b>	Intact	Intact	Compromised***	Capsid intact
<b>Anticipated conventional RT-PCR result</b>	Positive	Positive	Positive	Positive
<b>Anticipated viability RT-PCR result</b>	Positive	Positive	Negative	Positive
<b>Comments</b>	*Metabolic requirements and sensitivities may prevent growth on some media	** <i>In vitro</i> , VBNC can produce Shiga toxin at levels comparable to culturable STEC (76)	***Membrane may temporarily remain intact after death; will deteriorate without metabolic activity	Viral capsids have been reported to be impermeable to viability dyes (90)

VBNC: viable but non-culturable

Stx phage: Shiga toxin-converting bacteriophage

Viability dyes may not always perform as intended. In the viability RT-PCR context, a false positive occurs when DNA from dead cells is amplified. This may happen if the dye concentration is too low, light activation is not sufficient, the dye binds to other things (e.g. organic matter or plastic), or the membrane of the dead cells are not fully permeable (i.e., are “ghost cells”) (82). False negative results occur when live cell DNA is not amplified as expected (82). This can happen if the dye passively permeates the membrane of living cells, or if chemical substances facilitate its entry. As with all RT-PCR conducted on clinical specimens, sampling error can also contribute to false negative results.

#### **1.3.4 Viability RT-PCR with complex sample types**

Viability RT-PCR has been attempted with STEC in food matrices (**Table 1.2**): ground beef (91), vegetables (92,93), and low moisture foods (94). At present, few studies have attempted to conduct viability RT-PCR in stool. Those that have, did not target STEC and focused on fecal microbiota transplantation (95,96) and wastewater treatment (97,98) rather than diagnostics.

There are several challenges associated with applying viability RT-PCR to complex sample types, especially stool. Matrix interference is the primary concern that must be overcome. The organic matter found in stool specimens has the potential to affect the viability dye’s ability to associate with DNA. It is possible that the stool particulate may block the dye from accessing DNA, or that the dye may bind to the ions found in the specimen instead. There is also the possibility that light may not adequately penetrate the sample because of its turbidity, thus preventing complete activation of the viability dye molecules (99). Even if light activation occurs, the high load of DNA found in stool (both human and from commensal bacteria) might occupy the dye and reduce its efficiency on the target organism. Substances found in stool might also affect the membrane integrity of live cells.

**Table 1.2. Studies which have conducted viability PCR for STEC in complex samples.**

<b>Matrix</b>	<b>Target</b>	<b>PMA concentration</b>	<b>Dark incubation period</b>	<b>Photoactivation period</b>	<b>Other modifications</b>	<b>Reference</b>
<b>Beef burger</b>	<i>stx<sub>1</sub></i> & <i>stx<sub>2</sub></i>	100 µM	30 min	15 min	Added PMA enhancer 5X	(91)
<b>Lettuce &amp; spinach</b>	<i>stx<sub>1</sub></i>	50 µM	5 min	4 min	–	(92)
<b>Fresh-cut vegetables</b>	<i>92*uidA</i>	50 µM	5 min	15 min	PMA was dissolved in 20% Dimethyl sulfoxide	(93)
<b>Low moisture foods</b>	<i>92*uidA</i>	10 µM	30 min	5 min	–	(94)

*92\*uidA*: a conserved single nucleotide polymorphism in the beta-glucuronidase gene of O157:H7 STEC

## 1.4 Research rationale

### 1.4.1 Background

STEC is a common cause of acute gastroenteritis that can cause hemolytic uremic syndrome (HUS) and lead to death (10,15). Given its low infectious dose and potential to severely harm children, the elderly, and those who are immunocompromised, rigorous microbiological clearance testing is needed to ensure that infections are not transmitted in daycare, healthcare, or food handling settings (13). In Alberta, patients from these settings who are diagnosed with a STEC infection must exclude themselves and submit stools to the public health laboratory (ProvLab) until they produce two consecutive culture negative stools  $\geq 24$  hours apart (69). This testing is typically conducted using CHROMagar<sup>TM</sup> STEC. However, some non-O157 STEC strains are unable to grow on the media (42) so are instead enriched in tryptic soy broth before being tested by RT-PCR (referred to as “post-enrichment RT-PCR”) for *stx*. This thesis investigates whether a direct-from-stool viability RT-PCR assay can be used as an alternative testing method. If successful, it will determine with high sensitivity whether a patient’s sample contains live STEC without requiring an overnight growth period.

Viability RT-PCR involves the use of a viability dye like propidium monoazide (PMA), which irreversibly binds DNA when photoactivated and prevents amplification in subsequent RT-PCR (81). Since the dye is membrane impermeable and any excess will react with water to become inert, the DNA from live bacteria is not affected and will be selectively detected in RT-PCR (82). This technique has been successfully used to detect live STEC in other complex samples (91,92,94). Currently only a few studies have attempted viability RT-PCR in stool (95,96), none of which have used STEC as the target organism.

## 1.4.2 Hypothesis

Viability RT-PCR can exclusively detect live STEC in pure cell suspensions, spiked stools, and clinical stool specimens with a sensitivity comparable to conventional RT-PCR.

## 1.4.3 Objectives

**The aims of this study are to:**

1. Determine the optimum conditions for propidium monoazide treatment in order to develop a viability RT-PCR assay for STEC cell suspensions using a set of previously published *stx*<sub>1</sub> and *stx*<sub>2</sub> primers (**Chapter 2**).
2. Compare the sensitivity of viability RT-PCR, culture, and conventional RT-PCR in detecting live STEC using artificially spiked stools, artificially spiked rectal swabs, and clinical microbiological clearance stool specimens (**Chapter 3**).



## 1.5 References

1. Conrad C, Stanford K, McAllister T, Thomas J, Reuter T. Shiga toxin-producing *Escherichia coli* and current trends in diagnostics. *Anim Front*. 2016 Apr 1;6(2):37–43.
2. Melton-Celsa AR. Shiga Toxin (Stx) Classification, Structure, and Function. *Microbiol Spectr*. 2014;4(2):2–4.
3. Unkmeir A, Schmidt H. Structural Analysis of Phage-Borne stx Genes and Their Flanking Sequences in Shiga Toxin-Producing *Escherichia coli* and *Shigella dysenteriae* Type 1 Strains. *Infect Immun*. 2000 Sep;68(9):4856–64.
4. Chan YS, Ng TB. Shiga toxins: from structure and mechanism to applications. *Appl Microbiol Biotechnol*. 2016 Feb 1;100(4):1597–610.
5. Fratamico PM, DebRoy C, Liu Y, Needleman DS, Baranzoni GM, Feng P. Advances in Molecular Serotyping and Subtyping of *Escherichia coli*. *Front Microbiol*. 2016;7:644.
6. Zelyas N, Poon A, Patterson-Fortin L, Johnson RP, Lee W, Chui L. Assessment of commercial chromogenic solid media for the detection of non-O157 Shiga toxin-producing *Escherichia coli* (STEC). *Diagn Microbiol Infect Dis*. 2016 Jul 1;85(3):302–8.
7. Burger R. EHEC O104: H4 in Germany 2011: Large outbreak of bloody diarrhea and haemolytic uraemic syndrome by Shiga toxin-producing *E. coli* via contaminated food. [Internet]. *Improving Food Safety Through a One Health Approach: Workshop Summary*. National Academies Press (US); 2012 [cited 2022 Apr 20]. Available from: <https://www.ncbi.nlm.nih.gov/books/NBK114499/>
8. Glassman H, Ferrato C, Chui L. Epidemiology of Non-O157 Shiga Toxin-Producing *Escherichia coli* in the Province of Alberta, Canada, from 2018 to 2021. *Microorganisms*. 2022 Apr;10(4):814.
9. Awofisayo-Okuyelu A, Brainard J, Hall I, McCarthy N. Incubation Period of Shiga Toxin-Producing *Escherichia coli*. *Epidemiol Rev*. 2019 Oct 16;41(2):121–9.

10. Freedman SB, Eltorki M, Chui L, Xie J, Feng S, MacDonald J, et al. Province-Wide Review of Pediatric Shiga Toxin-Producing *Escherichia coli* Case Management. *J Pediatr*. 2017 Jan 1;180:184–90.
11. Tarr GAM, Stokowski T, Shringi S, Tarr PI, Freedman SB, Oltean HN, et al. Contribution and Interaction of Shiga Toxin Genes to *Escherichia coli* O157:H7 Virulence. *Toxins*. 2019 Oct;11(10):607.
12. Hughes JM, Wilson ME, Johnson KE, Thorpe CM, Sears CL. The Emerging Clinical Importance of Non-O157 Shiga Toxin—Producing *Escherichia coli*. *Clin Infect Dis*. 2006 Dec 15;43(12):1587–95.
13. Gyles CL. Shiga toxin-producing *Escherichia coli*: An overview. *J Anim Sci*. 2007 Mar 1;85(suppl\_13):E45–62.
14. Johannes L, Römer W. Shiga toxins — from cell biology to biomedical applications. *Nat Rev Microbiol*. 2010 Feb;8(2):105–16.
15. Joseph A, Cointe A, Mariani Kurkdjian P, Rafat C, Hertig A. Shiga Toxin-Associated Hemolytic Uremic Syndrome: A Narrative Review. *Toxins*. 2020 Jan 21;12(2):67.
16. Trachtman H, Austin C, Lewinski M, Stahl RAK. Renal and neurological involvement in typical Shiga toxin-associated HUS. *Nat Rev Nephrol*. 2012 Nov;8(11):658–69.
17. Louise CB, Obrig TG. Specific interaction of *Escherichia coli* O157:H7-derived Shiga-like toxin II with human renal endothelial cells. *J Infect Dis*. 1995 Nov;172(5):1397–401.
18. Persson S, Olsen KEP, Ethelberg S, Scheutz F. Subtyping Method for *Escherichia coli* Shiga Toxin (Verocytotoxin) 2 Variants and Correlations to Clinical Manifestations. *J Clin Microbiol*. 2007 Jun;45(6):2020–4.
19. Lienemann T, Salo E, Rimhanen-Finne R, Rönholm K, Taimisto M, Hirvonen JJ, et al. Shiga Toxin—producing *Escherichia coli* Serotype O78:H– in Family, Finland, 2009. *Emerg Infect Dis*. 2012 Apr;18(4):577–81.
20. Haugum K, Johansen J, Gabrielsen C, Brandal LT, Bergh K, Ussery DW, et al. Comparative

- Genomics to Delineate Pathogenic Potential in Non-O157 Shiga Toxin-Producing *Escherichia coli* (STEC) from Patients with and without Haemolytic Uremic Syndrome (HUS) in Norway. *PLOS ONE*. 2014 Oct 31;9(10):e111788.
21. Lisboa LF, Szelewicki J, Lin A, Latonas S, Li V, Zhi S, et al. Epidemiology of Shiga Toxin-Producing *Escherichia coli* O157 in the Province of Alberta, Canada, 2009–2016. *Toxins*. 2019 Oct 22;11(10):613.
  22. Alberta Health Services - *E. coli* (STEC) Info for Health Care Providers [Internet]. [cited 2022 Nov 4]. Available from:  
<https://www.albertahealthservices.ca/assets/info/hp/diseases/if-hp-dis-ecoli-stec.pdf>
  23. Ardissino G, Tel F, Possenti I, Testa S, Consonni D, Paglialonga F, et al. Early Volume Expansion and Outcomes of Hemolytic Uremic Syndrome. *Pediatrics*. 2016 Jan;137(1).
  24. Bauwens A, Kunsmann L, Karch H, Mellmann A, Bielaszewska M. Antibiotic-Mediated Modulations of Outer Membrane Vesicles in Enterohemorrhagic *Escherichia coli* O104:H4 and O157:H7. *Antimicrob Agents Chemother*. 61(9):e00937-17.
  25. Freedman SB, Xie J, Neufeld MS, Hamilton WL, Hartling L, Tarr PI, et al. Shiga Toxin-Producing *Escherichia coli* Infection, Antibiotics, and Risk of Developing Hemolytic Uremic Syndrome: A Meta-analysis. *Clin Infect Dis Off Publ Infect Dis Soc Am*. 2016 15;62(10):1251–8.
  26. Government of Canada. VTEC Illness Monitoring In Canada [Internet]. Innovation, Science and Economic Development Canada; [cited 2022 Jun 9]. Available from:  
[https://www.ic.gc.ca/eic/site/063.nsf/eng/h\\_98071.html#nesp](https://www.ic.gc.ca/eic/site/063.nsf/eng/h_98071.html#nesp)
  27. Baker CA, Rubinelli PM, Park SH, Carbonero F, Ricke SC. Shiga toxin-producing *Escherichia coli* in food: Incidence, ecology, and detection strategies. *Food Control*. 2016 Jan 1;59:407–19.
  28. Murinda SE, Nguyen LT, Landers TL, Draughon FA, Mathew AG, Hogan JS, et al. Comparison of *Escherichia coli* Isolates from Humans, Food, and Farm and Companion

- Animals for Presence of Shiga Toxin–Producing *E. coli* Virulence Markers. *Foodborne Pathog Dis.* 2004 Sep;1(3):178–84.
29. Large TM, Walk ST, Whittam TS. Variation in Acid Resistance among Shiga Toxin-Producing Clones of Pathogenic *Escherichia coli*. *Appl Environ Microbiol.* 2005 May;71(5):2493–500.
  30. Gill A, editor. Review of the State of Knowledge on Verotoxigenic *Escherichia coli* and the Role of Whole Genome Sequencing as an Emerging Technology Supporting Regulatory Food Safety in Canada [Internet]. Innovation, Science and Economic Development Canada; 2020 [cited 2022 Nov 4]. Available from:  
<https://science.gc.ca/site/science/en/blogs/cultivating-science/review-state-knowledge-verot-oxigenic-escherichia-coli-and-role-whole-genome-sequencing-emerging>
  31. Currie A, Honish L, Cutler J, Locas A, Lavoie MC, Gaulin C, et al. Outbreak of *Escherichia coli* O157:H7 Infections Linked to Mechanically Tenderized Beef and the Largest Beef Recall in Canada, 2012. *J Food Prot.* 2019 Sep 1;82(9):1532–8.
  32. Veneti L, Lange H, Brandal L, Danis K, Vold L. Mapping of control measures to prevent secondary transmission of STEC infections in Europe during 2016 and revision of the national guidelines in Norway. *Epidemiol Infect.* 2019 Jul 29;147(e267):1–10.
  33. Canadian Public Health Laboratory Network. Core Functions of Canadian Public Health Laboratories [Internet]. 2011 [cited 2022 Nov 4]. Available from:  
<https://nccid.ca/wp-content/uploads/sites/2/2020/03/CPHLN-Core-Functions.pdf>
  34. Chui L, Christianson S, Alexander D, Arseneau V, Bekal S, Berenger B, et al. CPHLN recommendations for the laboratory detection of Shiga toxin-producing *Escherichia coli* (O157 and non-O157). *Can Commun Dis Rep.* 2018 Nov 1;44:304–7.
  35. Berenger BM, Ferrato C, Chui L. Viability of bacterial enteropathogens in fecal samples in the presence or absence of different types of transport media. *Diagn Microbiol Infect Dis.* 2019 Nov 1;95(3):114862.
  36. Freedman SB, Xie J, Nettel-Aguirre A, Lee B, Chui L, Pang XL, et al. Enteropathogen

- detection in children with diarrhoea, or vomiting, or both, comparing rectal flocked swabs with stool specimens: an outpatient cohort study. *Lancet Gastroenterol Hepatol*. 2017 Sep;2(9):662–9.
37. Jean S, Yarbrough ML, Anderson NW, Burnham CAD. Culture of Rectal Swab Specimens for Enteric Bacterial Pathogens Decreases Time to Test Result While Preserving Assay Sensitivity Compared to Bulk Fecal Specimens. *J Clin Microbiol*. 2019 Jun;57(6):e02077-18.
  38. Kabayiza JC, Andersson ME, Welinder-Olsson C, Bergström T, Muhirwa G, Lindh M. Comparison of rectal swabs and faeces for real-time PCR detection of enteric agents in Rwandan children with gastroenteritis. *BMC Infect Dis*. 2013 Sep 27;13(1):447.
  39. Wine E. Rectal swabs: a diagnostic alternative in paediatric gastroenteritis? *Lancet Gastroenterol Hepatol*. 2017 Sep 1;2(9):623–4.
  40. March SB, Ratnam S. Sorbitol-MacConkey medium for detection of *Escherichia coli* O157:H7 associated with hemorrhagic colitis. *J Clin Microbiol*. 1986 May;23(5):869–72.
  41. Church DL, Emshey D, Semeniuk H, Lloyd T, Pitout JD. Evaluation of BBL CHROMagar O157 versus Sorbitol-MacConkey Medium for Routine Detection of *Escherichia coli* O157 in a Centralized Regional Clinical Microbiology Laboratory. *J Clin Microbiol*. 2007 Sep;45(9):3098–100.
  42. Fan R, Bai X, Fu S, Xu Y, Sun H, Wang H, et al. Tellurite resistance profiles and performance of different chromogenic agars for detection of non-O157 Shiga toxin-producing *Escherichia coli*. *Int J Food Microbiol*. 2018 Feb 2;266:295–300.
  43. Jenkins C, Perry NT, Godbole G, Gharbia S. Evaluation of chromogenic selective agar (CHROMagar STEC) for the direct detection of Shiga toxin-producing *Escherichia coli* from faecal specimens. *J Med Microbiol*. 2020 Mar;69(3):487–91.
  44. Hirvonen JJ, Siitonen A, Kaukoranta SS. Usability and Performance of CHROMagar STEC Medium in Detection of Shiga Toxin-Producing *Escherichia coli* Strains. *J Clin Microbiol*. 2012 Nov;50(11):3586–90.

45. Wylie JL, Van Caesele P, Gilmour MW, Sitter D, Guttek C, Giercke S. Evaluation of a New Chromogenic Agar Medium for Detection of Shiga Toxin-Producing *Escherichia coli* (STEC) and Relative Prevalences of O157 and Non-O157 STEC in Manitoba, Canada. *J Clin Microbiol.* 2013 Feb;51(2):466–71.
46. Lee JE, Reed J, Shields MS, Spiegel KM, Farrell LD, Sheridan PP. Phylogenetic analysis of Shiga toxin 1 and Shiga toxin 2 genes associated with disease outbreaks. *BMC Microbiol.* 2007 Dec 4;7(1):109.
47. Sánchez S, Llorente MT, Ramiro R, Herrera-León L, Herrera-León S. Evaluation of the SHIGA TOXIN QUIK CHEK after overnight enrichment as screening tool for Shiga toxin-producing *Escherichia coli* detection in human fecal samples. *Diagn Microbiol Infect Dis.* 2019 Jul 1;94(3):218–22.
48. SHIGA TOXIN QUIK CHEK™ Package insert [Internet]. TechLab; 2021 [cited 2022 Nov 4]. Available from:  
[https://www.techlab.com/wp-content/uploads/2021/09/SHIGA-TOXIN-QUIK-CHEK-PI-91-62-5-01-TL\\_7-2021.pdf](https://www.techlab.com/wp-content/uploads/2021/09/SHIGA-TOXIN-QUIK-CHEK-PI-91-62-5-01-TL_7-2021.pdf)
49. Chui L, Patterson-Fortin L, Kuo J, Li V, Boras V. Evaluation of Enzyme Immunoassays and Real-Time PCR for Detecting Shiga Toxin-Producing *Escherichia coli* in Southern Alberta, Canada. Munson E, editor. *J Clin Microbiol.* 2015 Mar;53(3):1019–23.
50. De Rauw K, Breynaert J, Piérard D. Evaluation of the Alere SHIGA TOXIN QUIK CHEK™ in comparison to multiplex Shiga toxin PCR. *Diagn Microbiol Infect Dis.* 2016 Sep;86(1):35–9.
51. Boone JT, Campbell DE, Dandro AS, Chen L, Herbein JF. A Rapid Immunoassay for Detection of Shiga Toxin-Producing *Escherichia coli* Directly from Human Fecal Samples and Its Performance in Detection of Toxin Subtypes. Tang YW, editor. *J Clin Microbiol.* 2016 Dec;54(12):3056–63.
52. Feng P, Weagant SD, Jinneman K. Bacteriological Analytical Manual Chapter 4A: Diarrheagenic *Escherichia coli* [Internet]. FDA; 2020 [cited 2022 Mar 22]. Available from:

<https://www.fda.gov/food/laboratory-methods-food/bam-chapter-4a-diarrheagenic-escherichia-coli>

53. Feng P. Identification of *Escherichia coli* serotype O157:H7 by DNA probe specific for an allele of uid A gene. *Mol Cell Probes*. 1993 Apr;7(2):151–4.
54. TaqMan. In: Wikipedia [Internet]. 2022 [cited 2022 Nov 4]. Available from: <https://en.wikipedia.org/w/index.php?title=TaqMan&oldid=1109226283>
55. Anderson NW, Buchan BW, Ledebner NA. Comparison of the BD MAX Enteric Bacterial Panel to Routine Culture Methods for Detection of *Campylobacter*, Enterohemorrhagic *Escherichia coli* (O157), *Salmonella*, and *Shigella* Isolates in Preserved Stool Specimens. *J Clin Microbiol*. 2014 Apr;52(4):1222–4.
56. Harrington SM, Buchan BW, Doern C, Fader R, Ferraro MJ, Pillai DR, et al. Multicenter Evaluation of the BD Max Enteric Bacterial Panel PCR Assay for Rapid Detection of *Salmonella* spp., *Shigella* spp., *Campylobacter* spp. (*C. jejuni* and *C. coli*), and Shiga Toxin 1 and 2 Genes. *J Clin Microbiol*. 2015 May;53(5):1639–47.
57. Berenger B, Chui L, Ferrato C, Lloyd T, Li V, Pillai DR. Performance of four commercial real-time PCR assays for the detection of bacterial enteric pathogens in clinical samples - ScienceDirect. *Int J Infect Dis*. 2021 Oct 20;114:195–201.
58. DeBurger B, Hanna S, Powell EA, Ventrola C, Mortensen JE. Utilizing BD MAX™ Enteric Bacterial Panel to Detect Stool Pathogens from Rectal Swabs. *BMC Clin Pathol*. 2017 Apr 8;17(1):7.
59. Schrader C, Schielke A, Ellerbroek L, Johne R. PCR inhibitors – occurrence, properties and removal. *J Appl Microbiol*. 2012;113(5):1014–26.
60. Yalamanchili H, Dandachi D, Okhuysen PC. Use and Interpretation of Enteropathogen Multiplex Nucleic Acid Amplification Tests in Patients With Suspected Infectious Diarrhea. *Gastroenterol Hepatol*. 2018 Nov;14(11):646–52.
61. Cronquist AB, Mody RK, Atkinson R, Besser J, D'Angelo MT, Hurd S, et al. Impacts of

- Culture-Independent Diagnostic Practices on Public Health Surveillance for Bacterial Enteric Pathogens. *Clin Infect Dis*. 2012 Jun 1;54(suppl\_5):S432–9.
62. Jenssen GR, Veneti L, Lange H, Vold L, Naseer U, Brandal LT. Implementation of multiplex PCR diagnostics for gastrointestinal pathogens linked to increase of notified Shiga toxin-producing *Escherichia coli* cases in Norway, 2007–2017. *Eur J Clin Microbiol Infect Dis*. 2019 Apr 1;38(4):801–9.
63. Berenger B, Chui L, Reimer A, Allen V, Alexander D, Domingo MC, et al. Canadian Public Health Laboratory Network position statement: Non-culture based diagnostics for gastroenteritis and implications for public health investigations. *Can Commun Dis Rep*. 2017 Dec 7;43(12):279–81.
64. Marder EP, Cieslak PR, Cronquist AB, Dunn J, Lathrop S, Rabatsky-Ehr T, et al. Incidence and Trends of Infections with Pathogens Transmitted Commonly Through Food and the Effect of Increasing Use of Culture-Independent Diagnostic Tests on Surveillance — Foodborne Diseases Active Surveillance Network, 10 U.S. Sites, 2013–2016. *MMWR Morb Mortal Wkly Rep*. 2017 Apr 21;66(15):397–403.
65. Gerner-Smidt P, Kincaid J, Kubota K, Hise K, Hunter SB, Fair MA, et al. Molecular Surveillance of Shiga Toxigenic *Escherichia coli* O157 by PulseNet USA. *J Food Prot*. 2005 Sep 1;68(9):1926–31.
66. Imdad A, Retzer F, Thomas LS, McMillian M, Garman K, Rebeiro PF, et al. Impact of Culture-Independent Diagnostic Testing on Recovery of Enteric Bacterial Infections. *Clin Infect Dis*. 2018 Jun 1;66(12):1892–8.
67. Macori G, McCarthy SC, Burgess CM, Fanning S, Duffy G. Investigation of the causes of shigatoxigenic *Escherichia coli* PCR positive and culture negative samples. *Microorganisms*. 2020;8(4):587.
68. Bording-Jorgensen M, Parsons BD, Tarr GAM, Shah-Gandhi B, Lloyd C, Chui L. Association of Ct Values from Real-Time PCR with Culture in Microbiological Clearance Samples for



- Shiga Toxin-Producing *Escherichia coli* (STEC). *Microorganisms*. 2020 Nov 16;8(11):1801.
69. Alberta Health. Alberta Public Health Disease Management Guidelines - *Escherichia coli* Verotoxigenic Infections [Internet]. 2021. Available from:  
<https://open.alberta.ca/dataset/2b77e542-cfcb-4f93-b825-dca7d140e024/resource/b3c01b4a-8541-47fa-a19a-b7c3835a1cee/download/health-phdmg-escherichia-coli-verotoxigenic-infections-2021-11.pdf>
70. Bai X, Mernelius S, Jernberg C, Einemo I, Monecke S, Ehricht R, et al. Shiga Toxin-Producing *Escherichia coli* Infection in Jönköping County, Sweden: Occurrence and Molecular Characteristics in Correlation With Clinical Symptoms and Duration of stx Shedding. *Front Cell Infect Microbiol*. 2018 May 1;8:125.
71. Mody RK, Griffin PM. Editorial Commentary: Fecal Shedding of Shiga Toxin–Producing *Escherichia coli*: What Should Be Done to Prevent Secondary Cases? *Clin Infect Dis*. 2013 Apr 15;56(8):1141–4.
72. Scavia G, Gianviti A, Labriola V, Chiani P, Maugliani A, Michelacci V, et al. A case of haemolytic uraemic syndrome (HUS) revealed an outbreak of Shiga toxin-2-producing *Escherichia coli* O26:H11 infection in a nursery, with long-lasting shedders and person-to-person transmission, Italy 2015. *J Med Microbiol*. 67(6):775–82.
73. Chekabab SM, Paquin-Veillette J, Dozois CM, Harel J. The ecological habitat and transmission of *Escherichia coli* O157:H7. *FEMS Microbiol Lett*. 2013 Apr 1;341(1):1–12.
74. Dinu LD, Bach S. Induction of Viable but Nonculturable *Escherichia coli* O157:H7 in the Phyllosphere of Lettuce: a Food Safety Risk Factor. *Appl Environ Microbiol*. 2011 Dec;77(23):8295–302.
75. Muniesa M, Hammerl JA, Hertwig S, Appel B, Brüssow H. Shiga Toxin-Producing *Escherichia coli* O104:H4: a New Challenge for Microbiology. *Appl Environ Microbiol*. 2012 Jun 15;78(12):4065–73.
76. Liu Y, Wang C, Tyrrell G, Li XF. Production of Shiga-like toxins in viable but nonculturable

- Escherichia coli* O157:H7. *Water Res.* 2010 Feb 1;44(3):711–8.
77. Croxen MA, Law RJ, Scholz R, Keeney KM, Wlodarska M, Finlay BB. Recent Advances in Understanding Enteric Pathogenic *Escherichia coli*. *Clin Microbiol Rev.* 2013 Oct;26(4):822–80.
  78. Yamasaki E, Watahiki M, Isobe J, Sata T, Nair GB, Kurazono H. Quantitative Detection of Shiga Toxins Directly from Stool Specimens of Patients Associated with an Outbreak of Enterohemorrhagic *Escherichia coli* in Japan—Quantitative Shiga toxin detection from stool during EHEC outbreak. *Toxins.* 2015 Oct;7(10):4381–9.
  79. McIngvale SC, Elhanafi D, Drake MA. Optimization of Reverse Transcriptase PCR To Detect Viable Shiga-Toxin-Producing *Escherichia coli*. *Appl Environ Microbiol.* 2002 Feb;68(2):799–806.
  80. Epand RM, Walker C, Epand RF, Magarvey NA. Molecular mechanisms of membrane targeting antibiotics. *Biochim Biophys Acta BBA - Biomembr.* 2016 May 1;1858(5):980–7.
  81. Nocker A, Camper AK. Novel approaches toward preferential detection of viable cells using nucleic acid amplification techniques. *FEMS Microbiol Lett.* 2009 Feb 1;291(2):137–42.
  82. van Frankenhuyzen JK, Trevors JT, Lee H, Flemming CA, Habash MB. Molecular pathogen detection in biosolids with a focus on quantitative PCR using propidium monoazide for viable cell enumeration. *J Microbiol Methods.* 2011;87(3):263–72.
  83. Lee AS, Lamanna OK, Ishida K, Hill E, Nguyen A, Hsieh MH. A Novel Propidium Monoazide-Based PCR Assay Can Measure Viable Uropathogenic *E. coli* In Vitro and In Vivo. *Front Cell Infect Microbiol.* 2022;12:40.
  84. Probst A, Mahnert A, Weber C, Haberer K, Moissl-Eichinger C. Detecting inactivated endospores in fluorescence microscopy using propidium monoazide. *Int J Astrobiol.* 2012 Apr;11(2):117–23.
  85. Nocker A, Cheung CY, Camper AK. Comparison of propidium monoazide with ethidium monoazide for differentiation of live vs. dead bacteria by selective removal of DNA from

- dead cells. *J Microbiol Methods*. 2006;67(2):310–20.
86. Codony F, Dinh-Thanh M, Agustí G. Key Factors for Removing Bias in Viability PCR-Based Methods: A Review. *Curr Microbiol*. 2020 Apr 1;77(4):682–7.
87. Thanh MD, Agustí G, Mader A, Appel B, Codony F. Improved sample treatment protocol for accurate detection of live *Salmonella* spp. in food samples by viability PCR. *PLOS ONE*. 2017 Dec 12;12(12):e0189302.
88. Propidium monoazide. In: Wikipedia [Internet]. 2022 [cited 2022 Nov 4]. Available from: [https://en.wikipedia.org/w/index.php?title=Propidium\\_monoazide&oldid=1117032474](https://en.wikipedia.org/w/index.php?title=Propidium_monoazide&oldid=1117032474)
89. Ethidium bromide monoazide [Internet]. ottokemi.com. [cited 2022 Nov 4]. Available from: <https://www.ottokemi.com/product/ethidium-bromide-monoazide-95-hplc-e-3676.aspx>
90. Elizaquível P, Aznar R, Sánchez G. Recent developments in the use of viability dyes and quantitative PCR in the food microbiology field. *J Appl Microbiol*. 2014;116(1):1–13.
91. Rey M de los Á, Cap M, Favre LC, Rodríguez Racca A, Dus Santos MJ, Vaudagna SR, et al. Evaluation of PMA-qPCR methodology to detect and quantify viable Shiga toxin-producing *Escherichia coli* in beef burgers. *J Food Process Preserv*. 2021;45(4):e15338.
92. Dinu LD, Bach S. Detection of viable but non-culturable *Escherichia coli* O157: H7 from vegetable samples using quantitative PCR with propidium monoazide and immunological assays. *Food Control*. 2013;31(2):268–73.
93. Elizaquível P, Sánchez G, Aznar R. Quantitative detection of viable foodborne *E. coli* O157:H7, *Listeria monocytogenes* and *Salmonella* in fresh-cut vegetables combining propidium monoazide and real-time PCR. *Food Control*. 2012 Jun 1;25(2):704–8.
94. Shekar A, Babu L, Ramlal S, Sripathy MH, Batra H. Selective and concurrent detection of viable *Salmonella* spp., *E. coli*, *Staphylococcus aureus*, *E. coli* O157:H7, and *Shigella* spp., in low moisture food products by PMA-mPCR assay with internal amplification control. *LWT*. 2017 Dec 1;86:586–93.

95. Papanicolas LE, Wang Y, Choo JM, Gordon DL, Wesselingh SL, Rogers GB. Optimisation of a propidium monoazide based method to determine the viability of microbes in faecal slurries for transplantation. *J Microbiol Methods*. 2019 Jan 1;156:40–5.
96. Takahashi M, Ishikawa D, Sasaki T, Lu Y j., Kuwahara-Arai K, Kamei M, et al. Faecal freezing preservation period influences colonization ability for faecal microbiota transplantation. *J Appl Microbiol*. 2019;126(3):973–84.
97. Li D, Tong T, Zeng S, Lin Y, Wu S, He M. Quantification of viable bacteria in wastewater treatment plants by using propidium monoazide combined with quantitative PCR (PMA-qPCR). *J Environ Sci*. 2014;26(2):299–306.
98. Varma M, Field R, Stinson M, Rukovets B, Wymer L, Haugland R. Quantitative real-time PCR analysis of total and propidium monoazide-resistant fecal indicator bacteria in wastewater. *Water Res*. 2009;43(19):4790–801.
99. Fu Y, Ye Z, Jia Y, Fan J, Hashmi MZ, Shen C. An Optimized Method to Assess Viable *Escherichia coli* O157:H7 in Agricultural Soil Using Combined Propidium Monoazide Staining and Quantitative PCR. *Front Microbiol*. 2020;11:1809.

## Chapter 2: Optimizing viability real-time PCR for STEC cell suspensions

### 2.1 Introduction

Shiga toxin-producing *Escherichia coli* (STEC) causes 1 - 2 cases of acute gastroenteritis per 100,000 Canadians each year (1). Children (< 10) are most at risk of acquiring STEC infection and experiencing severe complications (2,3). Between 5 - 10% of STEC infections in children lead to hemolytic uremic syndrome (HUS) which can cause fatal kidney failure (4). Since Shiga toxin is encoded by a lytic phage which can be induced by antibiotics, patients can only receive supportive hydration therapy (5,6). Fast and accurate STEC diagnosis is crucial so antibiotics are not wrongfully prescribed and intravenous fluids can be administered early (7).

Since 2018 the Canadian Public Health Laboratory Network (CPHLN) has permitted the use of nucleic acid amplification tests (NAATs) for preliminary STEC detection (8). These culture-independent assays involve extracting DNA from a patient's sample then conducting real-time PCR (RT-PCR) to identify the presence of *stx* (the Shiga toxin gene). This technique offers high sensitivity and a quicker turnaround time compared to overnight culture (9). Further, the process can be automated via commercially available systems like the BD MAX™ Enteric Bacterial Panel used in Albertan frontline laboratories. However, NAATs do not indicate viability, so positive results must be followed by culture to confirm the presence of live pathogens (8).

Culture-independent testing could be enhanced by viability RT-PCR. This technique involves the use of a viability dye that, when photoactivated, is supposed to irreversibly bind DNA and prevent subsequent amplification (10). Since these dyes are designed to be membrane-impermeable, they should not affect the DNA found in live cells (11). A successful viability RT-PCR protocol will efficiently eliminate the detection of dead cells, even at high

concentrations, while preserving the detection and viability of live cells. However, at present there is no consensus regarding the ideal viability RT-PCR treatment conditions.

In most studies, viability RT-PCR optimization begins by selecting a viability dye. The first generation viability dye ethidium monoazide (EMA) penetrates live cell membranes to an undesirable degree, so the second generation dye, propidium monoazide (PMA), was designed to be larger in size and to have an additional positive charge to reduce this effect (12). The proprietary PMAxx™ dye was chosen for this study as it has been shown to be even more effective than conventional PMA (13). The next step in optimization often involves determining the ideal dye concentration and photoactivation time. Previous studies have used concentrations ranging from 10 to 200 μM (14,15) and photoactivation times ranging from less than 5 min to up to 30 min (16,17). Lastly, modifications may be used to enhance performance. For example, some studies (12,18–20) add dimethyl sulfoxide (DMSO), which at low concentrations increases membrane fluidity, to help PMAxx™ better penetrate dead cells (e.g., those that are dead but retain a semi-intact membrane) (21,22).

The aim of Chapter 2 is to determine the optimum conditions for PMAxx™ treatment in order to develop a viability RT-PCR assay for STEC cell suspensions. This is to be achieved by first determining the limit of detection, sequence specificity, and subtype coverage of a previously published set of *stx*<sub>1</sub> and *stx*<sub>2</sub> primers and probes (23). Secondly, the claims that PMAxx™ is membrane-impermeable, binds DNA covalently, and that its fluorescence does not interfere with RT-PCR will be confirmed. Thirdly, the optimum buffer, PMAxx™ concentration, and photoactivation time will be selected for subsequent experiments. Fourthly, potential PMAxx™ treatment modifications (addition of DMSO, inclusion of a tube transfer step, and pre-photoactivation) will be trialed. Finally, the optimized protocol's ability to selectively detect DNA from live cells in the presence of dead (i.e., heat-killed) cells will be assessed.

## 2.2 Methods and Materials

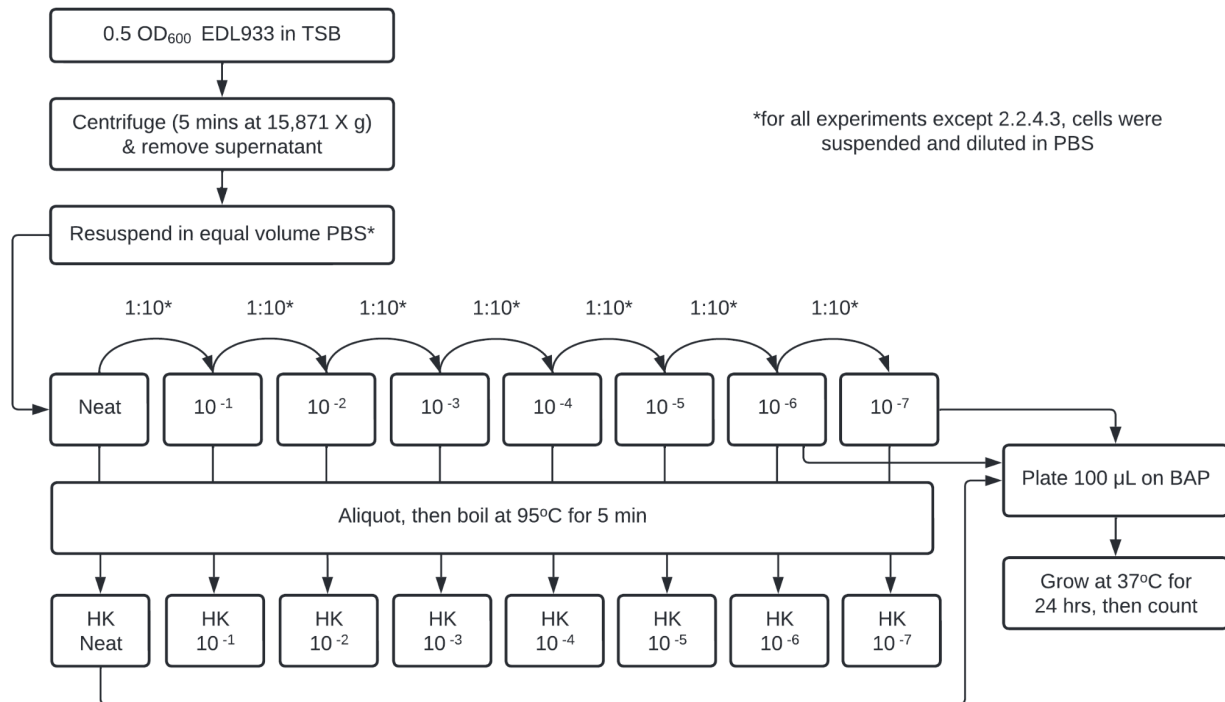
### 2.2.1 Cell suspensions

#### 2.2.1.1 Reference strain

EDL 933 is a well characterized STEC O157:H7 strain that is positive for both *stx*<sub>1</sub> and *stx*<sub>2</sub>. It had been stored in skim milk medium (prepared by APL-ProvLab) at -70°C as part of the Chui laboratory repository. The isolate was retrieved from the frozen stock by streaking onto a Blood Agar Plate (BAP; Dalynn Biologicals Inc, Calgary, AB, Canada) and incubating overnight (20 hours) at 37°C.

#### 2.2.1.2 Dilution series and preparation of heat-killed cells

To make a dilution series, one EDL 933 colony from a BAP was inoculated into Trypticase Soy Broth (TSB; Becton Dickinson, Mississauga, ON, Canada) with horizontal agitation at 225 rpm (MaxQ 2506 Reciprocating Shaker; Thermo Fisher Scientific, Waltham, MA, USA) at 37°C until an optical density ( $OD_{600}$ ) of 0.5 was reached (Microscan Turbidity Meter, Siemens, Oakville, ON, Canada). A 1 mL aliquot was centrifuged using an Eppendorf™ Centrifuge 5425 (ThermoFisher Scientific, Waltham, Massachusetts, USA) at 15,871 X g for 5 min, the supernatant was removed, and the cell pellet was resuspended in an equal volume of phosphate buffered saline (PBS; 1X, pH 7.4; ThermoFisher Scientific, Waltham, MA, USA). This “neat” suspension was then used to make ten-fold serial dilutions in PBS down to  $10^{-7}$  (**Figure 2.1**). A plate count was done in parallel with each dilution series to determine the colony forming units per milliliter (CFU/mL) in the cell suspensions. This involved spreading 100 µL of the  $10^{-6}$  and  $10^{-7}$  dilutions onto BAPs, incubating overnight (20 hours) at 37°C, then counting the colonies the following day. To calculate the CFU/mL of the  $10^{-6}$  and  $10^{-7}$  suspensions, the counted CFU/100 µL was multiplied by 10.



**Figure 2.1. Procedure used to prepare dilution series of live and heat-killed cells.**

Heat-killed (HK) cells were used to mimic naturally occurring membrane-compromised (i.e., dead) cells. HK suspensions were generated by boiling aliquots of the live dilution series in a water bath at 95°C for 5 min. The cells were cooled to room temperature before use in subsequent experiments. To verify the death of the cells, 100 µL of the neat HK suspension was spread onto BAP, incubated at 37°C overnight (20 hours), then observed to confirm the absence of growth.

### 2.2.2 DNA extraction

DNA was extracted from 100 µL cell suspension aliquots. First, each suspension was centrifuged for 5 min at 15,871 X g. Next, the supernatant was removed and the cell pellet was resuspended in an equal volume of an in-house rapid lysis buffer (100 mmol/L NaCl, 10 mmol/L Tris-HCl, pH 8.3, 1 mmol/L EDTA, pH 9.0, 1% Triton X-100). Lastly, this solution was boiled at 95°C for 15 min in a water bath.



## 2.2.3 Real-time PCR

### 2.2.3.1 Primers-probe sets and reaction conditions

Real-time PCR (RT-PCR) analysis utilized a set of multiplexed primers & probes (23) (Integrated DNA Technology, Skokie, IL, USA) to simultaneously detect *stx*<sub>1</sub> and *stx*<sub>2</sub> (**Table 2.1**). The probes used in this study were slightly modified from those originally published: the ZEN™ quencher (Integrated DNA Technologies, Coralville, Iowa, USA) was added to both probes and the *stx*<sub>2</sub> fluorescent reporter was been changed from Red640 to Yakima Yellow® (YAkYel; ELITech Group, Puteaux, France).

Each RT-PCR well contained 10 µL of 2X PrimeTime® Gene Expression Master Mix (Integrated DNA Technology, Coralville, Iowa, USA), 0.33 µM of each primer, 0.22 µM of each probe, 5 µL DNA extract and 2 µL molecular biology grade water in a total volume of 20 µL. An Applied Biosystems™ 7500 Fast Real-Time PCR instrument (Applied Biosystems, Life Technologies Corporation, Burlington, ON, Canada) was used to generate cycle threshold (Ct) values. The conditions were 95 °C for 20 seconds followed by 40 cycles of 95 °C for 3 seconds and 60 °C for 30 seconds. Each RT-PCR plate included a positive control (EDL 933 DNA extract) and a no template control (molecular biology grade water).

**Table 2.1. Primers and probes used for the multiplexed detection of *stx*<sub>1</sub> and *stx*<sub>2</sub> by real-time PCR.**

Target gene	Forward primer, reverse primer and probe sequences (5'–3')*	Location within sequence	Amplicon size (bp)	GenBank accession number
<i>stx</i> <sub>1</sub>	TTTGTYACTGT <u>S</u> ACAGCWGAAGCYTTACG	878–906	131	M16625
	CCCCAGTTCAR <u>W</u> GTRAG <u>R</u> TC <u>M</u> AC <u>R</u> TC	983–1008		
	56-FAM/CTGGATGAT/ZEN/CTCAGTGGGCGTTCTTATGTAA/3IABkFQ	941–971		
<i>stx</i> <sub>2</sub>	TTTGTYACTGT <u>S</u> ACAGC <u>W</u> GAAGCYTTACG	785–813	128	X07865
	CCCCAGTTCAR <u>W</u> GTRAG <u>R</u> TC <u>M</u> AC <u>R</u> TC	887–912		
	5YAkYeI/TCGTCAGGC/ZEN/ACTGTCTGAAACTGCTCC/3IABkFQ	838–864		

\* In the sequence: Y is (C, T), S is (C, G), W is (A, T), R is (A, G), M is (A, C).

### **2.2.3.2 Primer-probe sensitivity**

To determine the sensitivity of the primer-probe sets, a 1 in 10 dilution series was prepared in PBS ranging from neat to  $10^{-7}$  (as described in **2.2.1.2**). DNA was extracted from each dilution (as described in **2.2.2**) and analyzed by RT-PCR (as described in **2.2.3.1**). This experiment was performed independently three times. Each time, one fresh TSB culture was used to generate three dilution series (technical replicates). Standard curves were generated for *stx*<sub>1</sub> and *stx*<sub>2</sub> by plotting the Log CFU/mL values against the cycle threshold (Ct) values. The limit of detection (LOD) was established by identifying the lowest Log CFU/mL and corresponding Ct value that showed a detection frequency of  $\geq 95\%$ .

### **2.2.3.3 Primer-probe subtype coverage**

Previously frozen STEC DNA extracts of different *stx* subtypes were used to assess the primer-probe sets' subtype coverage. DNA from subtypes *1a*, *1c*, *1d*, and *2a - 2g* had previously been extracted and stored at  $-70^{\circ}\text{C}$  by the Chui research team (APL-ProvLab), whereas DNA from subtypes *2h*, *2i*, *2j*, and *2o* were received from Dr. Alexander Gill (Health Canada, Bureau of Microbial Hazards; Ottawa, ON, Canada). RT-PCR was performed on three independent occasions using each DNA extract (as described in **2.2.3.1**).

### **2.2.3.4 Primer-probe specificity**

A panel of 18 bacteria obtained from the quality control department of the Alberta Precision Laboratory, Public Health Laboratory, Edmonton, Alberta, Canada was used to determine the specificity of the primer-probe sets. It included: *Aeromonas hydrophila* (clinical isolate), *Salmonella* Enteritidis (clinical isolate), *Salmonella* Typhimurium (clinical isolate), *Shigella boydii*

(serotype 2; clinical isolate), *Shigella dysenteriae* (serotype 2; clinical isolate), *Shigella flexneri* (serotype 2; clinical isolate), *Shigella sonnei*, *Yersinia enterocolitica*, *Proteus mirabilis* (ATCC12453), *Citrobacter ferundii* (ATCC8090), *Klebsiella pneumoniae* (ATCC31488), *Enterobacter aerogenes* (ATCC13048), *Pseudomonas aeruginosa* (ATCC27853), *Enterobacter cloacae* (ATCC13047), *Staphylococcus aureus* (ATCC25923), *Staphylococcus aureus* (ATCC25913), *Bacillus cereus* (ATCC14579), and *Staphylococcus epidermidis* (ATCC12228). Each strain of bacteria was incubated overnight (20 hours) at 37°C on BAP from a frozen stock. A single colony from each plate was added to 100 µL of rapid lysis buffer and boiled for 15 min at 95°C. RT-PCR was performed on three independent occasions using each DNA extract (as described in 2.2.3.1).

## **2.2.4 PMAxx™ Optimization**

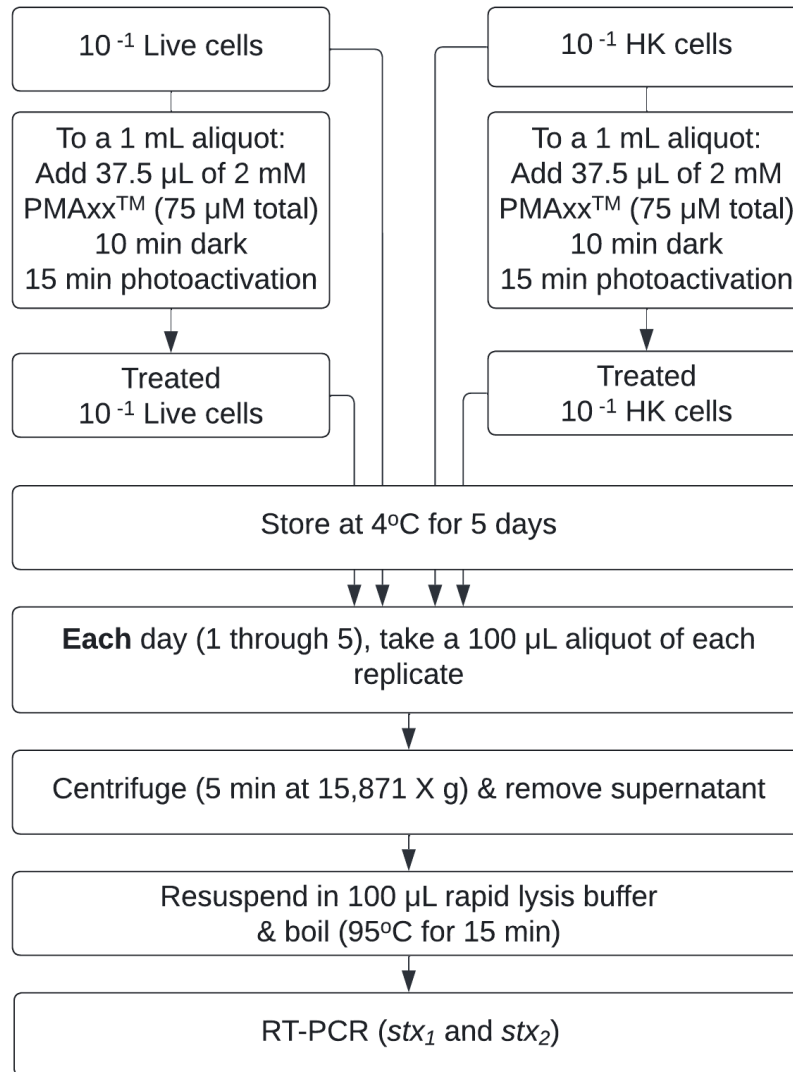
### **2.2.4.1 PMAxx™ stock solution and photolysis device**

PMAxx™ (Biotium, Fremont, California, USA) is commercially available in water at a concentration of 20 mM. To create a working stock solution, it was diluted 1 in 10 with UltraPure™ DNase/RNase-Free Distilled Water (Invitrogen™, Waltham, Massachusetts, USA) to a final concentration of 2 mM. This stock solution was stored in the dark at -20°C.

All experiments involving PMAxx™ were performed in dimly lit conditions. Photoactivation steps were conducted at room temperature in 1.5 mL Screw Cap Micro Tubes (Thermo Scientific™, Waltham, Massachusetts, USA) using a PMA-Lite™ LED Photolysis Device (Biotium, Fremont, California, USA). The device holds up to 18 microcentrifuge tubes at a time and each individual tube is exposed to an intense blue LED light (465 - 475 nm) which activates PMAxx™.

#### **2.2.4.2 Assessment of PMAxx™ binding irreversibility**

A time-course study was conducted to confirm that the effects of PMAxx™ treatment are immediate and irreversible (**Figure 2.2**). On day 1, live and HK  $10^{-1}$  cell suspensions were prepared (as described in **2.2.1.2**) and used to make 3 technical replicates (to be used in parallel). A 1 mL aliquot of each cell suspension was treated by adding 37.5  $\mu$ L of the 2 mM PMAxx™ solution (as prepared in **2.2.4.1**), giving a final concentration of 75  $\mu$ M. These samples were placed in the dark for 10 min at room temperature, and then were photoactivated for 15 min (as described in **2.2.4.1**). Immediately afterward, the treated and untreated samples were extracted and the first RT-PCR was performed. Following this, all of the samples were stored at 4°C in the dark for 4 subsequent days. On each day, a 100  $\mu$ L aliquot of each sample was extracted (as described in **2.2.2**) and analyzed by RT-PCR (as described in **2.2.3.1**). The mean Ct values of the 3 replicates were calculated for each condition (live untreated, live treated, HK untreated, and HK treated) on each day (1 - 5).



**Figure 2.2. Procedure used to determine whether PMAxx™ binds DNA irreversibly.**

### 2.2.4.3 Buffer suitability for PMAxx™ treatment

Live cells were diluted to  $10^{-1}$  (as described in 2.2.1.2) in either Tris (12 mM, pH 7.5) or PBS, and then 100 µL aliquots were treated with PMAxx™ at 50 µM (achieved by adding 2.5 µL of the 2 mM dye prepared in 2.2.4.1) or 100 µM (achieved by adding 5 µL of 2 mM dye). Once the dye was added, samples were placed in the dark at room temperature for 10 min and then were subjected to a 15 min photoactivation. Afterward, the samples were serially diluted (as in 2.2.1.2) in the same buffer to  $10^{-6}$  and  $10^{-7}$ , then 100 µL of each was spread onto BAP. The

plates were incubated overnight (20 hours) at 37°C and the colonies were counted the following day. The CFU/mL was calculated as described in **2.2.1.2**. This procedure was performed independently three times, and untreated cell suspensions in both buffers were plated in parallel each time.

#### **2.2.4.4 Photoactivation time and PMAxx™ Concentration**

DNA extract (100 ng/μL) from a clinical O157 STEC strain (positive for *stx*<sub>1</sub> and *stx*<sub>2</sub>) from the Chui Laboratory collection was used to assess the ideal PMAxx™ concentration and photoactivation time. The concentrations tested were 50 μM, 75 μM, and 100 μM. Respectively, this involved adding 2.5 μL, 3.75 μL, or 5 μL of 2 mM PMAxx™ (as prepared in **2.2.4.1**) to 100 μL aliquots of DNA extract. A control without PMAxx™ was also run in parallel. All conditions were placed in the dark for 10 min at room temperature then were subjected to a 15 or 30 min photoactivation. Afterward, RT-PCR was performed (as described in **2.2.3.1**) on the treated and untreated DNA. This procedure was conducted independently three times.

Next, a dilution series of HK cells ranging from neat to 10<sup>-7</sup> (prepared as described in **2.2.1.2**) was used to test the effectiveness of different PMAxx™ concentrations. Untreated controls were compared to those treated with concentrations of 50 μM, 75 μM, and 100 μM PMAxx™ as above. All treatments involved placing the samples in the dark for 10 min at room temperature and then conducting a 15 min photoactivation. Afterward samples were extracted (as described in **2.2.2**) and analyzed by RT-PCR (as described in **2.2.3.1**). This procedure was conducted independently three times.

#### **2.2.4.5 Effect of DMSO on viability RT-PCR and cell viability**

To make a stock solution of 2 mM PMAxx™ with 20% dimethyl sulfoxide (DMSO), 20 µL of 20 mM PMAxx™ was combined with 40 µL DMSO (ThermoFisher Scientific, Waltham, Massachusetts, USA) and 140 µL UltraPure™ DNase/RNase-Free Distilled Water (Invitrogen™, Waltham, Massachusetts, USA). This stock solution was stored in the dark at -20°C. A 10-fold dilution series of HK cells in PBS (neat to 10<sup>-7</sup>; prepared as described in **2.2.1.2**) was treated with 100 µM PMAxx™ and 1% DMSO by adding 5 µL of this stock solution to 100 µL aliquots. Samples were then placed in the dark at room temperature for 10 min, then a 15 min photoactivation was conducted. To control for the possibility that DMSO alone may impact Ct values, a condition was included where a final concentration of 1% DMSO was added to an aliquot of each HK cell dilution. All samples were extracted (as described in **2.2.2**) and analyzed by RT-PCR (as described in **2.2.3.1**).

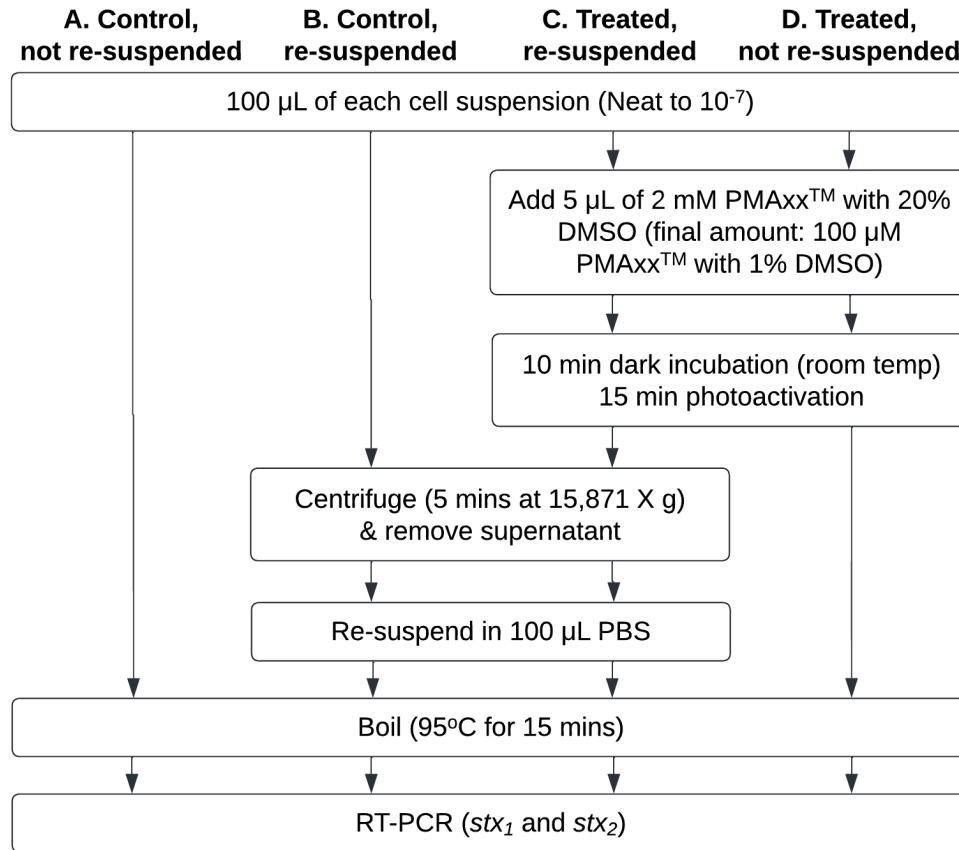
Additionally, live cell suspensions in PBS (neat, 10<sup>-3</sup>, and 10<sup>-5</sup>; prepared as in **2.2.1.2**) were treated with 100 µM PMAxx™ with and without 1% DMSO as above. Again, a condition was included where a final concentration of 1% DMSO was added to an aliquot of each cell suspension. Afterward, the suspensions were serially diluted to 10<sup>-6</sup> and 10<sup>-7</sup>, and a 100 µL aliquot of each was plated for overnight growth (20 hours at 37°C) on BAP. The cells were counted the next day to determine whether treatment caused any cell death. The CFU/mL was calculated as described in **2.2.1.2**.

Both the HK and live cell procedures were performed independently three times.



#### **2.2.4.6 PMAxx™ residual activity and resuspension of live cells**

To determine whether PMAxx™ loses the ability to bind DNA immediately following photoactivation or remains in its active form long enough to bind the DNA of live cells during DNA extraction, a dilution series (neat to  $10^{-7}$ ; prepared as described in **2.2.1.2**) of live cells was prepared. Two sets of 100  $\mu$ L aliquots were treated with 5  $\mu$ L of the stock solution prepared in **2.2.4.5** (2 mM PMAxx™ with 20% DMSO, giving a final concentration of 100  $\mu$ M PMAxx™ and 1% DMSO). This involved being placed in the dark for 10 mins and then undergoing a 15 min photoactivation. After treatment, one cell suspension series was kept in the supernatant from the treatment and boiled for 15 min at 95°C to release the DNA. The second set was centrifuged for 5 min at 15,871 X g, the supernatants were removed, then the pellets were resuspended in 100  $\mu$ L of fresh PBS before being boiled. A control with no PMAxx™ treatment was run in parallel for both conditions (remaining in the original supernatant and resuspension in fresh PBS), as described in **Figure 2.3**. The samples were then analyzed by RT-PCR (as described in **2.2.3.1**). This procedure was conducted independently three times.

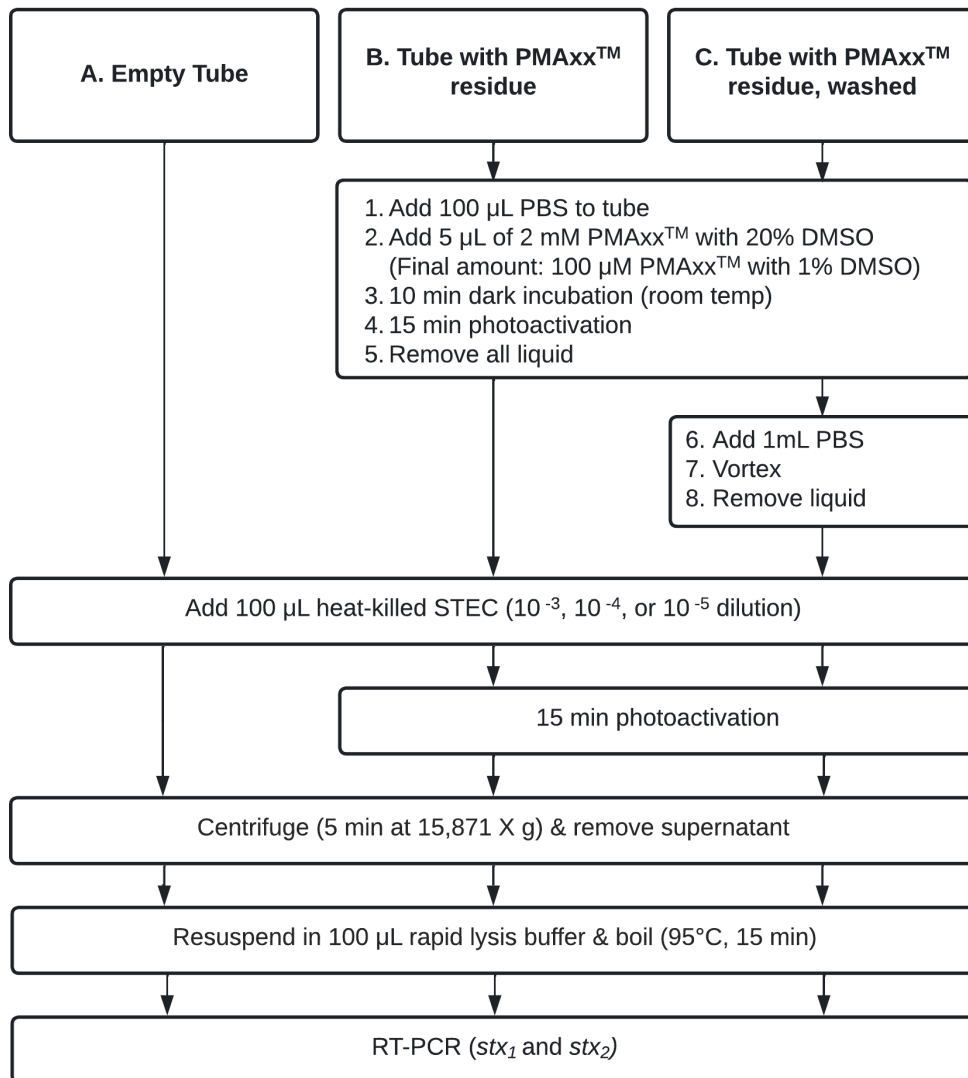


**Figure 2.3. Procedure used to determine whether PMAxx™ remains active following photoactivation.** Live cell suspensions ranging from neat to  $10^{-7}$  were used for each condition.

#### 2.2.4.7 PMAxx™ interactions with microcentrifuge tubes

The procedure in **Figure 2.4** was used to assess whether PMAxx™ is capable of adhering to the interior of microcentrifuge tubes and subsequently binding DNA. This involved adding 5 µL of the stock solution prepared in **2.2.4.5** (2 mM PMAxx™ with 20% DMSO, giving a final concentration of 100 µM PMAxx™ and 1% DMSO) to 100 µL PBS in micro tubes and simulating a treatment (10 min in the dark at room temperature followed by a 15 min photoactivation). Immediately following the photoactivation step, the liquid was removed. This procedure was repeated on a second set of tubes, but with the addition of the following wash step: 1 mL of PBS was added, the tube was vigorously mixed for 30 seconds to “wash” the tube’s interior, and then

the liquid was removed. To both the unwashed and washed tubes, 100  $\mu\text{L}$  aliquots of HK cells ( $10^{-3}$ ,  $10^{-4}$ , and  $10^{-5}$ ; prepared as described in 2.2.1.2) were added before undergoing a 15 min photoactivation. Aliquots (100  $\mu\text{L}$ ) of all three HK suspensions were also added to a third set of untreated tubes (that had no PMAxx<sup>TM</sup> exposure) as a control. Samples in all 3 conditions had their DNA extracted (as in 2.2.2) and were analyzed by RT-PCR (as in 2.2.3.1). This procedure was conducted independently three times.



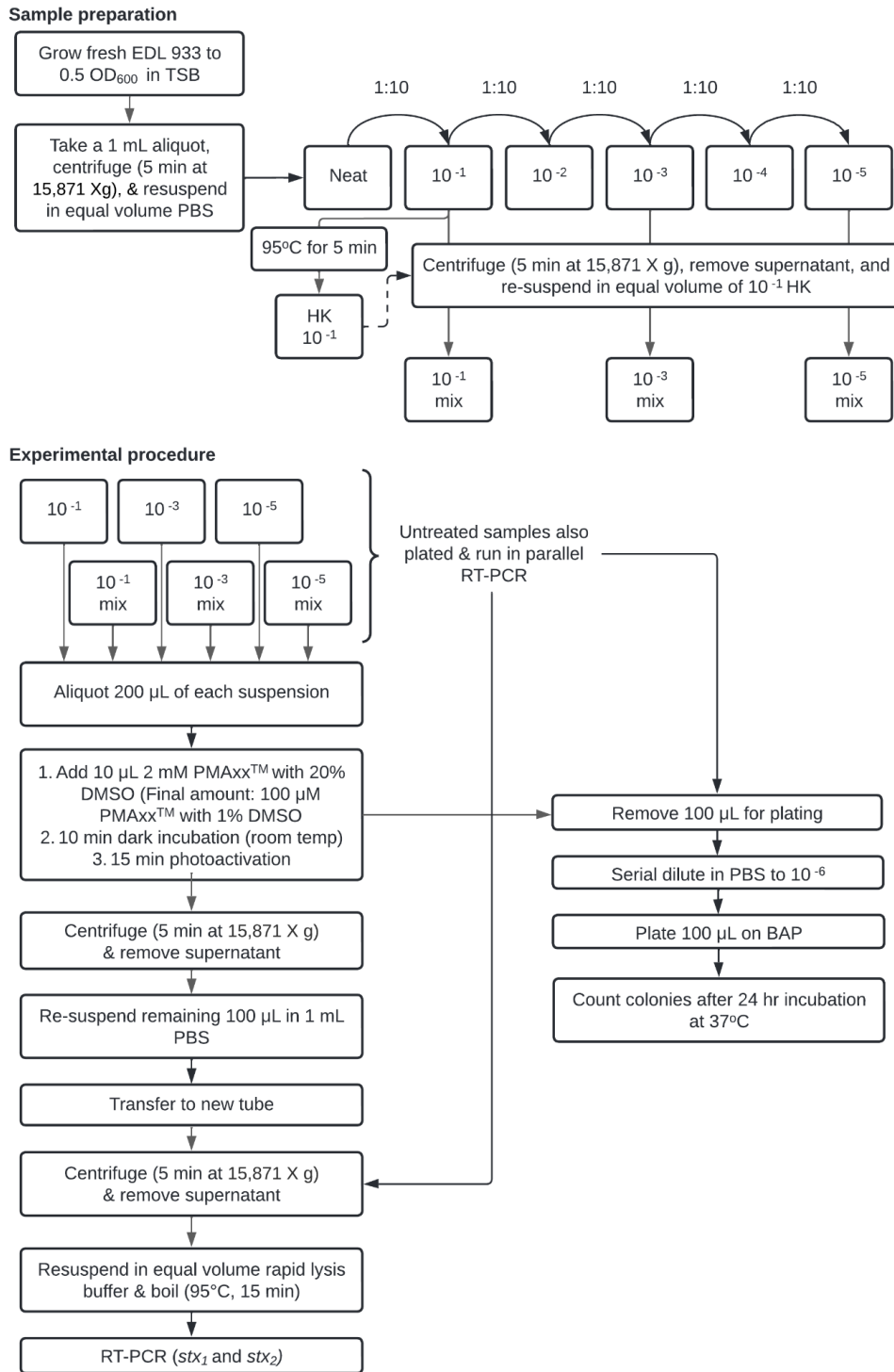
**Figure 2.4. Procedure used to determine whether PMAxx<sup>TM</sup> interacts with microcentrifuge tubes.**

#### **2.2.4.8 PMAxx™ pre-photoactivation**

A dilution series (neat to  $10^{-7}$ ; prepared as described in **2.2.1.2**) of HK cells was used to determine whether PMAxx™ could be photoactivated before being added to samples. The cell suspensions were treated with 100  $\mu$ M PMAxx™ and 1% DMSO, then photoactivation was either conducted as above (where the dye is activated in the presence of the cell suspension) or by photoactivating the dye before adding it to the sample (“pre-photoactivation”). The latter was conducted by first adding PMAxx™ to the tube, performing a 15 min photoactivation, adding the sample, mixing vigorously, then placing the tube in the dark at room temperature for 10 min. DNA was then extracted from the samples (as described in **2.2.2**) and examined by RT-PCR (as described in **2.2.3.1**). This procedure was conducted independently three times, and an untreated series was run in parallel each time.

#### **2.2.5 Final viability RT-PCR protocol for pure culture**

After the initial investigations above, a final protocol was established and tested using live and mixed (live and HK) cell suspensions (**Figure 2.5**). Live cell suspensions of  $10^{-1}$ ,  $10^{-3}$  and  $10^{-5}$  were prepared, and HK cells were generated by boiling a 1 mL aliquot of the  $10^{-1}$  suspension (as described in **2.2.1.2**). To combine the live and HK cells, an aliquot of each of the three live dilutions was centrifuged (5 min at 15,871 X g), the supernatant was removed, and then the cell pellet was resuspended in an equal volume of the heat-killed suspension. The final ratios of HK to live cells were respectively 1:1, 100:1 and 10,000:1 for the  $10^{-1}$  mix,  $10^{-3}$  mix, and  $10^{-5}$  mix. Logarithmic ratios were chosen so a Ct value difference could be discerned more easily.



**Figure 2.5. Procedure used to test the final viability RT-PCR protocol for STEC cell suspensions.**

Samples were treated with 100  $\mu$ M PMAxx™ and 1% DMSO. To achieve this, 10  $\mu$ L of the 2mM PMAxx™ stock solution with 20% DMSO (prepared in **2.2.4.5**) was added to 200  $\mu$ L of each cell suspension. Samples were briefly mixed, kept in the dark for 10 min at room temperature, and then subjected to a 15 min photoactivation. Afterward, 100  $\mu$ L was removed for plating and the remaining 100  $\mu$ L was centrifuged (5 min at 15,871 X g), the supernatant was removed, the cell pellet was resuspended in 1 mL of PBS, and then the solution was transferred to a new tube. Next, the suspensions were centrifuged (5 min at 15,871 X g), the supernatants were removed, then DNA was extracted (as described in **2.2.2**) and analyzed by RT-PCR (**2.2.3.1**).

Aliquots of the cell suspensions were taken immediately before and after PMAxx™ treatment. They were serially diluted to  $10^{-6}$  and then 100  $\mu$ L was spread on a BAP. The plates were incubated for 20 hours at 37°C, the colonies were counted, then the CFU/mL was calculated (as described in **2.2.1.2**).

This entire procedure was conducted independently three times, and untreated samples were run in parallel each time.

## **2.2.6 Statistical analyses**

Experiments were conducted independently three times. All numerical data is expressed as mean  $\pm$  standard deviation. The graphs in section **2.3.1.1** were generated using Google Sheets (Google LLC, Mountain View, CA, USA).

Statistical analysis was conducted on the final RT-PCR protocol results (section **2.3.9**) using ANOVA with post-hoc Tukey HSD. The alpha-level was set to 0.05 for all statistical tests, and all analyses were performed using R Statistical Software (v4.1.2; R Core Team 2021).

## 2.3 Results

### 2.3.1 Primer performance

#### 2.3.1.1 Sensitivity

Eight replicates were used for sensitivity calculations; one replicate was excluded because its Ct values were consistently higher than the others. The limit of detection for the *stx*<sub>1</sub> and *stx*<sub>2</sub> primer sets was 10<sup>3</sup> CFU/mL (**Table 2.2**). The Ct values associated with this concentration were just below 32, so this was established as a cut off in subsequent experiments. For both targets, the relationship between Log CFU/mL and Ct value can be described by the equation: *stx* Ct value = -3.32(log CFU/mL) + 41.2 (**Figures 2.6A** and **2.6B**).

**Table 2.2. Performance of the multiplexed RT-PCR *stx*<sub>1</sub> and *stx*<sub>2</sub> primer sets.**

Live cells (Log CFU/mL)	<i>stx</i> <sub>1</sub>		<i>stx</i> <sub>2</sub>	
	Ct value (Mean ± SD)	Detection frequency	Ct value (Mean ± SD)	Detection frequency
9.0	10.6 ± 1.1	100.0%	11.9 ± 0.4	100.0%
8.0	14.7 ± 0.4	100.0%	15.0 ± 0.3	100.0%
7.0	17.6 ± 0.7	100.0%	18.3 ± 0.3	100.0%
6.0	21.2 ± 0.8	100.0%	21.8 ± 0.5	100.0%
5.0	25.1 ± 0.5	100.0%	25.4 ± 0.4	100.0%
4.0	27.9 ± 0.9	100.0%	28.7 ± 0.4	100.0%
3.0	31.7 ± 0.8	100.0%	31.9 ± 0.7	100.0%
2.0	33.5 ± 1.2*	62.5%	34.8 ± 1.2*	87.5%
1.0	34.8 ± 1.0*	25.0%	36.4 ± 1.7*	25.0%

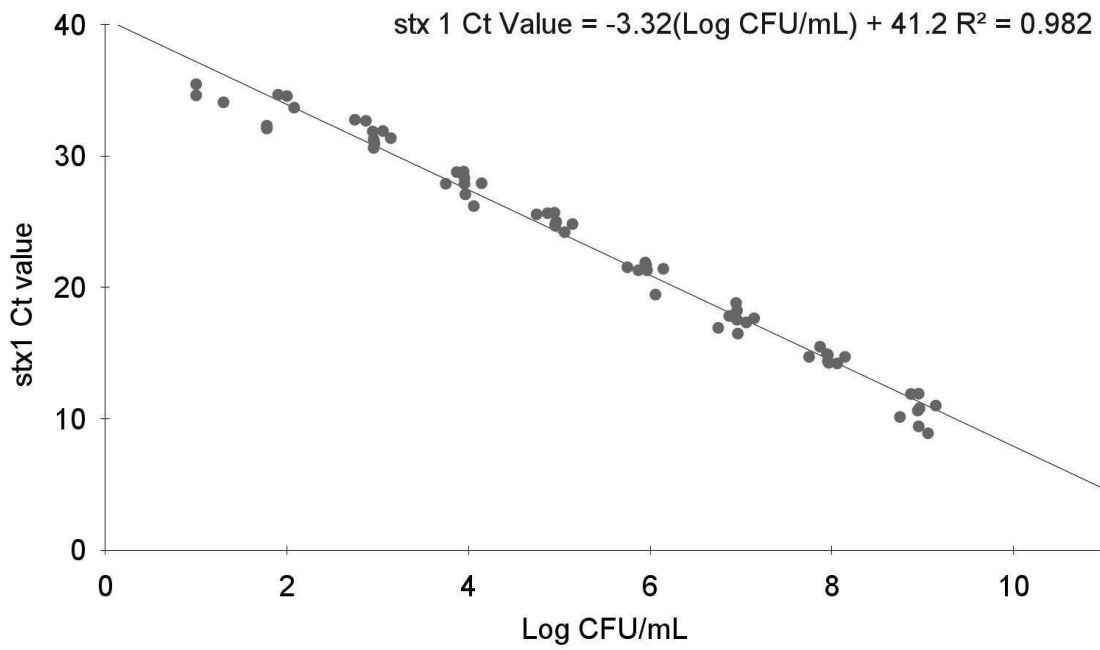
Ct values represent 8 replicates (3 independent experiments with 3 technical replicates each; one technical replicate was eliminated because it was consistently high)

Detection frequency: (8 – number of replicates with undetermined Ct values) / 8

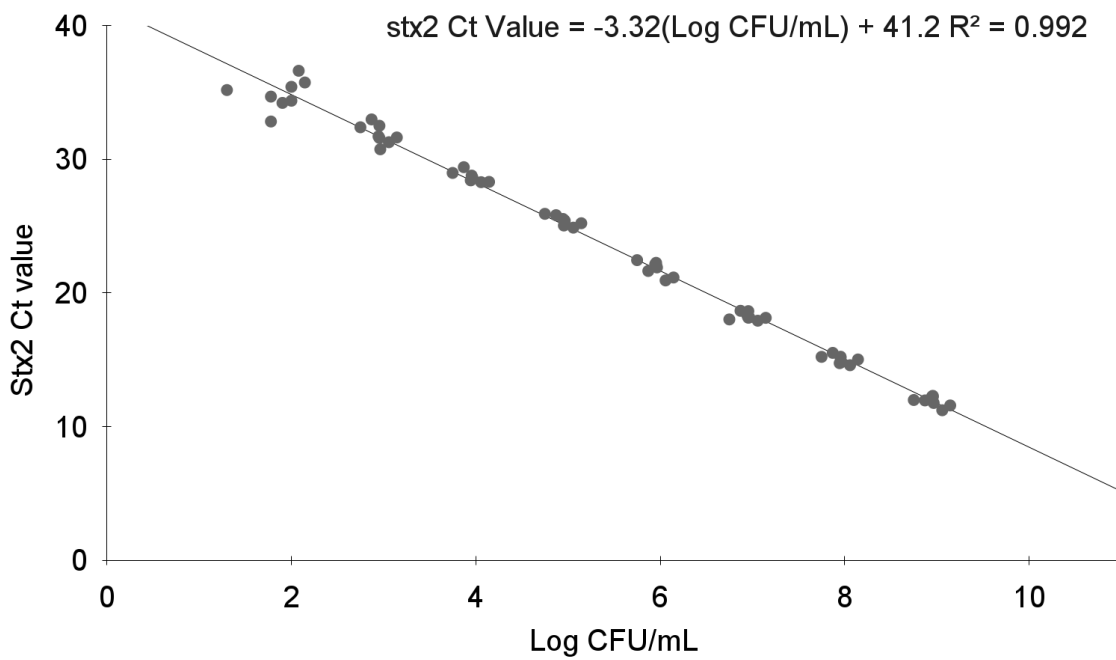
\*Undetermined Ct values were excluded from mean Ct value calculations

The dashed line indicates the limit of detection (≥ 95% detection frequency)

**A. *stx*<sub>1</sub>**



**B. *stx*<sub>2</sub>**



**Figure 2.6. Standard curve relating Log CFU/mL to *stx*<sub>1</sub> (A) and *stx*<sub>2</sub> (B) cycle threshold value.**



### 2.3.1.2 Subtype coverage

All of the *stx* subtypes (*1a*, *1c*, *1d*, and *2a* - *2e*, *2g* - *2j*, *2o*) except for *2f* were detected by the multiplexed primer sets (**Tables 2.3A** and **2.3B**).

**Table 2.3A. Subtypes amplified by the *stx*<sub>1</sub> primer set.**

<i>stx</i> <sub>1</sub> Subtype	Reference strain (GenBank Accession Number)	Amplified by <i>stx</i> <sub>1</sub> primer / probe set?
<i>1a</i>	M19473	Yes
<i>1c</i>	Z36901	Yes
<i>1d</i>	AY170851	Yes

**Table 2.3B. Subtypes amplified by the *stx*<sub>2</sub> primer set.**

<i>stx</i> <sub>2</sub> Subtype	Reference strain (GenBank Accession Number)	Amplified by <i>stx</i> <sub>2</sub> primer / probe set?
<i>2a</i>	Z37725	Yes
<i>2b</i>	AF043627	Yes
<i>2c</i>	L11079	Yes
<i>2d</i>	DQ059012	Yes
<i>2e</i>	M21534	Yes
<i>2f</i>	AJ010730	No
<i>2g</i>	AY286000	Yes
<i>2h</i>	CP076706	Yes
<i>2i</i>	OLC-1685	Yes
<i>2j</i>	CP076709	Yes
<i>2o</i>	CP076714	Yes

### 2.3.1.3 Specificity

No cross-reactivity was observed with the panel of bacteria tested.

### 2.3.2 PMAxx™ irreversibility

A time course (described in **Figure 2.2**) using live and HK cells (both  $10^7$  CFU/mL) assessed whether PMAxx™ would slowly penetrate live cells (resulting in an increased Ct value by RT-PCR) or detach from HK cell DNA (resulting in a decreased Ct value). The samples were stored in the dark at 4°C in their original supernatant (the “treated” sets contained PMAxx™, whereas the “untreated” sets did not) and an aliquot was extracted each day for 5 consecutive days. Three technical replicates were used for each condition. The mean Ct value across the 5 days was similar between the untreated live cells (5 day mean =  $17.1 \pm 2.5$ ) and treated live cells (5 day mean =  $17.9 \pm 2.5$ ), and differed minimally across the timepoints. Throughout the 5 days, the treated HK cell Ct value remained consistently higher (5 day mean =  $22.7 \pm 2.2$ ) than the HK that were untreated (5 day mean =  $17.4 \pm 1.5$ ).

### 2.3.3 Buffer suitability for PMAxx™ treatment

The effect of PMAxx™ treatment on live cell survival in Tris buffer versus PBS was compared to determine which buffer was ideal for subsequent experiments. The untreated live cell suspensions ( $10^7$  CFU/mL) in both Tris and PBS produced the  $10^2$  colonies expected for the dilution plated (**Table 2.4**). In PBS, treatment with 50  $\mu$ M and 100  $\mu$ M PMAxx™ did not reduce the mean colony count below this expected value. However, in the Tris buffer there was a 1-Log decrease in CFU with PMAxx™ treatment. This effect was especially pronounced in the 100  $\mu$ M condition.

**Table 2.4. Colony forming units counted after PMAxx™ treatment in different buffers.**

PMAxx™ concentration	Colony Forming Units (CFU, mean ± SD)	
	Tris Buffer	Phosphate-Buffered Saline
-	122 ± 32	147 ± 36
50 µM	34 ± 12	133 ± 37
100 µM	10 ± 8	109 ± 39

CFU represent 3 independent replicates

Live cells were treated with PMAxx™ at 10<sup>7</sup> CFU/mL, serially diluted to 10<sup>3</sup> CFU/mL, then 100 µL was grown on BAP overnight

### 2.3.4 Photoactivation time and PMAxx™ Concentration

In the preliminary inquiry, where PMAxx™ was applied to pure DNA (**Table 2.5**), increasing the concentration of PMAxx™ was overall associated with increased Ct values. When either photoactivation period was used with 100 µM, the Ct values crossed the 32-Ct cutoff established in **2.3.1.1**. Increasing the photoactivation time from 15 to 30 min did not have an appreciable effect. An increased Ct value (+13.5) was observed at 100 µM even when no photoactivation was conducted (i.e., when tubes were only briefly exposed to ambient light).

**Table 2.5. Effect of PMAxx™ concentration and photoactivation time on the mean *stx*<sub>1</sub> cycle threshold values associated with an extract of 1 ng/µL STEC DNA.**

Photoactivation time	PMAxx™ concentration (Mean <i>stx</i> <sub>1</sub> Ct value ± SD)			
	0 µM	50 µM	75 µM	100 µM
-	17.8 ± 0.2	18.4 ± 0.1	20.4 ± 1.2	31.3 ± 1.1
15 min	17.8 ± 0.1	21.6 ± 0.6	31.5 ± 0.8	-
30 min	18.2 ± 0.2	22.6 ± 0.5	27.2 ± 1.3	-

Average Ct values represent 3 independent replicates

Ct values above the 32 Ct cutoff are denoted “-”

When applied to heat-killed cells using a 15 min photoactivation (**Table 2.6**), the Ct values across all three PMAxx™ concentrations (50, 75, and 100 µM) increased by more than 10. As seen with the DNA above, higher PMAxx™ concentrations produced more drastic results. The 100 µM PMAxx™ treatment eliminated the detection of the highest concentration of HK cells tested (10<sup>8</sup> CFU/mL).

**Table 2.6. The effect of increasing PMAxx™ concentrations on the cycle threshold values of heat-killed cells.**

HK cells (Log CFU/mL)	PMAxx™ treatment (Mean <i>stx</i> <sub>1</sub> Ct value ± SD)			
	No treatment	50 µM	75 µM	100 µM
8	12.9 ± 0.5	28.3 ± 0.7	29.5 ± 4.8	–
7	16.5 ± 0.2	29.9 ± 0.9	–	–
6	19.8 ± 0.4	30.5 ± 0.7	–	–
5	23.5 ± 0.1	–	–	–
4	26.7 ± 0.1	–	–	–
3	29.5 ± 0.4	–	–	–

*stx*<sub>1</sub> Ct values represent 3 independent replicates

Values above the 32 Ct cutoff are denoted “–”

See **Table A.1** in **Appendix A** for raw values and ΔCt calculations

When the concentration optimization was conducted above, it was also assessed whether the fluorescent properties of PMAxx™ caused any interference with the RT-PCR process. When the raw data plot (i.e., which shows the amount of fluorescence detected by each filter in a given cycle) generated by the Applied Biosystems™ 7500 Fast Real-Time PCR instrument was observed (**Figure A.1** in **Appendix A**), the range of fluorescence was similar for untreated cell suspensions and those which had previously been treated with 100 µM PMAxx™. This overlap suggests that the fluorescence detected by Filter 4 (~610 nm) was only attributable to the

passive reference dye (ROX™) found in all of the wells (**Figure A.2** in **Appendix A**), while the impact of PMAxx™ fluorescence was negligible.

### 2.3.5 PMAxx™ and 1% DMSO

The addition of DMSO (20% in the 2 mM stock solution; 1% in the final volume) to 100 μM PMAxx™ enhanced performance (**Table 2.7**). While 100 μM PMAxx™ alone completely removed the detection of up to 10<sup>8</sup> CFU/mL HK cells, the combination of 100 μM PMAxx™ with 1% DMSO was able to eliminate 10<sup>9</sup> CFU/mL HK cells. When 1% DMSO alone was added, only negligible differences in Ct values (-0.2 to + 0.6) were observed (**Table A.2** in **Appendix A**).

**Table 2.7. Cycle threshold values of heat-killed cells treated with 1% DMSO, 100 μM PMAxx™, or 100 μM PMAxx™ + 1% DMSO.**

HK cells (Log CFU/mL)	Experimental condition (Mean <i>stx</i> <sub>1</sub> Ct value ± SD)			
	No treatment	1% DMSO	100 μM PMAxx™	100 μM PMAxx™ + 1% DMSO
9	12.6 ± 0.2	12.4 ± 0.1	31.3 ± 2.8	–
8	16.9 ± 0.1	17.5 ± 0.3	–	–
7	20.8 ± 0.1	21.2 ± 0.1	–	–

*stx*<sub>1</sub> Ct values represent 3 independent replicates

Values above the 32 Ct cutoff are denoted “–”

See **Table A.2** in **Appendix A** for raw values and ΔCt calculations

Live cells at 10<sup>8</sup>, 10<sup>5</sup>, and 10<sup>3</sup> CFU/mL were treated with 100 μM PMAxx™ alone, 100 μM PMAxx™ and 1% DMSO, or with 1% DMSO alone. The colony counts of all three treatment conditions (**Table 2.8**) are comparable (i.e., within 1-Log) to the counts of the live cells that did not receive any treatment.

**Table 2.8. Effect of treatment with 100  $\mu$ M PMAxx<sup>TM</sup>, 100  $\mu$ M PMAxx<sup>TM</sup> + 1% DMSO, or 1% DMSO on live cell survival.**

Live cells (Log CFU/mL)	DMSO	Experimental condition (Mean Log CFU/mL $\pm$ SD)	
		No treatment	100 $\mu$ M PMAxx <sup>TM</sup>
8	-	7.9 $\pm$ 0.1	7.8 $\pm$ 0.1
	1%	7.9 $\pm$ 0.1	7.8 $\pm$ 0.2
5	-	4.8 $\pm$ 0.2	4.7 $\pm$ 0.3
	1%	4.6 $\pm$ 0.2	4.7 $\pm$ 0.2
3	-	2.8 $\pm$ 0.2	2.6 $\pm$ 0.3
	1%	2.8 $\pm$ 0.2	2.6 $\pm$ 0.4

Log CFU/mL values represent 3 independent replicates

### 2.3.6 Effects of resuspension on live cells

An experiment was conducted to determine whether PMAxx<sup>TM</sup> remains active following photoactivation. Live cells boiled in PBS containing previously photoactivated 100  $\mu$ M PMAxx<sup>TM</sup> and 1% DMSO showed a complete loss of amplification (**Table 2.9**). When treated live cells were instead resuspended in fresh buffer (by centrifuging, removing the supernatant, and then adding PBS) this loss of amplification did not occur. The resuspension process did not affect detection ( $\pm$  1 Ct value).

**Table 2.9. Effect of resuspending live cells versus remaining in the original supernatant (with or without PMAxx™) during boiling.**

Live Cells (Log CFU/mL)	Treatment before boiling (Mean <i>stx</i> <sub>1</sub> Ct value ± SD)			
	No treatment		100 µM PMAxx™ + 1% DMSO	
	Original	Resuspended	Original	Resuspended
8	13.7 ± 0.6	14.7 ± 0.6	–	15.4 ± 1.1
7	18.8 ± 0.9	18.8 ± 0.5	–	19.5 ± 0.8
6	22.2 ± 0.8	20.7 ± 0.7	–	23.5 ± 1.6
5	26.1 ± 1.1	24.3 ± 0.9	–	26.8 ± 1.4
4	28.1 ± 0.9	27.6 ± 0.9	–	30.1 ± 1.8
3	31.4 ± 1.2	30.1 ± 0.6	–	–

*stx*<sub>1</sub> Ct values represent 3 independent replicates

Original = boiled in original supernatant immediately after photoactivation

Resuspended = pelleted, supernatant removed, cells resuspended in fresh PBS, then boiled

Values above the 32 Ct cutoff are denoted “–”

See **Table A.3** in **Appendix A** for raw values and ΔCt calculations

### 2.3.7 PMAxx™ interactions with microcentrifuge tubes

To determine whether PMAxx™ can adhere to the interior of polypropylene microcentrifuge tubes and subsequently bind free DNA, HK cells ( $10^5$ ,  $10^4$ , and  $10^5$  CFU/mL) were added to tubes that had previously been exposed to 100 µM of PMAxx™ and 1% DMSO (as described in **Figure 2.4**). Compared to the cells in the control tubes, the mean Ct values increased slightly (2.3 - 5.5) for HK cells in the exposed tubes regardless of whether they had been washed with 1 mL of PBS after PMAxx™ exposure (**Table 2.10**). Based on the standard curve from **2.3.1.1**, the PMAxx™ residue in these tubes caused the equivalent of a 1 - 2 Log CFU/mL reduction.

**Table 2.10. Effect of 100  $\mu\text{M}$  PMAxx<sup>TM</sup> + 1% DMSO residue in microcentrifuge tubes on the cycle threshold value of heat-killed cells.**

HK cells added (Log CFU/mL)	Microcentrifuge tube condition (Mean $stx_1$ Ct value $\pm$ SD)		
	Exposure to 100 $\mu\text{M}$ PMAxx <sup>TM</sup> + 1% DMSO		
	No exposure	No wash	Wash
5	24.5 $\pm$ 0.5	26.9 $\pm$ 1.5	28.5 $\pm$ 1.0
4	28.9 $\pm$ 0.6	–	–
3	31.6 $\pm$ 0.7	–	–

The  $stx_1$  Ct values represent 3 independent replicates

Exposure = PMAxx<sup>TM</sup> treatment simulated in PBS, supernatant removed, then HK cells added

Wash = 1 mL wash with PBS introduced between supernatant removal and HK cell addition

See **Table A.4** in **Appendix A** for raw values and  $\Delta\text{Ct}$  calculations

### 2.3.8 PMAxx<sup>TM</sup> Pre-photoactivation

A serial dilution of HK cells was used to assess whether PMAxx<sup>TM</sup> could be pre-photoactivated before being added to samples. Pre-photoactivation using 100  $\mu\text{M}$  of PMAxx<sup>TM</sup> and 1% DMSO resulted in minor Ct value increases (1.8 to 6.2) when compared to untreated HK cells (**Table 2.11**). This performance was more pronounced with decreasing cell concentrations, but was overall poor compared to standard photoactivation.



**Table 2.11. Effect of “pre-photoactivation” compared to standard photoactivation on the cycle threshold value of heat-killed cells treated with 100 µM PMAxx™ + 1% DMSO.**

HK cells (Log CFU/mL)	Experimental condition (Mean <i>stx</i> <sub>1</sub> Ct value ± SD)		
	100 µM PMAxx™ + 1% DMSO		
	No treatment	Standard photoactivation	Pre-photoactivation
8	12.8 ± 0.3	–	14.6 ± 0.5
7	15.9 ± 0.6	–	18.4 ± 0.4
6	19.5 ± 0.5	–	22.7 ± 0.2
5	23.3 ± 0.1	–	29.5 ± 0.5
4	27.0 ± 0.3	–	–
3	30.8 ± 0.5	–	–

*stx*<sub>1</sub> Ct values represent 3 independent replicates

Standard photoactivation: dye photoactivated after being added to cells

Pre-photoactivation: dye photoactivated prior to being added to cells

### 2.3.9 Final viability RT-PCR protocol performance

The Ct values generated when the final viability RT-PCR protocol was applied to mixes of live and heat-killed cell suspensions are summarized in **Tables 2.12A** and **2.12B**. For the 10<sup>8</sup> CFU/mL live cell suspensions, the Ct values of all conditions ([1] no treatment, [2] treatment, [3] no treatment + HK, and [4] treatment + HK) were statistically the same. For both the 10<sup>6</sup> CFU/mL and 10<sup>4</sup> CFU/mL live cell suspensions, the no treatment + HK condition was significantly lower ( $p < 0.05$ ) than the other Ct values. Notably, 100 µM PMAxx™ and 1% DMSO treatment increased the 10<sup>4</sup> CFU/mL live cell mean Ct value above the 32 Ct cutoff established in **2.3.1.1**. Although this increase was not statistically significant, two of the individual replicates in this condition would have been considered negative (*stx*<sub>1</sub> Ct values of 36.3 and 32.5) while only one would be considered positive (29.4).

**Table 2.12A. Impact of 100  $\mu$ M PMAxx™ + 1% DMSO treatment on the *stx*<sub>1</sub> cycle threshold values of live and mixed cell suspensions.**

Live cells (Log CFU/mL)	HK cells (8 Log CFU/mL)	Experimental condition (Mean <i>stx</i> <sub>1</sub> Ct value $\pm$ SD)	
		No treatment	100 $\mu$ M PMAxx™ + 1% DMSO
8	–	16.6 $\pm$ 0.6	17.5 $\pm$ 1.3
	+	16.5 $\pm$ 0.6	16.6 $\pm$ 1.7
6	–	23.1 $\pm$ 0.5	25.2 $\pm$ 2.5
	+	17.6 $\pm$ 0.9*	24.7 $\pm$ 2.5
4	–	30.0 $\pm$ 0.8	32.7 $\pm$ 3.5
	+	17.2 $\pm$ 1.5*	30.2 $\pm$ 2.3

*stx*<sub>1</sub> Ct values represent 3 independent replicates

HK: heat-killed

ANOVA analysis was conducted for each live cell concentration (delineated by horizontal lines)

\*indicates Ct values that were statistically different ( $p < 0.05$ ) from all others of the same live cell concentration

**Table 2.12B. Impact of 100  $\mu$ M PMAxx™ + 1% DMSO treatment on the *stx*<sub>2</sub> cycle threshold values of live and mixed cell suspensions.**

Live cells (Log CFU/mL)	HK cells (8 Log CFU/mL)	Experimental condition (Mean <i>stx</i> <sub>2</sub> Ct value $\pm$ SD)	
		No treatment	100 $\mu$ M PMAxx™ + 1% DMSO
8	–	14.8 $\pm$ 1.1	16.3 $\pm$ 0.9
	+	14.7 $\pm$ 1.3	15.3 $\pm$ 0.7
6	–	21.2 $\pm$ 0.6	23.7 $\pm$ 1.2
	+	15.9 $\pm$ 0.6*	23.0 $\pm$ 0.5
4	–	27.9 $\pm$ 0.6	32.1 $\pm$ 2.8
	+	16.2 $\pm$ 0.9*	28.8 $\pm$ 3.4

*stx*<sub>2</sub> Ct values represent 3 independent replicates

HK: heat-killed

ANOVA analysis was conducted for each live cell concentration (delineated by horizontal lines)

\*indicates Ct values that were statistically different ( $p < 0.05$ ) from all others of the same live cell concentration

The  $stx_1$  Ct values from **Table 2.12A** were converted to CFU/mL estimates in **Table 2.13A** using the line equation from **2.3.1.1**. For the  $10^8$  CFU/mL live cell suspensions, the Log CFU/mL estimates by both Ct and plate count were statistically the same for all conditions ([1] no treatment, [2] treatment, [3] no treatment + HK, and [4] treatment + HK). For the  $10^6$  CFU/mL and  $10^4$  CFU/mL live cell suspensions, the only Log CFU/mL estimate that statistically differed ( $p < 0.05$ ) from all others was the Ct-based estimate of the no treatment + HK condition. A similar trend is seen in the  $stx_2$  data (**Table 2.13B**) which was generated from the Ct values in **Table 2.12B**.

**Table 2.13A. Estimated CFU/mL by plate count and by  $stx_1$  cycle threshold value for live and mixed cell suspensions treated with 100  $\mu$ M PMAxx<sup>TM</sup> + 1% DMSO.**

Live cells (Log CFU/mL)	HK cells (8 Log CFU/mL)	Experimental condition (Mean Log CFU/mL estimate $\pm$ SD)			
		No treatment		100 $\mu$ M PMAxx <sup>TM</sup> + 1% DMSO	
		by $stx_1$ Ct	by count	by $stx_1$ Ct	by count
8	–	7.4 $\pm$ 0.2	7.9 $\pm$ 0.2	7.1 $\pm$ 0.4	7.7 $\pm$ 0.7
	+	7.4 $\pm$ 0.2	7.9 $\pm$ 0.1	7.4 $\pm$ 0.5	7.8 $\pm$ 0.3
6	–	5.5 $\pm$ 0.1	5.9 $\pm$ 0.2	4.8 $\pm$ 0.7	4.9 $\pm$ 0.4
	+	7.1 $\pm$ 0.3*	5.5 $\pm$ 0.1	5.0 $\pm$ 0.7	5.0 $\pm$ 0.1
4	–	3.4 $\pm$ 0.2	3.9 $\pm$ 0.2	2.6 $\pm$ 1.0	3.7 $\pm$ 0.3
	+	7.2 $\pm$ 0.4*	3.1 $\pm$ 0.2	3.3 $\pm$ 0.7	2.7 $\pm$ 0.2

Each estimate represents 3 independent replicates

HK: heat-killed

by  $stx_1$  Ct: calculated from the data in **Table 2.12A** and equation in **2.3.1.1**

by count: calculated using the method described in **2.2.1.2**

ANOVA analysis was conducted for each live cell concentration (delineated by horizontal lines)

\*indicates Log CFU/mL estimates that were statistically different ( $p < 0.05$ ) from all others of the same live cell concentration

**Table 2.13B. Estimated CFU/mL by plate count and by *stx*<sub>2</sub> cycle threshold value for live and mixed cell suspensions treated with 100 µM PMAxx™ + 1% DMSO.**

Live cells (Log CFU/mL)	HK cells (8 Log CFU/mL)	Experimental condition (Mean Log CFU/mL estimate ± SD)			
		No treatment		100 µM PMAxx™ + 1% DMSO	
		by <i>stx</i> <sub>2</sub> Ct	by count	by <i>stx</i> <sub>2</sub> Ct	by count
8	–	8.0 ± 0.3	7.9 ± 0.2	7.5 ± 0.3	7.7 ± 0.7
	+	8.0 ± 0.4	7.9 ± 0.1	7.8 ± 0.2	7.8 ± 0.3
6	–	6.0 ± 0.2	5.9 ± 0.2	5.3 ± 0.4	4.9 ± 0.4
	+	7.6 ± 0.2*	5.5 ± 0.1	5.5 ± 0.2	5.0 ± 0.1
4	–	4.0 ± 0.2	3.9 ± 0.2	2.8 ± 0.8	3.7 ± 0.3
	+	7.5 ± 0.3*	3.1 ± 0.2	3.7 ± 1.0	2.7 ± 0.2

Each estimate represents 3 independent replicates

HK: heat-killed

by *stx*<sub>2</sub> Ct: calculated from the data in **Table 2.12B** and equation in **2.3.1.1**

by count: calculated using the method described in **2.2.1.2**

ANOVA analysis was conducted for each live cell concentration (delineated by horizontal lines)

\*indicates Log CFU/mL estimates that were statistically different ( $p < 0.05$ ) from all others of the same live cell concentration

## 2.4 Discussion

### 2.4.1 Primer set performance

Commercial nucleic acid amplification tests (NAATs) used for STEC detection often target *stx*<sub>1</sub> and *stx*<sub>2</sub> (though such assays will often call a sample *stx*-positive without differentiation) (24).

Accordingly, a set of published primers and probes (23) targeting both genes was chosen for this project. For both, the RT-PCR target corresponds to the B subunit of the toxin which has a more conserved sequence than the A subunit (25). The set enables duplexed detection within the same RT-PCR well, which reduces the overall number of wells needed for testing samples with both genes.

The primer and probe sequences determine the baseline sensitivity of the final viability RT-PCR assay. Their limit of detection ( $10^3$  CFU/mL, **Table 2.2**) is on par with the limit of detection of other *stx* primer sets (26). Additionally, it is promising that they showed no cross-reactivity with other bacteria, especially the *Shigella* species (*S. boydii* (serotype 2), *S. dysenteriae* (serotype 2), *S. flexneri* (serotype 2), and *S. sonnei*). However, the major limitation of this set of primers is their inability to detect *stx*<sub>2f</sub> (**Table 2.3B**). Although Stx-2f is considered a “rarer” subtype and cannot be detected by some commercial NAATs (27) or enzyme immunoassays (28), it can still be associated with severe disease (29).

#### **2.4.2 PMAxx™ performance and treatment conditions**

Viability RT-PCR depends on two fundamental characteristics of viability dyes: i) they do not penetrate the membrane of live cells, and ii) after photoactivation they covalently (i.e., irreversibly) bind DNA. If either characteristic is not reliably true, then the Ct values generated by viability RT-PCR will not accurately reflect the DNA of intact cells. That is, if i) is not consistently true, then the dye might penetrate live cells and cause an underestimation of intact cell DNA (increased Ct value). On the other hand, if ii) is inaccurate, then the dye molecules might detach from dead cell DNA and cause an overestimation of intact cell DNA (decreased Ct value). In this study, PMAxx™ appeared to bind irreversibly to DNA (**Section 2.3.2**). This concurs with the proposed mechanism of action and means that delays between DNA extraction and RT-PCR are inconsequential. Further, it completed its action within the first day of application and did not affect live cell DNA as the time course progressed. This agrees with the claim that excess photoactivated PMAxx™ binds with water (or other organic molecules) to become inert (11).

This study's preliminary trials (**Table 2.4**) showed that PBS is preferable to Tris buffer for PMAxx™ application because the live cell recovery was higher. Although Tris buffer is widely used in many laboratories, some evidence suggests that it can increase membrane permeability (30). It is likely that this feature allowed PMAxx™ to penetrate the live bacteria and cause death.

According to the manufacturer, PMAxx™ has an emission spectra of ~610 nm when bound to DNA after photolysis, so it is possible that it could interfere with the fluorescence measured by the thermocycler if not sufficiently removed (31). The Real-Time PCR instrument used in this study has 5 filters to detect fluorescent signals; those with a wavelength of 610 nm would be detected by filter 4 (**Figure A.2 in Appendix A**). The reporters used for the *stx*<sub>1</sub> (6-FAM) and *stx*<sub>2</sub> (YAkYel) probes are detected by filters 1 and 2 respectively, so there is no concern for overlap. However, the Master Mix used here utilizes ROX™ as a passive reference dye. Although ROX™ has an emission spectrum similar to PMAxx™ and is detected by filter 4 (32), PMAxx™ treatment did not interfere with fluorescence readings (**Figure A.1 in Appendix A**).

When PMAxx™ was added to STEC DNA and photoactivated for 15 mins, it performed comparably to PMAxx™ which had been photoactivated for 30 mins (**Table 2.5**). Consequently a 15 min photoactivation was used for subsequent experiments. Ambient light was also found to be capable of activating the dye to a degree. To prevent the dye from becoming inactivated before application in later experiments, dye addition steps were conducted in the dark and the dye was stored in an opaque or covered tube.

Each PMAxx™ concentration tested (50, 75, and 100 µM) was able to drastically increase the Ct values associated with HK cells (**Table 2.6**). The addition of DMSO further enhanced this performance (**Table 2.7**). A high concentration of PMAxx™ (100 µM, with or without DMSO) was associated with a certain degree of live cell loss (**Table 2.8**), but caused less than a 1-Log loss

of cells even at low cell concentrations. It is possible that this effect is inherent to the dye itself; although it is meant to be membrane-impermeable, the design might still allow a certain amount to passively cross as seen to a greater extent with the earlier viability dye, EMA (12).

Alternatively, it is possible that a certain proportion of the live cells are especially susceptible to the dye crossing their membrane because of their deteriorating membrane integrity.

The lack of amplification that occurred when live cell suspensions were boiled immediately after PMAxx™ photoactivation confirms that the dye remains active for a period of time after photoactivation is completed (**Table 2.9**). Consequently, removal of any supernatant containing PMAxx™ is necessary prior to DNA extraction. The act of resuspension as it was conducted in this experiment (i.e. by centrifugation, removing the supernatant, and adding fresh buffer) introduced a tolerable ( $\pm 1$  Ct value) amount of error which outweighs the risk of leaving residual PMAxx™. It was also confirmed that PMAxx™ can stick to the interior of the microcentrifuge tube and bind to a proportion of free DNA (**Table 2.10**). For these reasons, a step involving re-suspension in 1 mL PBS and a subsequent transfer to a new tube for DNA extraction was incorporated into the final viability RT-PCR protocol for STEC cell suspensions (**Figure 2.5**).

In theory, pre-photoactivation could be useful for complex samples where turbidity might interfere with photoactivation. However its poor performance at 100  $\mu$ M PMAxx™ (with 1% DMSO) suggests that only a small proportion of the dye molecules remain activated for long enough to bind the DNA once added to the sample (**Table 2.11**). The moderate Ct value increases attributable to pre-photoactivated PMAxx™ observed in the lower cell suspensions ( $\leq 10^4$  CFU/mL) could potentially be improved upon by increasing the dye concentration to much higher levels. This, however, would be undesirable given the cost and potential negative effects on live cells.

### 2.4.3 Viability RT-PCR protocol performance with mixes of live and heat-killed culture

The viability RT-PCR protocol was successful in eliminating the contaminating signal of the  $10^8$  CFU/mL heat-killed cells (**Tables 2.13A** and **2.13B**). This effect is less noticeable in the  $10^8$  live CFU/mL suspension because the ratio of HK to live cells is 1:1, which means that the CFU change is within the same Log. However, the ability to selectively-detect only live cells is readily apparent in the  $10^6$  and  $10^4$  live CFU/mL suspensions: the Ct value-based estimates of the untreated mixes reflect the presence of the dead cells, while the treated Ct value-based estimates only reflect the number of live cells that can also be counted on a plate. However, PMAxx™ randomly binds DNA so it follows that most treated conditions showed more variability compared to the untreated controls.

PMAxx™ treatment produced false negative results (2/3 replicates in **Table 2.12A**) when applied to live cells at low bacterial loads despite efforts (e.g. tube transfer via 1 mL PBS resuspension) to mitigate this occurrence. Although the average Ct value across the replicates was not statistically significant compared to the untreated control, its inflation may suggest that the dye interacts with live cells in an adverse manner. Alternatively it is also possible that a certain amount of live cells were lost during the tube transfer step, which would be more easily observed at low cell concentrations.

## 2.5 Conclusion

A viability RT-PCR assay for pure STEC culture was developed. The *stx*<sub>1</sub> and *stx*<sub>2</sub> primer-probe sets (23) were found to have a limit of detection of  $10^3$  CFU/mL, showed no cross-reactivity with other bacteria (including four *Shigella* species), and detected all of the *stx* subtypes tested except for *stx*<sub>2f</sub>. PMAxx™ was confirmed to be a membrane-impermeable dye, bind DNA irreversibly, and to not interfere with RT-PCR via its fluorescence. The following conditions were



selected: PBS as the buffer, a PMAxx™ concentration of 100 µM, and a photoactivation time of 15 min. The final viability RT-PCR protocol was enhanced by adding DMSO (to a final concentration of 1%) and transferring the cell suspension to a new tube before DNA extraction. This protocol was able to eliminate the detection of heat-killed cells, but negatively impacted (i.e., increased beyond the threshold of 32) live cell Ct values at a low cell concentration (10<sup>4</sup> CFU/mL).

## 2.6 References

1. Government of Canada. VTEC Illness Monitoring In Canada [Internet]. Innovation, Science and Economic Development Canada; [cited 2022 Jun 9]. Available from: [https://www.ic.gc.ca/eic/site/063.nsf/eng/h\\_98071.html#nesp](https://www.ic.gc.ca/eic/site/063.nsf/eng/h_98071.html#nesp)
2. Glassman H, Ferrato C, Chui L. Epidemiology of Non-O157 Shiga Toxin-Producing *Escherichia coli* in the Province of Alberta, Canada, from 2018 to 2021. *Microorganisms*. 2022 Apr;10(4):814.
3. Lisboa LF, Szelewicki J, Lin A, Latonas S, Li V, Zhi S, et al. Epidemiology of Shiga Toxin-Producing *Escherichia coli* O157 in the Province of Alberta, Canada, 2009–2016. *Toxins*. 2019 Oct 22;11(10):613.
4. Freedman SB, Eltorki M, Chui L, Xie J, Feng S, MacDonald J, et al. Province-Wide Review of Pediatric Shiga Toxin-Producing *Escherichia coli* Case Management. *J Pediatr*. 2017 Jan 1;180:184–90.
5. Freedman SB, Xie J, Neufeld MS, Hamilton WL, Hartling L, Tarr PI, et al. Shiga Toxin-Producing *Escherichia coli* Infection, Antibiotics, and Risk of Developing Hemolytic Uremic Syndrome: A Meta-analysis. *Clin Infect Dis Off Publ Infect Dis Soc Am*. 2016 15;62(10):1251–8.
6. McGannon CM, Fuller CA, Weiss AA. Different Classes of Antibiotics Differentially Influence Shiga Toxin Production. *Antimicrob Agents Chemother*. 2010 Sep;54(9):3790–8.
7. Ake JA, Jelacic S, Ciol MA, Watkins SL, Murray KF, Christie DL, et al. Relative Nephroprotection During *Escherichia coli* O157:H7 Infections: Association With Intravenous Volume Expansion. *Pediatrics*. 2005 Jun 1;115(6):e673–80.
8. Chui L, Christianson S, Alexander D, Arseneau V, Bekal S, Berenger B, et al. CPHLN recommendations for the laboratory detection of Shiga toxin-producing *Escherichia coli* (O157 and non-O157). *Can Commun Dis Rep*. 2018 Nov 1;44:304–7.

9. Harrington SM, Buchan BW, Doern C, Fader R, Ferraro MJ, Pillai DR, et al. Multicenter Evaluation of the BD Max Enteric Bacterial Panel PCR Assay for Rapid Detection of *Salmonella* spp., *Shigella* spp., *Campylobacter* spp. (*C. jejuni* and *C. coli*), and Shiga Toxin 1 and 2 Genes. *J Clin Microbiol*. 2015 May;53(5):1639–47.
10. Nocker A, Camper AK. Novel approaches toward preferential detection of viable cells using nucleic acid amplification techniques. *FEMS Microbiol Lett*. 2009 Feb 1;291(2):137–42.
11. van Frankenhuyzen JK, Trevors JT, Lee H, Flemming CA, Habash MB. Molecular pathogen detection in biosolids with a focus on quantitative PCR using propidium monoazide for viable cell enumeration. *J Microbiol Methods*. 2011 Dec 1;87(3):263–72.
12. Nocker A, Cheung CY, Camper AK. Comparison of propidium monoazide with ethidium monoazide for differentiation of live vs. dead bacteria by selective removal of DNA from dead cells. *J Microbiol Methods*. 2006;67(2):310–20.
13. Codony F, Dinh-Thanh M, Agustí G. Key Factors for Removing Bias in Viability PCR-Based Methods: A Review. *Curr Microbiol*. 2020 Apr 1;77(4):682–7.
14. Shekar A, Babu L, Ramlal S, Sripathy MH, Batra H. Selective and concurrent detection of viable *Salmonella* spp., *E. coli*, *Staphylococcus aureus*, *E. coli* O157:H7, and *Shigella* spp., in low moisture food products by PMA-mPCR assay with internal amplification control. *LWT*. 2017 Dec 1;86:586–93.
15. Bhatta TR, Chamings A, Alexandersen S. Exploring the Cause of Diarrhoea and Poor Growth in 8–11-Week-Old Pigs from an Australian Pig Herd Using Metagenomic Sequencing. *Viruses*. 2021 Aug;13(8):1608.
16. Dinu LD, Bach S. Detection of viable but non-culturable *Escherichia coli* O157: H7 from vegetable samples using quantitative PCR with propidium monoazide and immunological assays. *Food Control*. 2013;31(2):268–73.
17. Álvarez G, González M, Isabal S, Blanc V, León R. Method to quantify live and dead cells in multi-species oral biofilm by real-time PCR with propidium monoazide. *AMB Express*. 2013

Jan 4;3(1):1.

18. Schnetzinger F, Pan Y, Nocker A. Use of propidium monoazide and increased amplicon length reduce false-positive signals in quantitative PCR for bioburden analysis. *Appl Microbiol Biotechnol*. 2013 Mar 1;97(5):2153–62.
19. Seinige D, Krischek C, Klein G, Kehrenberg C. Comparative analysis and limitations of ethidium monoazide and propidium monoazide treatments for the differentiation of viable and nonviable *Campylobacter* cells. *Appl Environ Microbiol*. 2014;80(7):2186.
20. Bonetta S, Pignata C, Bonetta S, Meucci L, Giacosa D, Marino E, et al. Viability of *Legionella pneumophila* in Water Samples: A Comparison of Propidium Monoazide (PMA) Treatment on Membrane Filters and in Liquid. *Int J Environ Res Public Health*. 2017 May;14(5):467.
21. Gurtovenko AA, Anwar J. Modulating the structure and properties of cell membranes: the molecular mechanism of action of dimethyl sulfoxide. *J Phys Chem B*. 2007 Sep 6;111(35):10453–60.
22. Notman R, Noro M, O'Malley B, Anwar J. Molecular Basis for Dimethylsulfoxide (DMSO) Action on Lipid Membranes. *J Am Chem Soc*. 2006 Nov 1;128(43):13982–3.
23. Perelle S, Dilasser F, Grout J, Fach P. Detection by 5'-nuclease PCR of Shiga-toxin producing *Escherichia coli* O26, O55, O91, O103, O111, O113, O145 and O157:H7, associated with the world's most frequent clinical cases. *Mol Cell Probes*. 2004 Jun 1;18(3):185–92.
24. Margot H, Cernela N, Iversen C, Zweifel C, Stephan R. Evaluation of Seven Different Commercially Available Real-Time PCR Assays for Detection of Shiga Toxin 1 and 2 Gene Subtypes. *J Food Prot*. 2013 May 1;76(5):871–3.
25. Melton-Celsa AR. Shiga Toxin (Stx) Classification, Structure, and Function. *Microbiol Spectr*. 2014;4(2):2–4.
26. Reischl U, Youssef MT, Kilwinski J, Lehn N, Zhang WL, Karch H, et al. Real-Time

- Fluorescence PCR Assays for Detection and Characterization of Shiga Toxin, Intimin, and Enterohemolysin Genes from Shiga Toxin-Producing *Escherichia coli*. *J Clin Microbiol*. 2002 Jul;40(7):2555–65.
27. Berenger B, Chui L, Ferrato C, Lloyd T, Li V, Pillai DR. Performance of four commercial real-time PCR assays for the detection of bacterial enteric pathogens in clinical samples - ScienceDirect. *Int J Infect Dis*. 2021 Oct 20;114:195–201.
28. De Rauw K, Breynaert J, Piérard D. Evaluation of the Alere SHIGA TOXIN QUIK CHEK™ in comparison to multiplex Shiga toxin PCR. *Diagn Microbiol Infect Dis*. 2016 Sep;86(1):35–9.
29. Friesema IHM, Keijzer-Veen MG, Koppejan M, Schipper HS, van Griethuysen AJ, Heck MEOC, et al. Hemolytic Uremic Syndrome Associated with *Escherichia coli* O8:H19 and Shiga Toxin 2f Gene. *Emerg Infect Dis*. 2015 Jan;21(1):168–9.
30. Irvin RT, MacAlister TJ, Costerton JW. Tris(hydroxymethyl)aminomethane buffer modification of *Escherichia coli* outer membrane permeability. *J Bacteriol*. 1981 Mar;145(3):1397–403.
31. PMAxx™ Dye, 20 mM in H<sub>2</sub>O [Internet]. Biotium. [cited 2022 Nov 8]. Available from: <https://biotium.com/product/pmaxx-20-mm-in-h2o/>
32. Applied Biosystems 7500/7500 Fast Real-Time PCR Systems Manual [Internet]. Available from: <https://tools.thermofisher.com/content/sfs/manuals/4387777d.pdf>

## **Chapter 3: Development and application of a direct-from-stool viability real-time PCR assay for STEC detection**

### **3.1 Introduction**

Shiga toxin-producing *Escherichia coli* (STEC) is a major cause of acute gastroenteritis (AGE). Each strain carries at least one Shiga toxin-converting phage which encodes the *stx* genes (1). The infection causes watery and/or bloody diarrhea, and usually resolves without intervention within a week (2,3). However, Stx can affect the kidneys and brain, which may lead to potentially fatal complications like hemolytic uremic syndrome (HUS) (4). Children (< 10) and the elderly are most at risk of these severe complications because of their weakened immune systems (1). Canadian guidelines contraindicate the use of antibiotics for STEC (5) because they can increase toxin expression (6,7) and increase the risk of HUS (8). Instead, the early administration of intravenous fluids is the main method used to minimize sequelae (9,10).

As a zoonotic pathogen, STEC can naturally be found in ruminants and water (11). Consequently, contaminated food (especially meats, dairy products, and vegetables grown using manure) is the primary mode of STEC transmission (11). However, it has been estimated that person-to-person transmission causes around 11% of all STEC infections (12). In the USA there were forty outbreaks at childcare facilities between 1982 - 2002 linked to person-to-person transmission (13). To prevent secondary spread, public health guidelines are used to remove STEC patients from sensitive settings until they have fully cleared their infection. The clearance process takes a median 2.5 weeks, but can last for several months (14). Younger and symptomatic patients tend to shed STEC for a longer period of time (15).

In Alberta, STEC patients who work in food handling, healthcare, and childcare or who attend childcare must exclude themselves and submit stool samples to the Public Health laboratory (ProvLab) for microbiological clearance testing until they produce two consecutively negative stool specimens more than 24 hours apart (16). Currently, the majority of this testing is conducted using CHROMagar™ STEC. However, some non-O157 serotypes have documented difficulties growing on this media (17,18). Post-enrichment real-time PCR (PE RT-PCR) is used for such strains. In this case, the specimen is first enriched in tryptic soy broth (TSB) or on MacConkey agar before being tested by real-time PCR (RT-PCR) for the *stx* genes (See **Figure B.1** in **Appendix B** for the workflow used in Alberta for STEC microbiological clearance testing).

STEC has a low infectious dose (1), so the ideal microbiological clearance testing method should be sensitive enough to detect low bacterial loads. At the same time, the method ought to only reflect active infections (i.e., live bacteria are present) so patients can return to work or daycare as soon as they are not at risk of transmitting their infection to others. This study investigates whether viability RT-PCR could be used as a culture-independent alternative for STEC microbiological clearance testing. This technique uses a photoactivated viability dye, like propidium monoazide, to bind free DNA from dead bacteria and prevent amplification in subsequent RT-PCR. Since the dye is designed to be impermeable to intact cell membranes, this method should allow for the exclusive detection of live STEC in patient samples.

Chapter 3 aims to compare the sensitivity of viability RT-PCR, conventional RT-PCR, and culture in detecting live STEC using artificially spiked stools, artificially spiked rectal swabs (RS), and clinical stool specimens. To achieve this, a viability RT-PCR assay for stool samples and RS will be developed by optimizing sample dilution, DNA extraction, and PMAxx™ treatment. Next, the optimized protocol's ability to selectively detect DNA from live STEC in the presence of dead

STEC will be tested using artificially spiked stools and artificially spiked RS. Lastly, the sensitivity of the direct-from-stool (DFS) viability RT-PCR assay will be compared to conventional RT-PCR, culture, EIA, and PE RT-PCR using clinical microbiological clearance samples.

## **3.2 Methods and Materials**

### **3.2.1 Artificially spiked stool**

#### **3.2.1.1 Reference strain**

Spiking experiments were conducted using ProvLab's STEC positive control (ATCC 35150), a O157:H7 strain positive for both *stx*<sub>1</sub> and *stx*<sub>2</sub>. It had been stored in skim milk medium (prepared by APL-ProvLab) at -70°C as part of the Chui laboratory repository. The isolate was retrieved from the frozen stock by streaking onto a blood agar plate (BAP; Dalynn Biologicals Inc, Calgary, AB, Canada) and incubating overnight (20 hours) at 37°C.

#### **3.2.1.2 STEC-free stool used for spiking experiments**

A liquid clinical stool specimen from the University of Alberta Hospital Microbiology department which had been determined to be STEC-negative was used for all stool spiking experiments. Upon receipt, a 100 µL aliquot was spread onto a CHROMagar™ STEC (CHROMagar™, Paris, France) plate, incubated for 20 hours at 37°C, and observed to confirm the absence of mauve colonies. Additionally, to confirm that no substances (e.g. antibiotics) were present in the stool that would interfere with the reference strain, a 1:1 mix was prepared using stool and ATCC 35150 grown in trypticase soy broth (TSB; Becton Dickinson, Mississauga, ON, Canada) to an optical density (OD<sub>600</sub>) of 0.5 (Microscan Turbidity Meter, Siemens, Oakville, ON, Canada). A 100 µL aliquot of this mixture was grown on CHROMagar™ STEC as above.

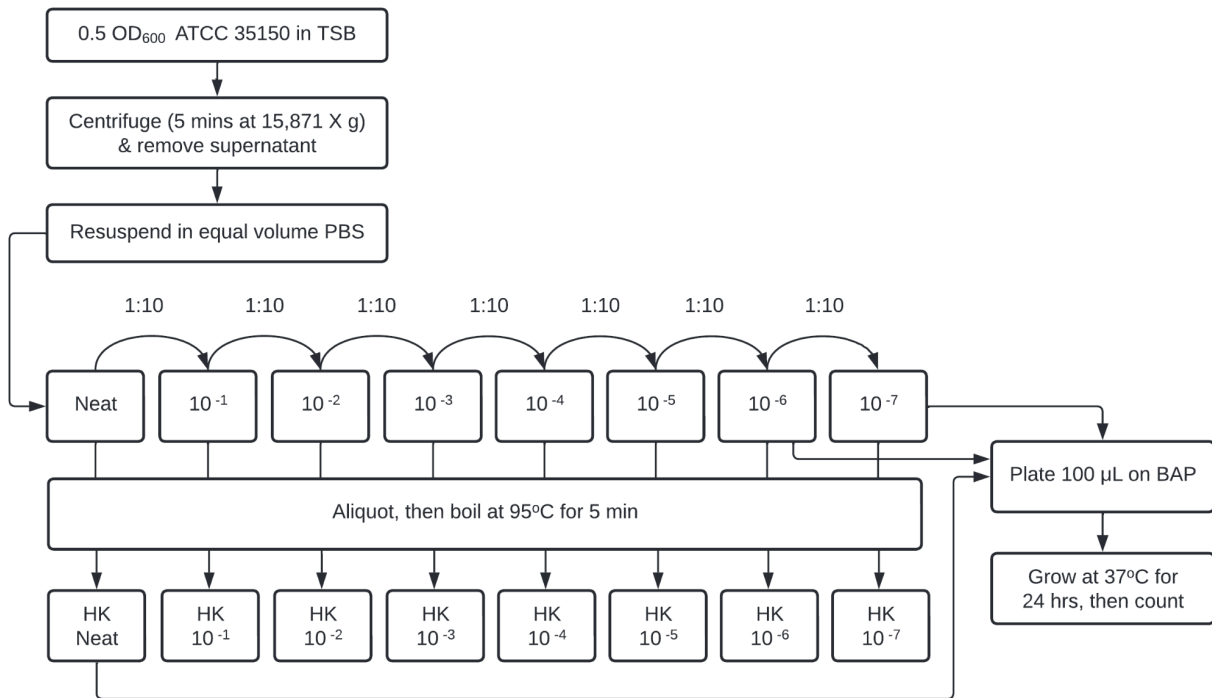


### 3.2.1.3 Stool spiking

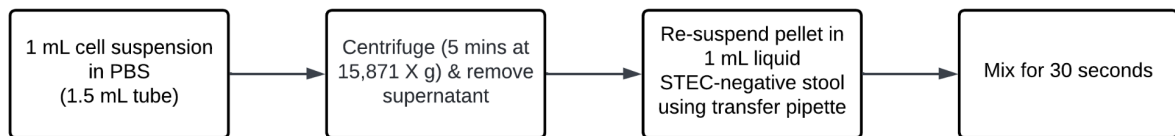
The protocol used to generate live and heat-killed (HK) suspensions of ATCC 35150 is described in **Figure 3.1A**. One colony from an overnight BAP was inoculated into TSB and grown at 37°C with horizontal agitation at 225 rpm (MaxQ 2506 Reciprocating Shaker; Thermo Fisher Scientific, Waltham, MA, USA) until an OD<sub>600</sub> of 0.5 was reached. A 1 mL aliquot was centrifuged using an Eppendorf™ Centrifuge 5425 (ThermoFisher Scientific, Waltham, Massachusetts, USA) at 15,871 X g for 5 min, the supernatant was removed, and the cell pellet was resuspended in an equal volume of PBS (pH 7.4). This neat suspension was then used to make ten-fold serial dilutions in PBS down to 10<sup>-7</sup>. To determine the number of colony forming units per milliliter (CFU/mL), 100 µL of the 10<sup>-6</sup> and 10<sup>-7</sup> dilutions were spread onto BAP, incubated overnight (20 hours) at 37°C, then the colonies were counted the following day. HK suspensions were generated by boiling aliquots of the live dilution series in a water bath at 95°C for 5 min. To verify the death of the cells, 100 µL of the neat HK suspension was spread on BAP, kept at 37°C overnight (20 hours), and confirmed to produce no observable growth.

To artificially spike stool, 1 mL of each cell suspension was centrifuged (5 min at 15,871 X g) in a 1.5 mL Screw Cap Micro Tube (Thermo Scientific™, Waltham, Massachusetts, USA) (**Figure 3.1B**). The supernatant was removed and 1 mL of the STEC-free liquid stool from **3.2.1.2** was added using a transfer pipette (TechLab®, Blacksburg, Virginia, USA). The pipette was used to mix the specimen, and then the tube was mixed vigorously (speed 8 - 10) for 30 seconds using an analog Vortex Mixer (VWR International, Radnor, Pennsylvania, USA).

### A) Dilution series preparation



### B) Stool spiking

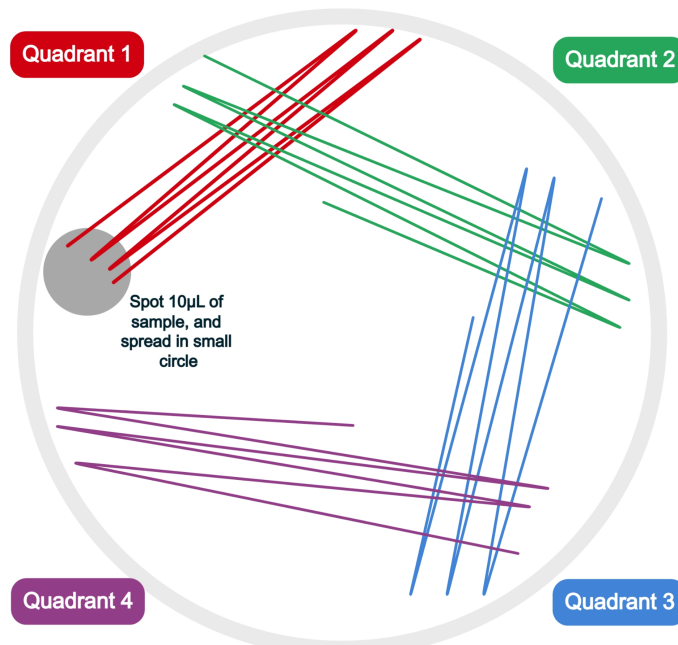


**Figure 3.1. Workflow used to (A) prepare dilution series of live and heat-killed STEC and (B) spike STEC-negative liquid stool.**

#### 3.2.1.4 Growth on CHROMagar™ STEC

Stool samples were plated on CHROMagar™ STEC using a protocol standardized to produce distinct quadrants (**Figure 3.2**). This involved first spotting 10 µL of sample on the plate using a disposable 10 µL inoculation loop (Globe Scientific Inc., Mahwah, NJ, USA). This was allowed to dry, then the rounded tip of a sterile glass spreader was used to streak out 3 overlapping lines from the spot. The spreader was changed and 3 more streaks were made by crossing over the

previous streaks at a 90° angle. This process was repeated to produce 4 quadrants. As per the manufacturer's instructions, plates were incubated for 20 hours at 37°C and then visualized for mauve colonies. Plates were scored according to the highest quadrant to show growth of ≥ 3 mauve colonies. This is based on the approach of a previous Chui laboratory study (19), which documented a relationship between growth in higher quadrants and a higher bacterial load (as indicated by a lower RT-PCR cycle threshold value).



**Figure 3.2. Illustration of the quadrant streaking method used for CHROMagar™ STEC.**

### **3.2.2 Real-time PCR analysis of stool and rectal swabs**

#### **3.2.2.1 Sample preparation for direct-from-stool (DFS) detection**

The direct-from-stool (DFS) workup involved first creating a 10% stool suspension. For the liquid STEC-free stool used for spiking, a 1 in 10 dilution was prepared by adding 100 µL stool to 900 µL PBS using a transfer pipette. The suspension was briefly mixed then left at room temperature for 15 min to allow the stool particulate to settle at the bottom. After this period, 100

$\mu\text{L}$  aliquots of the liquid phase were carefully transferred to 1.5 mL microcentrifuge tubes for use in subsequent experiments.

### **3.2.2.2 Sample preparation for rectal swab (RS) detection**

The rectal swabs (RS) used in this study were 5U002S FLOQSwabs® (COPAN Diagnostics, Murrieta, California, USA). To artificially collect a sample, a swab was removed from its plastic packaging, inserted into a 1.5 mL tube with 1 mL of undiluted spiked stool, and gently rotated 360° one time. After removal, the swab was inserted into a sterile Falcon® 5 mL round bottom polystyrene test tube (Corning Incorporated, Corning, New York, USA) with 1 mL of PBS. The shaft of the swab was snapped at the breakpoint in the tube, the snap cap was secured, and the tube was vigorously mixed for 30 seconds. A pair of sterilized tongs were used to remove and dispose of the swab head. The rectal swab suspension was left to settle for 15 min at room temperature before 100  $\mu\text{L}$  aliquots of the liquid phase were carefully transferred to 1.5 mL microcentrifuge tubes for use in subsequent experiments.

### **3.2.2.3 Comparison of rapid lysis buffer and MagaZorb® DNA Mini-Prep Kit**

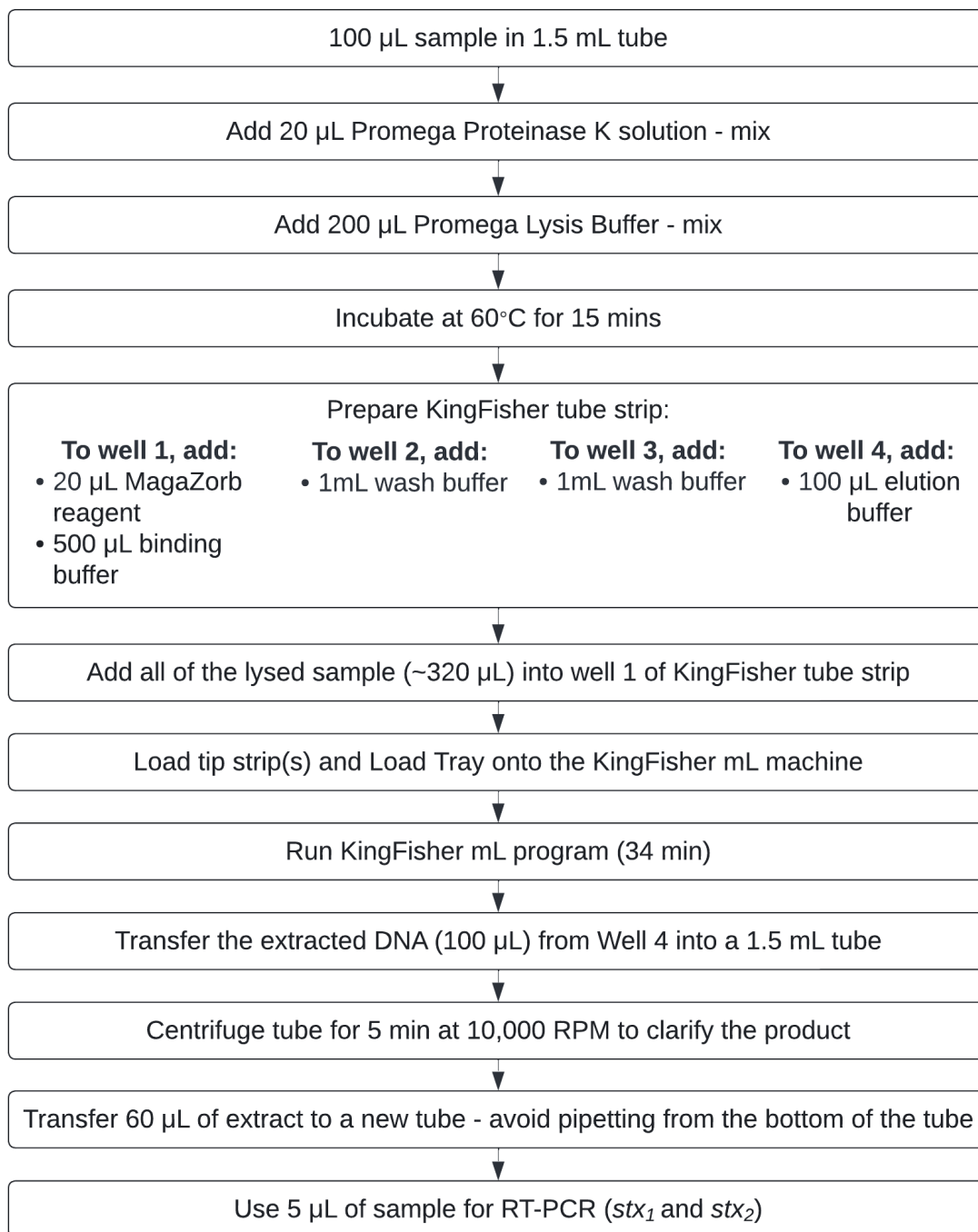
To determine which DNA extraction method should be used, liquid stool was spiked with three different live cell suspensions ( $10^{-1}$ ,  $10^{-3}$ , and  $10^{-5}$  as prepared in **3.2.1.3**). The spiked stools were prepared according to the direct-from-stool (**3.2.2.1**) and rectal swab (**3.2.2.2**) procedures above. Afterward, DNA was extracted from an aliquot of each liquid phase using either rapid lysis buffer or the MagaZorb® DNA Mini-Prep Kit (Promega, Madison, Wisconsin, USA) and KingFisher™ mL Purification System (Thermo Scientific™, Waltham, Massachusetts, USA)

before being analyzed by RT-PCR. The original live cell suspensions in PBS were also diluted 1 in 10 (to match the dilution of the DFS method) and run in parallel for comparison.

The rapid lysis buffer (RLB) DNA extraction method (described in **Chapter 2** section **2.2.2**) extracted DNA from 100  $\mu$ L aliquots in 1.5 mL microcentrifuge tubes. First, suspensions were centrifuged for 5 min at 15,871 X g using an Eppendorf<sup>TM</sup> Centrifuge 5425. Next, the supernatant was removed and the pellet was resuspended in an equal volume of rapid lysis buffer (100 mmol/L NaCl, 10 mmol/L Tris-HCl, pH 8.3, 1 mmol/L EDTA, pH 9.0, 1% Triton X-100). Lastly, this suspension was boiled at 95°C for 15 min in a water bath.

The MagaZorb<sup>®</sup> DNA Mini-Prep Kit and KingFisher<sup>TM</sup> mL Purification System (MZ-KF) were used together as described in **Figure 3.3**. First, 20  $\mu$ L of Promega proteinase K solution was added to each 100  $\mu$ L aliquot and mixed using a Vortex Mixer. Next, 200  $\mu$ L of Promega lysis buffer was added and the tubes were mixed again. The tubes were pulse centrifuged (2,000 X g) in a PicoFuge microcentrifuge (Stratagene, San Diego, California, USA), and placed in a 60°C water bath for 15 min. After this incubation step, the entirety of each lysed sample (~320  $\mu$ L) was combined with 20  $\mu$ L MagaZorb<sup>®</sup> reagent and 500  $\mu$ L binding buffer in well 1 of a KingFisher<sup>TM</sup> tube strip. DNA bound to the MagaZorb<sup>®</sup> reagent was washed 2 times with Promega wash buffer using The KingFisher<sup>TM</sup> mL Purification System and DNA was eluted in 100  $\mu$ L of elution buffer. The DNA extract was transferred into a fresh microcentrifuge tube and centrifuged for 5 min at 15,871 X g. A 60  $\mu$ L aliquot of this clarified DNA extract was then transferred to a new tube.

Extracted samples were then analyzed by RT-PCR as described below. This procedure was performed independently three times. .



**Figure 3.3. Flow chart describing the MagaZorb® DNA Mini-Prep Kit and KingFisher™ mL Purification System DNA extraction protocol.**

#### **3.2.2.4 RT-PCR Reaction conditions**

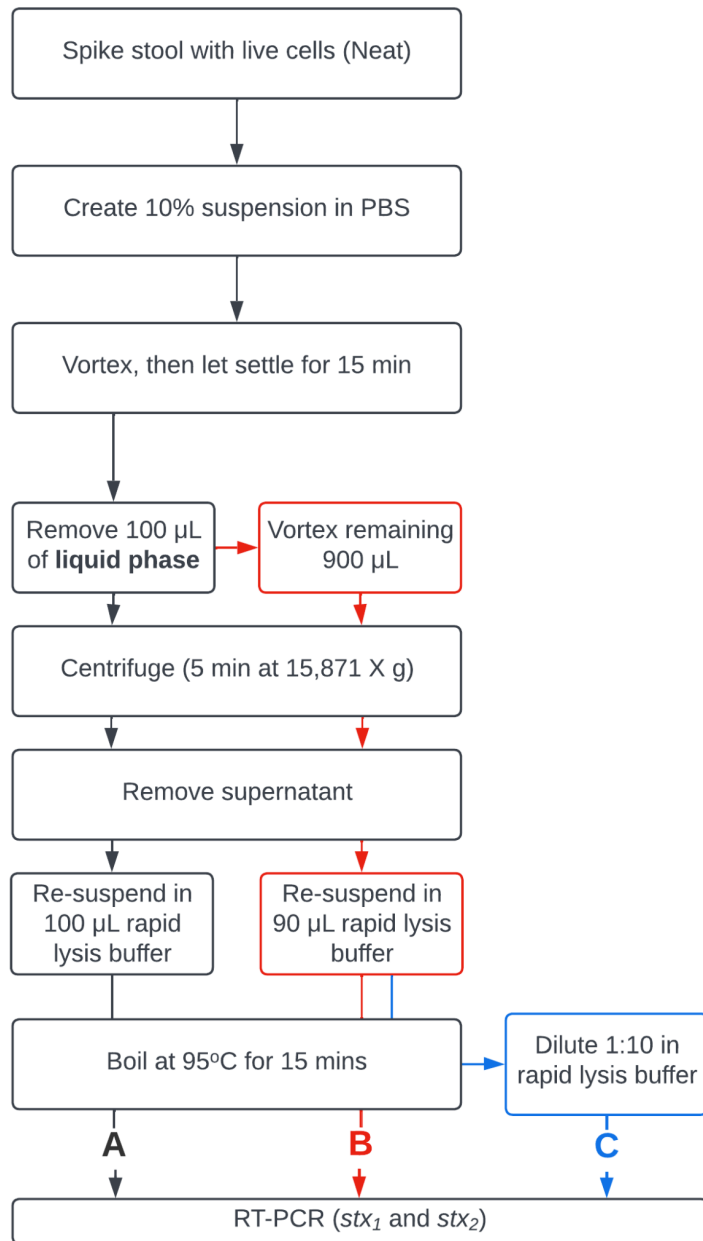
DNA extracts from stool and rectal swab suspensions were analyzed by RT-PCR using the same methods described previously (**Chapter 2**, section **2.2.3.1**). Each RT-PCR well contained 10  $\mu\text{L}$  of 2X PrimeTime® Gene Expression Master Mix (Integrated DNA Technology, Coralville, Iowa, USA), 0.33  $\mu\text{M}$  of each  $stx_1$  and  $stx_2$  primer (**Chapter 2**, **Table 2.1**), 0.22  $\mu\text{M}$  of each probe, 5  $\mu\text{L}$  DNA extract and 2  $\mu\text{L}$  molecular biology grade water in a total volume of 20  $\mu\text{L}$ . An Applied Biosystems™ 7500 Fast Real-Time PCR instrument (Applied Biosystems, Life Technologies Corporation, Burlington, ON, Canada) was used to generate cycle threshold (Ct) values, and the conditions were 95 °C for 20 seconds followed by 40 cycles of 95 °C for 3 seconds and 60 °C for 30 seconds. Each run included a positive control (ATCC 35150 DNA extract) and a no template control (molecular biology grade water). For each spiking experiment, an aliquot of unspiked stool was run in parallel to confirm the absence of STEC by RT-PCR.

#### **3.2.2.5 Comparison of DNA extracted from the liquid phase of a settled 10% stool suspension versus that of the total sample**

The procedure outlined in **Figure 3.4** was used to determine whether the liquid phase DNA extract sufficiently approximates the DNA extract of the total sample. STEC-free liquid stool was spiked with neat live cells (as described in **Figure 3.1**), then a 1:10 suspension was prepared (as described in **3.2.2.1**). This suspension was left to settle for 15 mins, and 100  $\mu\text{L}$  of the liquid phase was transferred to a new tube. The liquid phase DNA extract (“A”) was made by centrifuging this tube (5 min at 15,871 Xg), removing the supernatant, and resuspending the pellet in an equal volume of rapid lysis buffer (as in **3.2.2.3**). The remaining 900  $\mu\text{L}$  of the 1:10 stool suspension was mixed, centrifuged (5 min at 15,871 X g) to pellet all particulates, and then

the supernatant was removed. This pellet was resuspended in 90  $\mu$ L of rapid lysis buffer to produce the [reconstituted] stool DNA extract ("B"). Both tubes were boiled at 95°C for 15 min. Afterward, the stool DNA extract ("B") was diluted 1:10 in rapid lysis buffer to produce the 1:10 stool DNA extract ("C"). All three DNA extracts were then analyzed by RT-PCR (as described in **3.2.2.4**). This procedure was conducted independently 3 times.





**Figure 3.4. Flow chart describing the experiment used to determine whether the liquid phase DNA extract of a 10% stool suspension approximates the DNA found in the undiluted sample.**

A: liquid phase DNA extract, B: stool DNA extract (reconstituted), C: 1:10 stool DNA extract/

### **3.2.2.6 Baseline performance of DFS and RS RT-PCR protocol using live and HK cells**

To determine which cell suspensions should be used for subsequent viability RT-PCR experiments, a dilution series of live cells ranging from neat to  $10^{-6}$  was prepared and spiked into the liquid stool (as described in **3.2.1.3**). The spiked stools were processed using the DFS (as in **3.2.2.1**) and RS (as in **3.2.2.2**) methods before DNA was extracted using rapid lysis buffer (as in **3.2.2.3**) and analyzed by RT-PCR (as in **3.2.2.4**). This procedure was conducted independently three times.

### **3.2.3 Spiked stool and rectal swab viability RT-PCR**

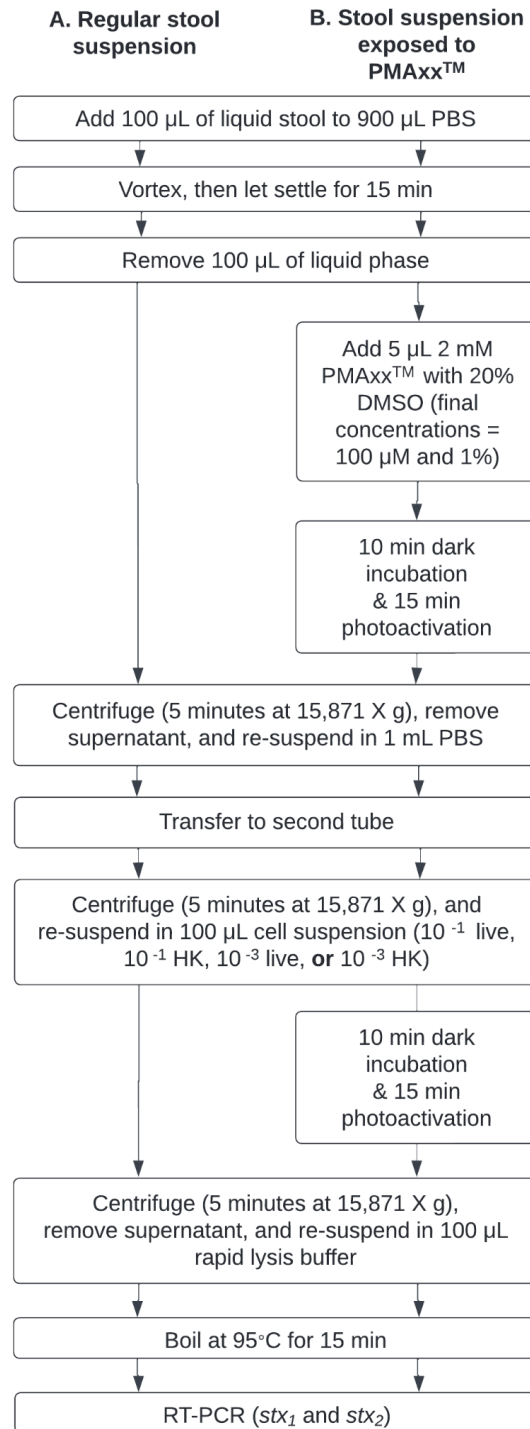
#### **3.2.3.1 Effect of tube transfer on cells treated with PMAxx™**

Live ( $10^{-3}$ ) cells were spiked into STEC-free liquid stool (**3.2.1.3**). The stool was prepared using the DFS (**3.2.2.1**) method, and three 100  $\mu$ L aliquots of the liquid phase were taken for use in the following conditions: no treatment, PMAxx™ treatment, and PMAxx™ treatment followed by transfer to a new tube. All steps involving PMAxx™ were performed in a dimly lit room.

Treatment involved the addition of 5  $\mu$ L of 2 mM PMAxx™ with 20% DMSO (final concentrations = 100  $\mu$ M PMAxx™ and 1% DMSO), placing the tubes in the dark for 10 min at room temperature, then conducting a 15 min photoactivation. For the tube transfer condition, the aliquot was centrifuged (5 min at 15,871 X g), the pellet was resuspended in 1 mL of PBS, and then the suspension was transferred to a new tube. All conditions were then centrifuged (5 min at 15,871 X g), the supernatants were removed, and the pellets were resuspended in 100  $\mu$ L of rapid lysis buffer before being boiled for 5 min at 95°C. Each DNA extract was analyzed RT-PCR (**3.2.2.4**). This procedure was conducted independently three times.

### 3.2.3.2 PMAxx™ interactions with substances in the liquid phase

To determine whether PMAxx™ adheres to substances that remain suspended in the liquid phase, a 10% suspension of the liquid STEC-free stool specimen was prepared (without spiking STEC) (**Figure 3.5**). After the suspension was left to settle for 15 min, eight 100 µL aliquots of the liquid phase were transferred to microcentrifuge tubes. Four 100 µL aliquots were subjected to a PMAxx™ treatment, which involved the addition of 5 µL of 2 mM PMAxx™ with 20% DMSO (final concentrations = 100 µM PMAxx™ and 1% DMSO), placing the tubes in the dark for 10 min, then conducting a 15 min photoactivation. The treated and untreated samples were centrifuged (5 min at 15,871 X g), the supernatants were removed, and then the pellets were resuspended in 1 mL of PBS. The samples were then each transferred to a fresh tube. In the new tubes, the samples were centrifuged (5 min at 15,871 X g), the supernatants were removed, and then the pellets were resuspended in 100 µL of live ( $10^{-1}$  or  $10^{-3}$ ) or HK ( $10^{-1}$  or  $10^{-3}$ ) cell suspensions (prepared as in **3.2.1.3**). After this, the set of tubes containing “PMAxx™ exposed liquid phase” were subjected to a 10 mins in the dark followed by a 15 min photoactivation. Afterward, the DNA from each sample was extracted using rapid lysis buffer (**3.2.2.3**) and analyzed by RT-PCR (**3.2.2.4**). This procedure was conducted independently three times.



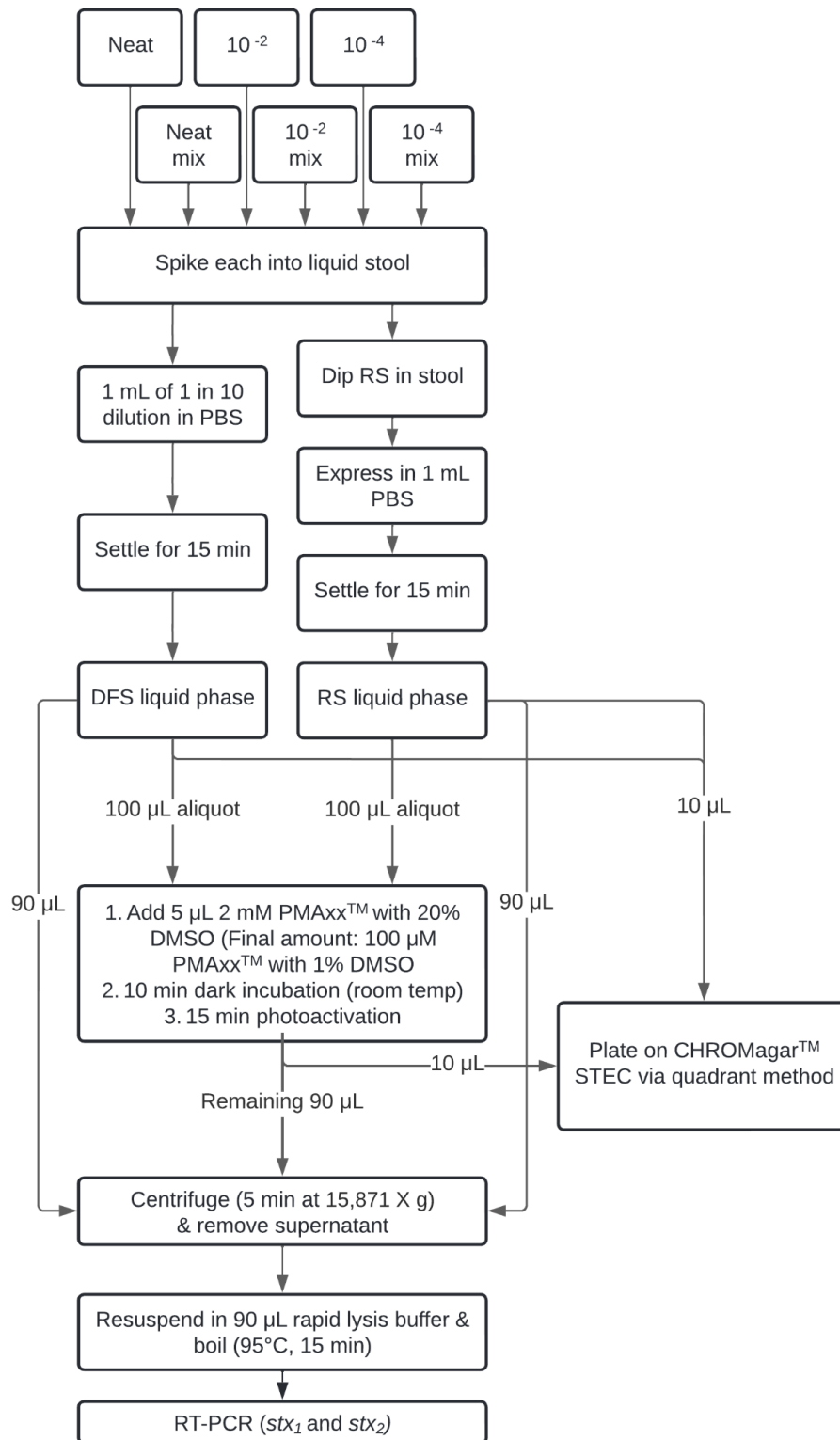
**Figure 3.5. Workflow used to determine whether PMAxx™ adheres to substances found in the liquid phase of a settled 10% stool suspension.**

### 3.2.3.3 Final viability RT-PCR protocol for spiked stool and rectal swab specimens

After the initial investigations above, the final DFS and RS viability RT-PCR protocols were established and tested using live and mixed (live and HK) suspensions (**Figure 3.6**). Live suspensions of neat,  $10^{-2}$  and  $10^{-4}$  were prepared, and HK cells were generated by boiling a 1 mL aliquot of the neat suspension (as in **3.2.1.3**). To combine the live and HK cells, an aliquot of each of the three live dilutions was centrifuged (5 min at 15,871 X g) and resuspended in an equal volume of the heat-killed suspension. The final ratios of HK to live cells were respectively 1:1, 100:1 and 10,000:1 for the neat mix,  $10^{-2}$  mix, and  $10^{-4}$  mix. Logarithmic ratios were chosen so a Ct value difference could be discerned more easily.

The live and mixed cell suspensions were spiked into liquid STEC-free stool (as in **3.2.1.3**) and were processed using the DFS (as in **3.2.2.1**) and RS (as in **3.2.2.2**) methods. All steps involving PMAxx™ were performed in a dimly lit room. Aliquots of each liquid phase were treated with 100 µM PMAxx™ and 1% DMSO. To achieve this, 5 µL of 2 mM PMAxx™ stock solution with 20% DMSO was added to 100 µL of each. Samples were briefly mixed, kept in the dark for 10 min at room temperature, and then subjected to a 15 min photoactivation. Afterward, 10 µL was streaked onto a CHROMagar™ STEC plate using the quadrant method (**3.2.1.4**), while the remaining 90 µL was centrifuged (5 min at 15,871 X g). After the supernatant was removed, the pellet was resuspended in 90 µL of rapid lysis buffer and boiled for 15 min at 95°C. The samples were then analyzed by RT-PCR (as described in **3.2.2.4**).

This procedure was conducted independently three times, and an aliquot of each untreated liquid phase was also analyzed by RT-PCR and plated on CHROMagar™ STEC in parallel each time.



**Figure 3.6. Flow chart describing how the final direct-from-stool and rectal swab viability real-time PCR protocols were tested using spiked stool.**

### 3.2.4 Microbiological clearance samples

#### 3.2.4.1 Specimens and inclusion criteria

A total of 30 unpreserved bulk stool samples from four patients undergoing microbiological clearance testing (as ordered by the Alberta Ministry of Health) were received from ProvLab (**Table 3.1**). The duration of STEC clearance was defined as the number of days from the first microbiological clearance stool sample to the last positive stool submission. As per Alberta's exclusion guidelines (16), a consecutive negative sample (taken > 24 hours after the first was collected) was used to confirm that each patient had successfully cleared their infection. Each specimen's collection date and consistency according to the Bristol stool scale (**Figure B.2** in **Appendix B**) were recorded. Stools were stored at 4°C until testing could be conducted.

**Table 3.1. Characteristics of the STEC microbiological clearance specimens used in this study.**

Patient	Number of stool submissions	STEC Serotype(s)	stx carriage	Colony appearance on CHROMagar™ STEC
A	7	O121:H19	<i>stx</i> <sub>2</sub> +	Mauve
B	12	O88:H25	<i>stx</i> <sub>1</sub> + & <i>stx</i> <sub>2</sub> +	No growth*
		O75:H38	<i>stx</i> <sub>1</sub> +	No growth*
		O145:HUN	<i>stx</i> <sub>2</sub> +	No growth*
C	4	O157:H7	<i>stx</i> <sub>2</sub> +	Mauve
D	7	O117:H7	<i>stx</i> <sub>1</sub> +	Mauve

Isolation, serotyping, and initial *stx* testing was performed by ProvLab

Non-O157 serotyping was performed by the National Microbiology Laboratory

HUN = undetermined H antigen

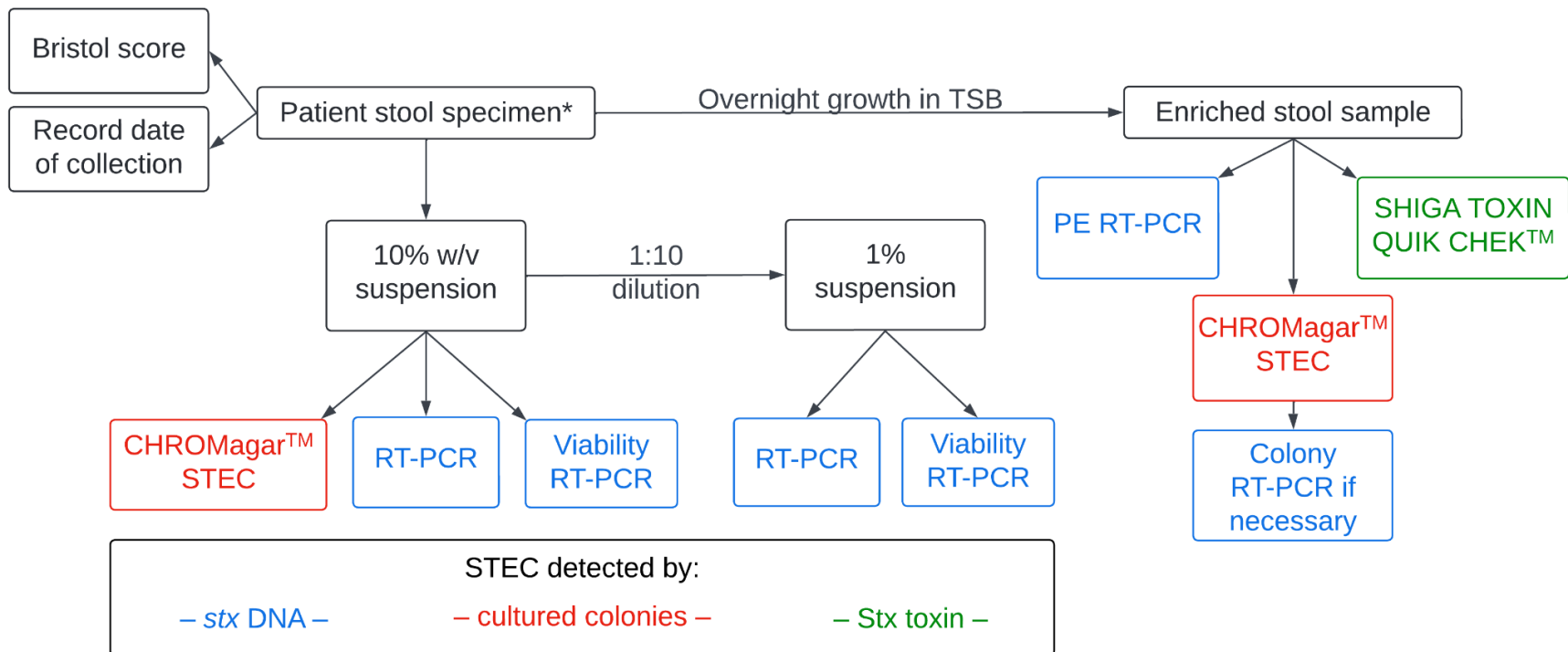
\*Strain isolated by ProvLab using MacConkey agar

Isolation of the causative strain(s) was conducted by ProvLab (**Figure B.1** in **Appendix B**) by plating each patient's first submission on either CHROMagar™ STEC (Patients A, C, and D) or MacConkey agar (Patient B). The isolates were tested for *stx*<sub>1</sub> and *stx*<sub>2</sub> by RT-PCR, and the O157 agglutination test was conducted. The non-O157 isolates were forwarded to the Canadian National Microbiology Laboratory for conventional serotyping. The microbiological clearance testing conducted by ProvLab on subsequent submissions for all patients involved a combination of CHROMagar™ STEC (except for Patient B) as well as post-enrichment RT-PCR where TSB was used as the enrichment medium.

#### **3.2.4.2 Microbiological clearance specimen testing**

All clinical stool submissions were tested once by each method described in **Figure 3.7**. First, a 10% w/v stool suspension in PBS was made from each. This was achieved by adding 300 mg of stool to 3 mL PBS in a sterile container. Each 10% suspension was left to settle for 15 mins at room temperature, and then three 100 µL aliquots of the liquid phase were transferred to 1.5 mL tubes. The first aliquot was used to create a 1 in 10 dilution (making a 1% suspension). Viability RT-PCR was performed on an aliquot of the 10% liquid phase and an aliquot of the 1% suspension. To do this, 100 µL was treated with 100 µM PMAxx™ and 1% DMSO by adding 5 µL of 2 mM PMAxx™ stock solution with 20% DMSO. The tubes were briefly mixed, placed in the dark for 10 min at room temperature, and then subjected to a 15 min photoactivation. The DNA was then extracted using rapid lysis buffer (as described in **3.2.2.3**) and analyzed for *stx* by RT-PCR (**3.2.2.4**). This process was repeated without PMAxx™ treatment to generate [conventional] RT-PCR results. To assess the relative bacterial load of the 10% suspension by culture, 10 µL was plated on CHROMagar™ STEC using the quadrant method (**3.2.1.4**).





**Figure 3.7. Workflow used to analyze clinical microbiological clearance stool specimens in this study.**

\*All stool specimens were first tested by ProvLab (See **Figure B.1** in **Appendix B**)

Bristol score: assessment of stool texture using **Figure B.2** in **Appendix B**

CHROMagar™ STEC: sample plated on differential media via quadrant method (**3.2.1.4**)

RT-PCR: sample DNA extracted (**3.2.2.3**) and analyzed for  $stx_1$  and  $stx_2$  (**3.2.2.4**)

Viability: RT-PCR conducted after treatment with 100  $\mu$ M PMAxx™ and 1% DMSO (**3.2.3.3**)

PE: post-enrichment; specimen grown in TSB overnight, then broth used for RT-PCR

Colony: isolated colony from CHROMagar™ STEC plate used for RT-PCR

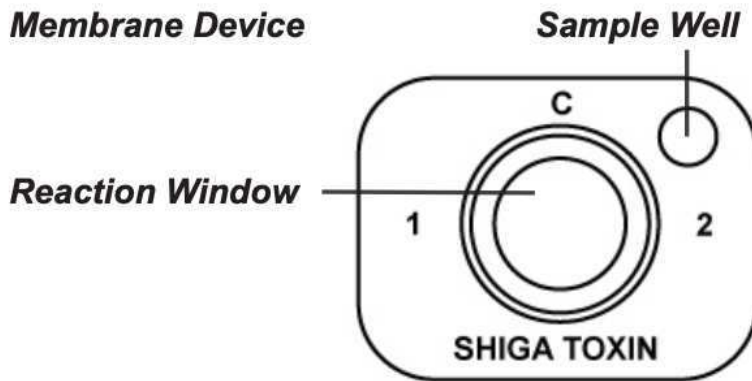
SHIGA TOXIN QUIK CHEK™: enzyme immunoassay used to detect Stx-1 and Stx-2

TSB: trypticase soy broth

The stool specimens were also enriched by adding a pea-sized amount of stool to 3 mL of tryptic soy broth (TSB) and incubating at 37°C overnight (20 hours). The next day, 100 µL of the enriched broth was used for rapid lysis buffer DNA extraction (3.2.2.3) and analyzed by RT-PCR (3.2.2.4). This is referred to as post-enrichment (PE) RT-PCR. A 10 µL loop of broth was also plated on CHROMagar™ STEC using the quadrant method (3.2.1.4).

When the growth on CHROMagar™ STEC plates (from either the 10% suspension or TSB-enrichment) was not distinctly mauve (e.g., grey or brown instead), RT-PCR was used to verify whether the colonies were *stx*-positive. To do this, a colony was sampled using a sterile wooden stick, added to 100 µL of rapid lysis buffer, and boiled for 15 min at 95°C before being analyzed by RT-PCR (3.2.2.4).

Lastly, SHIGA TOXIN QUIK CHEK™ (STQC; TechLab®, Blacksburg, Virginia, USA) was performed on the broth according to the manufacturer's instructions to determine if detectable levels of Shiga toxin (Stx-1 or Stx-2) were present (20). The *Diluent* (650 µL) and *Conjugate* (1 drop) provided in the kit were added to a glass test tube, then 100 µL of the broth was added via a transfer pipette. After gently mixing, 500 µL of this combination was added to the sample well of the STQC *Membrane Device* (Figure 3.8). The device was left at room temperature for 15 min to allow the sample to migrate. Next, 300 µL of *Wash Buffer* was added to the reaction window and allowed to absorb before 2 drops of *Substrate* were added to the reaction window. This was visualized after 10 mins to confirm the presence of a dotted blue control line (in the center of the window) and to assess whether solid lines could be seen on either the left (indicating Stx1 detection) or right (indicating Stx2 detection) side of the control line.



**Figure 3.8. Diagram of a SHIGA TOXIN QUIK CHEK™ membrane device.**  
Image from package insert (20)

### 3.2.5 Statistical analyses

Optimization experiments (i.e., all except for the clinical stool specimen testing in **3.2.4.2**) were conducted independently three times. All corresponding numerical data are expressed as mean  $\pm$  standard deviation. An ANOVA with post-hoc Tukey HSD was performed on the data in section **3.3.4**. The alpha-level was set to 0.05 for all statistical tests, and all analyses were performed using R Statistical Software (v4.1.2; R Core Team 2021).

## 3.3 Results

### 3.3.1 DNA extraction optimization for DFS and RS specimens

#### 3.3.1.1 Rapid lysis buffer versus MagaZorb® DNA Mini-Prep Kit

The effectiveness of the in-house rapid lysis buffer DNA extraction was compared with the MagaZorb® DNA Mini-Prep Kit and KingFisher™ mL Purification System. The  $stx_1$  Ct values generated from aliquots extracted by RLB were on average  $3.5 \pm 0.6$  lower than the Ct values of aliquots extracted using MZ-KF (**Table 3.2**). This was consistent across the cell concentrations ( $10^7$ ,  $10^5$ , and  $10^3$  CFU/mL) tested by all three conditions (PBS suspension, DFS, and RS).

**Table 3.2. Rapid lysis buffer (RLB) compared to MagaZorb® DNA Mini-Prep Kit and KingFisher™ mL Purification System (MZ-KF) for DNA extraction.**

Live cells* (Log CFU/mL)	Sample type and extraction method (Mean <i>stx</i> <sub>1</sub> Ct value ± SD)					
	PBS suspension		DFS LP		RS LP	
	RLB	MZ-KF	RLB	MZ-KF	RLB	MZ-KF
7	14.1 ± 0.2	18.5 ± 0.3	16.0 ± 0.6	19.3 ± 0.5	15.3 ± 0.5	18.4 ± 1.0
5	21.1 ± 0.1	24.7 ± 0.4	22.2 ± 0.7	26.4 ± 0.9	21.7 ± 0.8	25.3 ± 0.8
3	30.6 ± 0.4	32.9 ± 0.6	29.5 ± 0.8	32.8 ± 1.1	28.7 ± 0.8	32.0 ± 0.9

*stx*<sub>1</sub> Ct values represent 3 independent replicates

PBS suspension = cells in phosphate buffered saline

DFS = direct-from-stool (3.2.2.1)

RS = rectal swab (3.2.2.2)

LP = liquid phase

\*The concentrations reflect the number of cells in the DFS LP; the PBS suspension was diluted 1 in 10 for consistency

### 3.3.1.2 Liquid phase versus total stool sample DNA extraction

The procedure in **Figure 3.4** was performed independently three times to determine whether (“A”) liquid phase DNA extract (e.g., from the layer that forms at the top of a 10% stool suspension after 15 min of settling) accurately reflects the total amount of DNA in the stool sample. After the liquid phase aliquot was taken, the stool sample was reconstituted and extracted (“B”). Then this extract was diluted 1 in 10 (to produce “C”) for consistency with the liquid phase extract. The mean *stx*<sub>1</sub> Ct value of the liquid phase DNA extract (“A”,  $18.8 \pm 0.6$ ) was comparable to that of “C” ( $18.4 \pm 0.3$ ). On the other hand, the reconstituted extract (“B”) showed inhibition (two replicates had undetermined Ct values while the third Ct value was 22.2).

### 3.3.2 DFS and RS RT-PCR sensitivity for live cells

To establish the limit of detection (LOD) and determine which cell concentrations should be used to test the final viability RT-PCR protocols (**3.2.3.3**), serial dilutions of live cells were spiked into the STEC-free liquid stool and subject to the direct-from-stool and rectal swab protocols. For all of the cell concentrations tested, the DFS and RS conditions were within 1 Ct value of each other (**Table 3.3**). Both could detect live cells when they were spiked into stool at  $10^5$  CFU/mL (equivalent to  $10^4$  CFU/mL in the DFS liquid phase). The DFS and RS data points were slightly higher (2 - 4 Ct values for suspensions above the LOD) than the PBS suspensions (which were diluted 1:10 for consistency with the DFS concentrations).

**Table 3.3. Sensitivity of the direct-from-stool (DFS) and rectal swab (RS) protocols in detecting live cells spiked into liquid stool.**

Live cells spiked into liquid stool (Log CFU/mL)	STEC detection method (Mean $stx_1$ Ct value $\pm$ SD)		
	PBS*	Direct-from-stool	Rectal swab
8	16.0 $\pm$ 0.3	18.9 $\pm$ 0.5	17.8 $\pm$ 0.6
7	19.4 $\pm$ 0.1	22.3 $\pm$ 0.3	21.2 $\pm$ 0.5
6	22.8 $\pm$ 0.2	24.8 $\pm$ 0.7	24.9 $\pm$ 0.4
5	26.5 $\pm$ 0.3	29.7 $\pm$ 0.5	28.7 $\pm$ 0.4
4	28.0 $\pm$ 0.3	34.2 $\pm$ 1.1	34.3 $\pm$ 1.7

$stx_1$  Ct values represent 3 independent replicates

“----” indicates the limit of detection based on the 32 Ct cutoff established in Chapter 2 (2.3.1.1)

\*PBS: cells in phosphate buffered saline were diluted 1 in 10 for consistency with the DFS protocol; shown to highlight the effect of stool

### 3.3.3 DFS and RS PMAxx™ treatment optimization using spiked samples

#### 3.3.3.1 Tube transfer to improve live cell detection

The final viability RT-PCR protocol in **section 2.2.5** of **Chapter 2** included a tube transfer step prior to DNA extraction to preserve the detection of live cells. To assess whether this is necessary in the stool context, liquid stool was spiked with a relatively low concentration of live cells ( $10^5$  CFU/mL in the undiluted spiked stool, which is equivalent to  $10^4$  CFU/mL in the DFS liquid phase) and analyzed by the DFS procedure. The mean  $stx_1$  Ct value (N = 3) for the untreated spiked stool was  $28.7 \pm 0.6$ , whereas the aliquots treated with 100  $\mu$ M PMAxx™ with 1% DMSO had higher Ct values regardless of whether they were transferred to a new tube prior to extraction ( $32.5 \pm 2.4$ ) or not ( $33.6 \pm 1.7$ ).

### 3.3.3.2 PMAxx™ interactions with substances found in the liquid phase

The liquid phase (LP) generated from settled 10% stool suspensions was generally light yellow in color (**Figure 3.9**). This suggests that pigmented substances remain suspended even after 15 min of particulate settling. An experiment was conducted (as described in **Figure 3.5**) to determine whether PMAxx™ could attach to these substances in the LP and subsequently bind STEC DNA. When  $10^5$  CFU/mL HK cells were added to LP previously exposed to PMAxx™ there was a minor increase in Ct value compared to the control (**Table 3.4**). However, this effect was negligible ( $\pm 1$  Ct) for live cells.

**Control liquid phase**



**Liquid phase previously exposed to PMAxx™**



**Figure 3.9. Supernatant color of original liquid phase compared to liquid phase exposed to PMAxx™ after tube transfer and the addition of cells in PBS.**

An unspiked stool was prepared according to the DFS procedure, then an aliquot of the liquid phase (LP) was treated with 100  $\mu$ M PMAxx™ and 1% DMSO. Afterward the LP was transferred to a new tube, the tube was centrifuged, the supernatant was removed, and then cell suspensions in PBS were added.

**Table 3.4. Effect of exposing direct-from-stool liquid phase to PMAxx™ prior to adding live and HK cells.**

Cells added to LP (Log CFU/mL)		DFS LP treatment condition (Mean <i>stx</i> <sub>1</sub> Ct value ± SD)	
		Not exposed	Exposed to 100 μM PMAxx™ + 1% DMSO
Live	7	18.8 ± 0.6	17.2 ± 0.8
	5	23.7 ± 0.6	23.6 ± 0.7
HK	7	15.4 ± 0.7	15.8 ± 0.8
	5	22.6 ± 0.9	24.4 ± 1.2

*stx*<sub>1</sub> Ct values represent 3 independent replicates

LP: liquid phase generated from DFS procedure (3.2.2.1)

Exposed: An unspiked stool was prepared according to the DFS procedure, then an LP aliquot was treated with 100 μM PMAxx™ and 1% DMSO. Afterward the LP was transferred to a new tube, the tube was centrifuged, the supernatant was removed, and then cell suspensions in PBS were added.

### 3.3.4 DFS and RS viability RT-PCR performance for stools spiked with mixes of live and HK cells

The Ct values generated when the final DFS and RS viability RT-PCR protocols were applied to mixes of live and heat-killed cells spiked in stool are summarized in **Table 3.5**. The findings are the same for both protocols. For stools spiked with 10<sup>9</sup> CFU/mL live STEC, the Ct values of all conditions ([1] no treatment, [2] treatment, [3] no treatment + HK, and [4] treatment + HK) were statistically the same. For stool spiked with 10<sup>7</sup> CFU/mL live STEC, only the no treatment + HK condition was significantly lower ( $p < 0.05$ ) than the other Ct values.

For stool spiked with 10<sup>5</sup> CFU/mL live STEC, the no treatment + HK condition was significantly lower ( $p < 0.05$ ) than the other Ct values. However, the treatment (live only) condition at this concentration was also significantly higher than all other Ct values ( $p < 0.05$ ). All of these replicates were negative ( $> 32$ ).



**Table 3.5. Mean *stx*<sub>1</sub> Ct value for live and mixed cell suspensions spiked into stool and analyzed using the direct-from-stool and rectal swab RT-PCR and viability RT-PCR protocols.**

Cells spiked into liquid stool*		STEC detection method (Mean <i>stx</i> <sub>1</sub> Ct value ± SD)			
		Direct-from-stool		Rectal swab	
Live (Log CFU/mL)	Heat-killed (9 Log CFU/mL)	RT-PCR	Viability RT-PCR	RT-PCR	Viability RT-PCR
9	–	15.7 ± 0.5	16.2 ± 0.6	15.3 ± 0.3	15.8 ± 0.2
	+	15.2 ± 0.7	17.2 ± 1.2	14.8 ± 0.6	16.1 ± 0.1
7	–	22.6 ± 0.7	23.9 ± 0.7	22.0 ± 0.3	22.9 ± 0.6
	+	16.7 ± 1.1*	23.8 ± 0.9	16.8 ± 0.3*	22.6 ± 0.8
5	–	28.7 ± 0.6	33.6 ± 1.6*	28.8 ± 0.2	33.1 ± 0.2*
	+	16.5 ± 0.5*	25.6 ± 1.2	16.2 ± 0.5*	27.6 ± 1.7

*stx*<sub>1</sub> Ct values represent 3 independent replicates

Viability RT-PCR: sample treated with PMAxx™ before DNA extraction (3.2.3.3)

ANOVA analysis was conducted separately for each live cell concentration (delineated by horizontal lines) and method (DFS or RS)

\*indicates Ct values that were statistically different ( $p < 0.05$ ) from all others of the same live cell concentration and method

### 3.3.5 Analysis of microbiological clearance samples

#### 3.3.5.1 Patient A (O121:H19)

Patient A was infected by an O121:H19 strain that was positive for *stx*<sub>2</sub>. The day 8 stool submission was the last to be positive by any method (in this case, only the 1% RT-PCR and PE RT-PCR) (**Table 3.6**). All other methods were positive up to day 5. There was also a gradual upward trend in the RT-PCR and PE RT-PCR Ct values as sample submissions progressed, with the last positive date being the highest (see **Table C.1** in **Appendix C** for raw Ct values).

All of the viability RT-PCR Ct values were higher than their corresponding RT-PCR values for the 10% (min  $\Delta$ Ct = 0.8; max  $\Delta$ Ct  $\geq$  13.9) and 1% (min  $\Delta$ Ct = 2.5; max  $\Delta$ Ct = 6.5) suspensions (**Appendix C, Table C.1**). One 10% suspension and one 1% suspension showed potential false negative viability RT-PCR results (i.e., RT-PCR and PE RT-PCR were both positive, but the viability RT-PCR Ct  $\geq$  32).

RT-PCR detected the *stx*<sub>2</sub> gene in all five Patient A specimens, regardless of sample preparation (10%, 1%, or TSB-enriched). On the other hand, only four Patient A TSB-enriched specimens (days 0 - 5) were positive for Stx2 expression by STQC EIA. The mean PE RT-PCR Ct value of these samples was  $15.9 \pm 1.0$ .

**Table 3.6. Shiga toxin assay results for Patient A stool submissions.**

Days since first clearance submission	Bristol stool type	10% Stool		1% stool		TSB-enriched stool	
		<i>stx</i> <sub>2</sub> Ct		<i>stx</i> <sub>2</sub> Ct		<i>stx</i> <sub>2</sub> Ct	Stx
		RT-PCR	Viability RT-PCR	RT-PCR	Viability RT-PCR	PE RT-PCR	STQC EIA
0	4	22.3	23.6	23.3	25.8	15.4	Stx2+
2	4	26.1	–	25.2	29.5	15.4	Stx2+
3	3	25.1	28.6	25.1	31.6	17.4	Stx2+
5	4	26.7	27.5	25.5	29.4	15.5	Stx2+
8	4	31.4	–	29.8	–	22.1	–
-----							
11	5	–	–	–	–	–	–
17	3	–	–	–	–	–	–

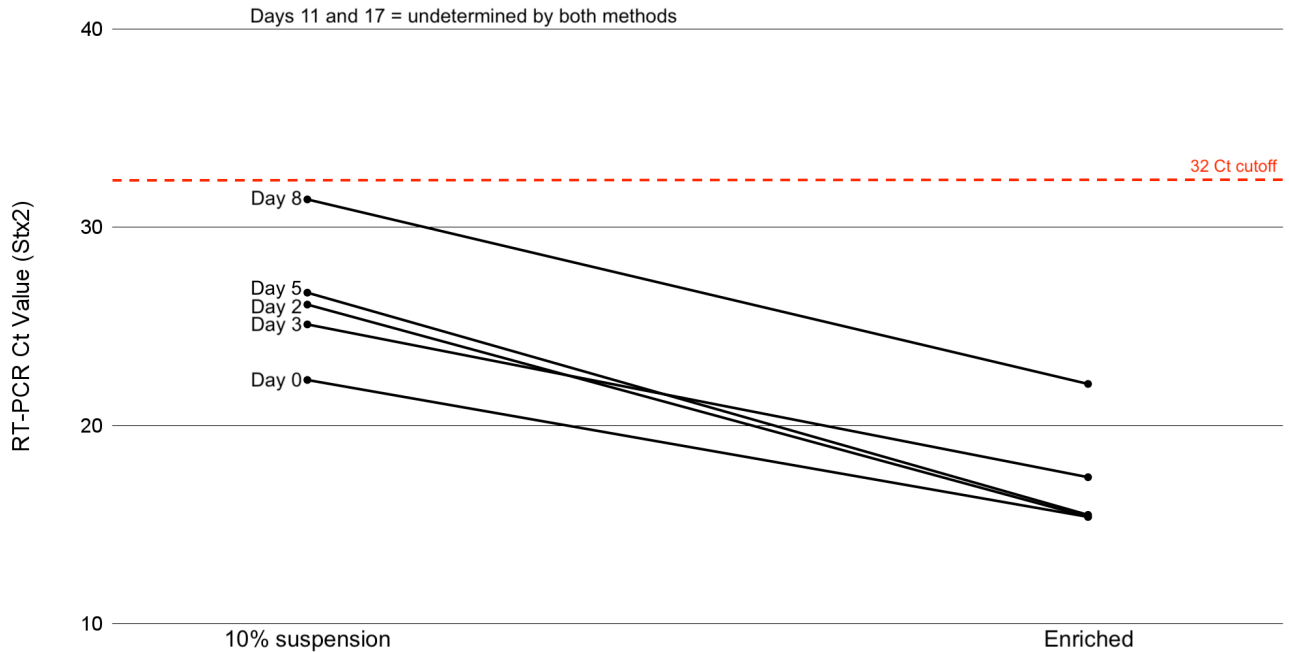
PE: Post-enrichment

STQC EIA: SHIGA TOXIN QUIK CHEK™ enzyme immunoassay.

“–” = Ct value was above the 32 Ct value cutoff. See **Table C.1** in **Appendix C** for raw Ct values.

“-----” Specimens below the dashed line were determined to be negative by ProvLab.

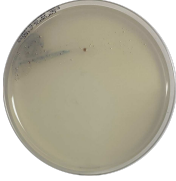

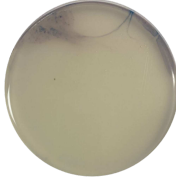
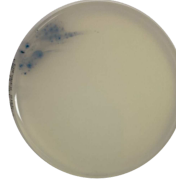
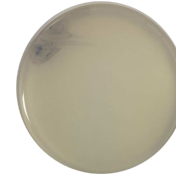









All Patient A specimens that tested positive for STEC showed a decreased *stx*<sub>2</sub> Ct value after TSB-enrichment compared to the 10% (-6.9 to -11.2) and 1% suspensions (-7.7 to -10.0) (Figure 3.10). This indicates that the organism grew overnight.



**Figure 3.10. RT-PCR *stx*<sub>2</sub> Ct values of Patient A 10% and TSB-enriched stool specimens.**

The O121:H19 organism infecting Patient A successfully grew mauve colonies on CHROMagar™ STEC (Table 3.7). In general, the samples that were enriched in TSB overnight showed more growth (1 - 2 more quadrants) compared to the 10% suspensions. However, the day 8 enriched specimen did not have mauve colonies (i.e., a potential false negative) despite the PE RT-PCR being positive.

**Table 3.7. Growth on CHROMagar™ STEC compared to RT-PCR Ct for Patient A 10% and TSB-enriched stool specimens.**

Sample	Days since first clearance submission						
	0	2	3	5	8	11	17
<b>Undiluted stool*</b>	Mauve colonies	Mauve colonies	Mauve colonies	Mauve colonies	Mauve colonies	No mauve colonies	No mauve colonies
<b>10% suspension</b>							
Quadrant	1 <sup>st</sup>	Smear - 1 <sup>st</sup>	Smear - 1 <sup>st</sup>	Smear - 1 <sup>st</sup>	Negative	Negative	Negative
RT-PCR <i>stx</i> <sub>2</sub> Ct	22.3	26.1	25.1	26.7	31.4	—	—
<b>TSB-Enriched</b>							
Quadrant	2 <sup>nd</sup>	2 <sup>nd</sup>	2 <sup>nd</sup>	2 <sup>nd</sup>	Negative	Negative	Negative
PE RT-PCR <i>stx</i> <sub>2</sub> Ct	15.4	15.4	17.4	15.5	22.1	—	—
STQC EIA	Stx2+	Stx2+	Stx2+	Stx2+	—	—	—

\*Undiluted stool refers to ProvLab's findings during testing

“---” indicates when the samples became negative according to ProvLab

Quadrant: the highest quadrant on CHROMagar™ STEC to show the growth of ≥ 3 mauve colonies

### 3.3.5.2 Patient B (Mixed infection)

Patient B was infected with 3 different STEC serotypes: O88:H25 ( $stx_1^+$  and  $stx_2^+$ ), O75:H38 ( $stx_1^+$  only), and O145:H undetermined ( $stx_2^+$  only). Their day 28 submission was the last to be positive by any method (i.e., only PE RT-PCR) (**Table 3.8**).

Only three Patient B 1% stool suspensions were positive by viability RT-PCR (day 17, 21, and 24), and none of the 10% suspensions were viability RT-PCR positive. The  $stx_2$  results in **Table 3.8** are paralleled (within a few Ct values) by the  $stx_1$  data shown in **Table C.2** in **Appendix C**. Given that PE RT-PCR was positive, there were 4 potential false-negative viability RT-PCR results for the 1% suspensions, and 7 for the 10% suspensions. The 1% suspension from day 10 was negative for both RT-PCR and viability RT-PCR which, given the high Ct value (31.9) of the corresponding 10% suspension, is likely attributable to a low bacterial load.

Three Patient B enriched specimens (Days 17, 21, and 24) were Stx2 positive by STQC EIA. These samples had a mean  $stx_2$  Ct value of  $12.9 \pm 0.4$ , which was lower than that of the enriched specimens that were not positive ( $17.8 \pm 5.1$ ). These Stx2 positive submissions had the lowest observed unenriched RT-PCR Ct values (10% and 1% suspensions) in the series, and were the only ones within the 32 Ct value cutoff when viability RT-PCR was performed on the 1% stool.

**Table 3.8. Shiga toxin assay results for Patient B stool submissions.**

Days since first clearance submission	Bristol stool type	10% Stool		1% stool		TSB-enriched stool		
		<i>stx</i> <sub>2</sub> Ct		<i>stx</i> <sub>2</sub> Ct		<i>stx</i> <sub>2</sub> Ct	Stx	
		RT-PCR	Viability RT-PCR	RT-PCR	Viability RT-PCR	PE RT-PCR	STQC EIA	
0	6	27.6	–	28.7	–	28.5	–	
5	6	30.6	–	31.5	–	14.1	–	
10	6	31.9	–	–	–	14.3	–	
12	6	27.9	–	30.6	–	15.2	–	
17	6	23.7	–	26	26.8	12.8	Stx2+	
19	6	27.1	–	29.7	–	20.1	–	
21	6	24.4	–	24.6	26.6	12.6	Stx2+	
24	6	–	–	24.2	25.5	13.3	Stx2+	
26	6	–	–	–	–	16.3	–	
28	6	–	–	–	–	16.3	–	
-----								
33	6	–	–	–	–	–	–	
38	6	–	–	–	–	–	–	

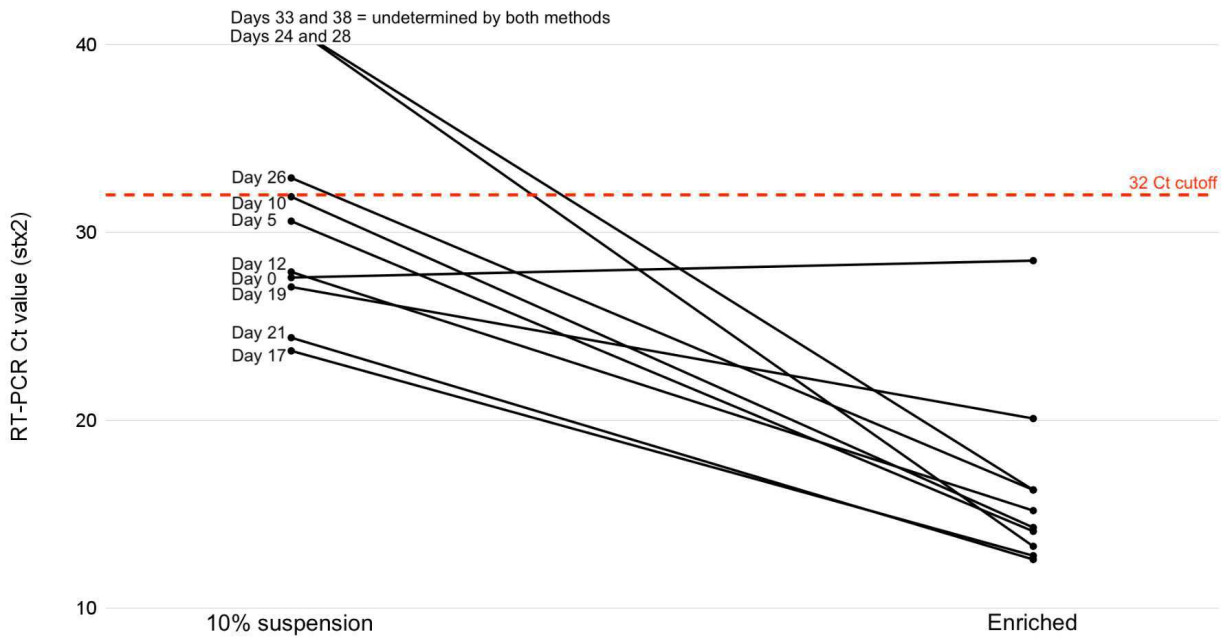
PE: Post-enrichment

STQC EIA: SHIGA TOXIN QUIK CHEK™ enzyme immunoassay.

“–” = Ct value was above the 32 Ct value cutoff. See **Table C.2** in **Appendix C** for raw *stx*<sub>1</sub> data, and **Table C.3** for raw *stx*<sub>2</sub> data.

“-----” Specimens below the dashed line were determined to be negative by ProvLab.

For all Patient B submissions except for the first, the PE RT-PCR *stx*<sub>2</sub> Ct values were consistently lower than that of the 10% (-7 to ≤ -26.7) and 1% suspensions (-9.6 to -20.4) (Figure 3.11). The similarity between the 10% suspension and the PE RT-PCR Ct values (27.6 and 28.5 respectively) for the day 0 submission suggests that the bacteria in that sample may have died during transport and storage.







**Figure 3.11. RT-PCR *stx*<sub>2</sub> Ct values of Patient B 10% and TSB-enriched stool specimens.**

No Patient B samples grew mauve colonies when either the 10% stool suspension or the enriched culture was plated on CHROMagar™ STEC; only blue colonies or no growth was observed (Table 3.9). This finding was corroborated by ProvLab’s unsuccessful attempt to culture all three isolated strains on CHROMagar™ STEC. Although blue colonies started appearing on the plates from days 21 to 38, colony PCR confirmed that these colonies were not *stx*-positive (Figure C.1 in Appendix C)



**Table 3.9. Growth on CHROMagar™ STEC compared to RT-PCR Ct for Patient B 10% and TSB-enriched stool specimens.**

Sample	Days since first clearance submission	
	0 (Representative of days 0 - 19)	28 (Representative of days 21 - 38)
<b>Undiluted stool*</b>	No growth	Blue colonies
<b>10% suspension</b>		
Quadrant	Negative	Negative
RT-PCR <i>stx</i> <sub>2</sub> Ct (range of other days)	$d_0 = 27.6$ (23.7 - 31.9)	$d_{28} \geq 32$ (23.3 - $\geq 32$ )
<b>TSB-Enriched</b>		
Quadrant	Negative	Negative <sup>†</sup>
PE RT-PCR <i>stx</i> <sub>2</sub> Ct (range of other days) STQC EIA	$d_0 = 28.5$ (12.8 - 20.1) $d_{17} = \text{Stx2}$	$d_{28} = 16.3$ (12.6 - 16.3) $d_{21}$ and $d_{24} = \text{Stx2}$

\*Undiluted stool refers to ProvLab's findings during testing

Quadrant: the highest quadrant on CHROMagar™ STEC to show the growth of  $\geq 3$  mauve colonies

<sup>†</sup>See **Appendix C, Figure C.1** for colony RT-PCR results (blue colony = *stx* neg)

### 3.3.5.3 Patient C (O157:H7)

Patient C was infected by an O157:H7 strain that was positive for *stx*<sub>2</sub> only (See **Table C.4** in **Appendix C** for raw *stx*<sub>2</sub>Ct values). They cleared their infection after day 7 according to PE RT-PCR (**Table 3.10**). The 10% and 1% stool suspensions were only positive on day 0. The day 7 RT-PCR results of the 1% and 10% suspensions constitute false negative results when compared to PE RT-PCR. This is also true of the viability RT-PCR results, which were negative on both day 0 and day 7 for both suspensions. Finally, no Patient C enriched specimens were positive by STQC EIA.

**Table 3.10. Shiga toxin assay results for Patient C stool submissions.**

Days since first clearance submission	Bristol stool type	10% Stool		1% stool		TSB-enriched stool	
		<i>stx</i> <sub>2</sub> Ct		<i>stx</i> <sub>2</sub> Ct		<i>stx</i> <sub>2</sub> Ct	Stx
		RT-PCR	Viability RT-PCR	RT-PCR	Viability RT-PCR	PE RT-PCR	STQC EIA
0	5	27.9	–	29.6	–	21.5	–
7	4	–	–	–	–	26.9	–
11	3	–	–	–	–	–	–
12	4	–	–	–	–	–	–

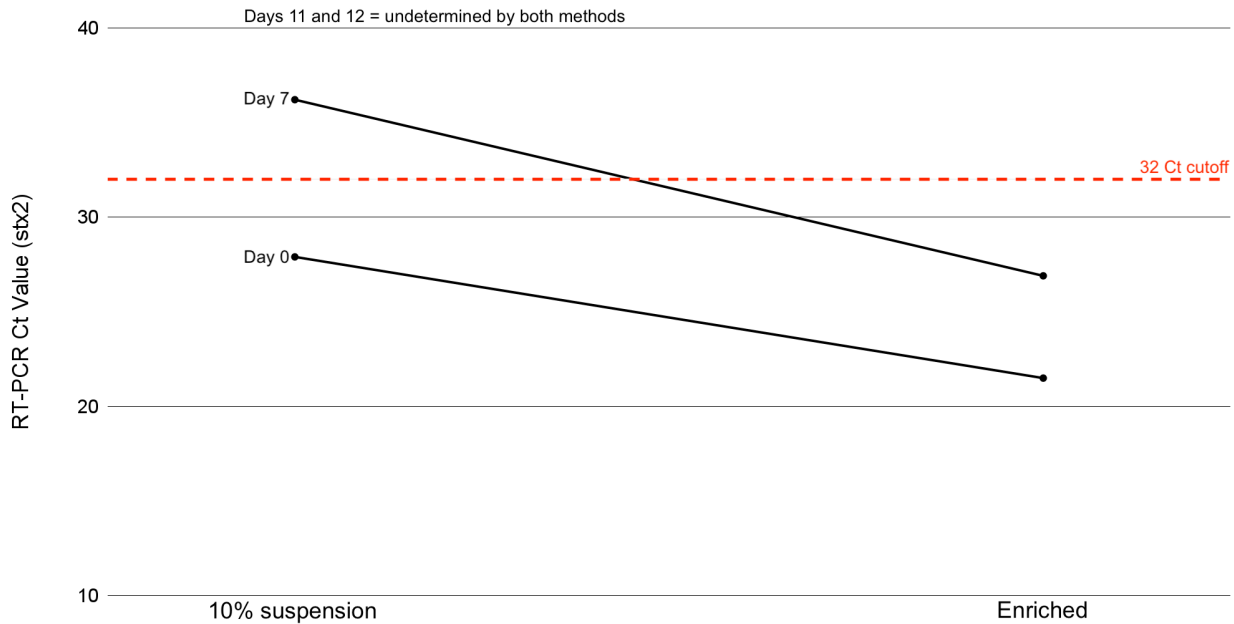
PE: Post-enrichment

STQC EIA: SHIGA TOXIN QUIK CHEK™ enzyme immunoassay.

“–” = Ct value was above the 32 Ct value cutoff. See **Table C.4** in **Appendix C** for raw Ct values.

“----” Specimens below the dashed line were determined to be negative by ProvLab

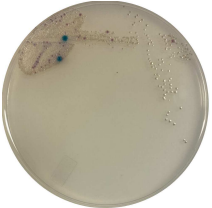


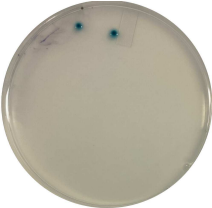

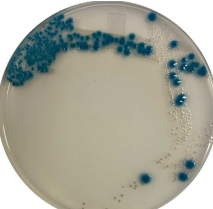
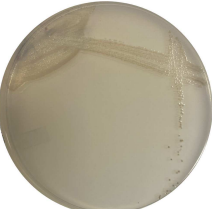

Both PE RT-PCR positive samples had decreased Ct values compared to the 10% and 1% suspensions, which suggests that the strain grew overnight (**Figure 3.12**).



**Figure 3.12. RT-PCR *stx*<sub>2</sub> Ct values of Patient C 10% and TSB-enriched stool specimens.**

The first submission (both 10% and enriched) and day 7 10% suspension were the only CHROMagar™ STEC plates for Patient C specimens with mauve colonies (**Table 3.11**), some of which were confirmed to be *stx*<sub>2</sub>-positive by colony RT-PCR (**Figures C.2 and C.3 in Appendix C**). The colony RT-PCR on a grey-mauve colony from the TSB-enriched day 7 plate was *stx*<sub>2</sub> negative (**Figure C.4**). This constitutes a false negative because the corresponding PE RT-PCR was positive. Although a representative grey-mauve colony was chosen, it is possible that other similar colonies were *stx* positive. Alternatively the blue colonies (i.e., other gram negative bacteria) may have masked STEC growth. Grey-mauve colonies also grew when the enriched day 11 and day 12 specimens were plated. Some were confirmed to be *stx*<sub>2</sub>-negative (**Figures C.5 and C.6**) which corresponds with the negative PE RT-PCR results. For Patient C specimens overall, enrichment in TSB did not seem to be correlated with growth in higher quadrants.

**Table 3.11. Growth on CHROMagar™ STEC compared to RT-PCR Ct for Patient C 10% and TSB-enriched stool specimens.**

Sample	Days since first clearance submission			
	0	7	11	12
<b>Undiluted stool*</b>	Mauve colonies	Mauve smear	No growth	No growth
<b>10% suspension</b>				
Quadrant	2 <sup>nd</sup> †	1 <sup>st</sup> †	Negative	Negative
RT-PCR <i>stx</i> <sub>2</sub> Ct	27.9	—	—	—
<b>TSB-Enriched</b>				
Quadrant	1 <sup>st</sup>	Negative †	Negative †	Negative †
RT-PCR <i>stx</i> <sub>2</sub> Ct	21.5	26.9	—	—

\*Undiluted stool refers to ProvLab's findings during testing

“—” indicates when the samples became negative according to ProvLab

†See **Figures C.2 - C.6** in **Appendix C** for colony PCR results

Quadrant: the highest quadrant on CHROMagar™ STEC to show the growth of ≥ 3 mauve colonies

All TSB-enriched broths were Stx neg by STQC EIA

#### **3.3.5.4 Patient D (O117:H7)**

Patient D was infected by an O117:H7 organism that was positive for *stx*<sub>1</sub> only. They were positive by RT-PCR, viability RT-PCR, and PE RT-PCR for at least 35 days (**Table 3.12**). This patient was likely positive for longer but stopped submitting specimens to ProvLab.

**Table 3.12. Shiga toxin assay results for Patient D stool submissions.**

Days since first clearance submission	Bristol stool type	10% Stool		1% stool		TSB-enriched stool	
		<i>stx</i> <sub>1</sub> Ct		<i>stx</i> <sub>1</sub> Ct		<i>stx</i> <sub>1</sub> Ct	Stx
		RT-PCR	Viability RT-PCR	RT-PCR	Viability RT-PCR	PE RT-PCR	STQC EIA
0	4	21.1	28.9	26.7	31.3	21.8	–
3	3	24.8	–	25.7	30.1	22.8	–
12	3	23.3	25.7	26.0	29.5	20.6	–
16	2	22.0	24.8	26.2	29.5	20.0	–
21	2	20.4	22.8	23.9	27.4	15.8	–
27	2	25.1	28.0	28.9	31.0	22.6	–
35	2	24.8	26.9	28.1	29.7	23.2	–

PE: Post-enrichment

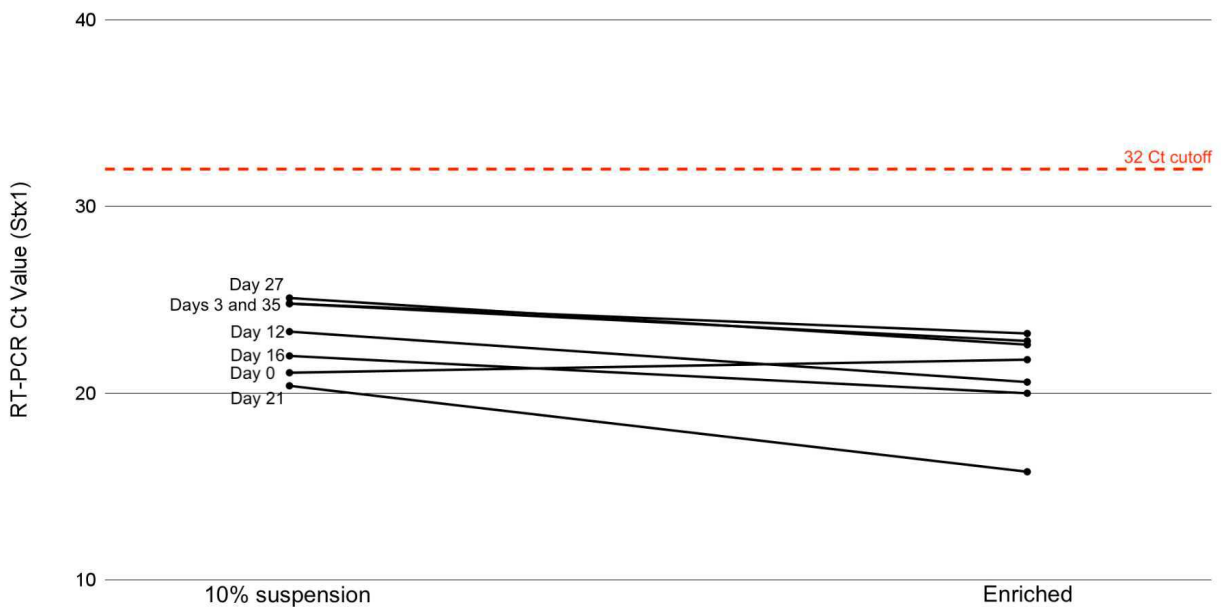
STQC EIA: SHIGA TOXIN QUIK CHEK™ enzyme immunoassay

“–” = Ct value was above the 32 Ct value cutoff. See **Table C.5** in **Appendix C** for raw Ct values.

“----” Specimens below the dashed line were determined to be negative by ProvLab.

Only one Patient D suspension (day 3, 10%) had a potential false negative associated with viability RT-PCR. For the other 10% and 1% suspensions, the increase in viability RT-PCR Ct values compared to the RT-PCR Ct values ranged from 1.6 to 4.6 (10% suspensions) and 1.6 to 4.6 (1% suspensions).

The range in differences between the PE RT-PCR Ct values compared to their corresponding 10% suspensions (range +0.7 to - 4.6) and 1% suspensions (range -2.9 to -8.1) suggests that not all samples were effectively enriched (**Figure 3.13**). Further, all of the RT-PCR and PE RT-PCR Ct values were within a relatively narrow range. Thus, there was no discernible relationship between later submission dates and Ct value.


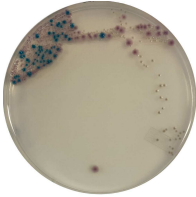
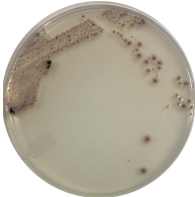

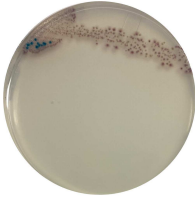


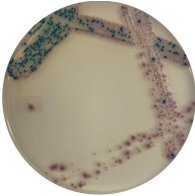

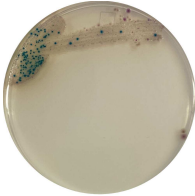
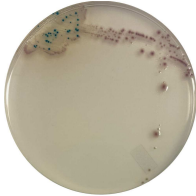

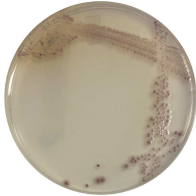
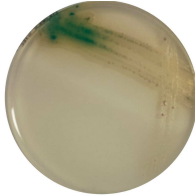


**Figure 3.13. RT-PCR *stx*<sub>1</sub> Ct values of Patient D 10% and TSB-enriched stool specimens.**

Patient D specimens readily grew mauve colonies on CHROMagar™ STEC (**Table 3.13**). Most days showed similar growth in the 10% and enriched specimens, whereas Days 0, 21, and 27 showed an increase of 1 - 2 quadrants.



**Table 3.13. Growth on CHROMagar™ STEC compared to RT-PCR Ct for Patient D 10% and TSB-enriched stool specimens.**

Sample	Days since first clearance submission						
	0	3	12	16	21	27	35
<b>Undiluted stool*</b>	Mauve colonies	Mauve colonies	Mauve colonies	Mauve colonies	Mauve colonies	Mauve colonies	Mauve colonies
<b>10% suspension</b>							
Quadrant	2 <sup>nd</sup>	2 <sup>nd</sup>	2 <sup>nd</sup>	2 <sup>nd</sup>	2 <sup>nd</sup>	2 <sup>nd</sup>	2 <sup>nd</sup>
RT-PCR <i>stx</i> <sub>1</sub> Ct	21.1	24.8	23.3	22.0	20.4	25.1	24.8
<b>TBS-enriched</b>							
Quadrant	4 <sup>th</sup>	2 <sup>nd</sup>	2 <sup>nd</sup>	2 <sup>nd</sup>	3 <sup>rd</sup>	3 <sup>rd</sup>	2 <sup>nd</sup>
RT-PCR <i>stx</i> <sub>1</sub> Ct	21.8	22.8	20.6	20.0	15.8	22.6	23.2

\*Undiluted stool refers to ProvLab's findings during testing

"---" indicates when the samples became negative according to ProvLab

Quadrant: the highest quadrant on CHROMagar™ STEC to show the growth of ≥ 3 mauve colonies

All TSB-enriched broths were Stx neg by STQC EIA

### 3.3.5.5 Summary of positive stool samples by microbiological clearance detection method.

**Table 3.14. Summary of STEC positive microbiological clearance stool samples by testing method.**

Patient (STEC pos stools, n <sup>†</sup> ) Strain(s) Serotype - <i>stx</i> type	Bristol stool form score	Number of STEC positive stool samples per patient							
		10% stool			1% stool		TSB-enriched stool		
		CHROM -agar <sup>™</sup> STEC (Culture)	RT-PCR ( <i>stx</i> )	Viability RT-PCR ( <i>stx</i> )	RT-PCR ( <i>stx</i> )	Viability RT-PCR ( <i>stx</i> )	CHROM -agar <sup>™</sup> STEC (Culture)	PE RT-PCR ( <i>stx</i> )	STQC (Stx)
<b>Patient A (5)</b> O121:H19 - <i>stx</i> <sub>2</sub>	3 - 5	4	5	3	5	4	4	5	4
<b>Patient B (10)</b> O88:H25 - <i>stx</i> <sub>1</sub> & <i>stx</i> <sub>2</sub> O75:H38 - <i>stx</i> <sub>1</sub> O145:HUN - <i>stx</i> <sub>2</sub>	6	NG	7	0	7	3	NG	10	3
<b>Patient C (2)</b> O157:H7 - <i>stx</i> <sub>2</sub>	3 - 5	2	1	0	1	0	1	2	0
<b>Patient D (7)</b> O117:H7 - <i>stx</i> <sub>1</sub>	2 - 4	7	7	6	7	7	7	7	0
<b>Total (24)</b>	–	13	20	9	20	14	12	24	7

<sup>†</sup>Number of STEC positive stool samples according to Provlab (undiluted specimen on CHROMagar<sup>™</sup> STEC and/or PE RT-PCR)  
Bristol stool form score: from a scale defining range of specimen textures (**Figure B.2 in Appendix B**)

TSB: trypticase soy broth

NG: isolated strains do not grow on CHROMagar<sup>™</sup> STEC

PE: Post-enrichment

STQC EIA: SHIGA TOXIN QUIK CHEK<sup>™</sup> enzyme immunoassay

### **3.4 Discussion**

#### **3.4.1 Direct-from-stool and Rectal Swab sample preparation**

Detecting STEC directly from stool presents several challenges. Stools are highly complex specimens which can vary depending on a person's diet and microflora. They contain PCR inhibitors, such as complex polysaccharides (e.g., from vegetables), bile salts, lipids, and urate (21). They also can vary in texture, ranging from pure liquid with no solid pieces to hard clumps (See **Appendix B, Figure B.2**). For these reasons, direct-from-stool RT-PCR assays usually involve a dilution step before or after the DNA extraction process. Previous studies have shown that highly turbid complex samples can interfere with the photoactivation of viability dyes, so stool dilution is especially important in the context of viability RT-PCR (22). The use of 10% stool suspensions for DNA extraction prior to RT-PCR is common in diagnostic microbiology (23,24).

A protocol for rectal swabs (RS) was also developed in this study because major Canadian hospitals have begun implementing RS for pediatric inpatients with diarrhea (26). This collection method is easier for health care practitioners (26) and performs comparably to bulk stool (27,28). A successful viability RT-PCR assay would be especially beneficial in this context given the need for a quick turnaround time.

If a 10% stool or expressed RS suspension is left standing for a brief period of time, larger pieces of stool particulate will settle at the bottom while DNA and bacterial cells remain suspended in the "liquid phase". The data in **3.3.1.2** show that liquid phase DNA extract (generated from 10% stool suspensions that were left to settle for 15 mins) reflects the Ct value of the corresponding total sample DNA extract after a 1 in 10 dilution. Thus, this method of removing large particulates before DNA extraction is acceptable.

The similarity ( $\pm 2$  Ct values) between the conventional RT-PCR Ct values of RS DNA extracts and the corresponding DFS DNA extracts suggests that the RS procedure used here had an effect comparable to a 1 in 10 dilution (**Table 3.3** and **Table 3.5**). Given that RS were dipped directly into the spiked stool and then expressed in 1 mL PBS, this suggests that it was able to transfer (i.e., take up and release during expression)  $\sim 100$   $\mu$ L of stool sample. This is consistent with what studies have found for Copan FLOQ swabs using other bacteria (29,30).

### 3.4.2 DNA Extraction

The MagaZorb<sup>®</sup> DNA Mini-Prep Kit uses magnets coated with DNA-binding antibodies to isolate DNA from complex samples. The kit can be used in conjunction with The KingFisher<sup>™</sup> mL Purification System, which uses inducible electromagnets to purify the DNA from samples. When used together, DNA can be extracted from up to 15 samples in less than an hour. Alternatively, in-house rapid lysis buffer (RLB) may serve as a more cost-effective DNA extraction option which requires no specialized equipment and can be completed in approximately 15 min. However, RLB DNA extraction occurs in one tube and does not include wash steps, so DNA extracts may contain contaminants.

The DNA extracts generated by the MagaZorb<sup>®</sup> DNA Mini-Prep Kit and KingFisher<sup>™</sup> mL Purification System (MZ-KF) had a higher average Ct value ( $\sim 3$ ) than the RLB DNA extracts (**Table 3.2**). A repeat DNA extraction using a different MZ kit showed the same trend, suggesting that this difference was not attributable to the underperformance of one lot of antibody-coated magnetic beads (MagaZorb<sup>®</sup> reagent). Instead, it is likely that the two 1 mL wash steps in the MZ-KF protocol caused a certain proportion of DNA to be lost during the purification process. Given the shorter processing time, equipment availability, and lower Ct

values seen with RLB compared to MZ-KF, RLB was chosen as the DNA extraction method for the rest of the project.

### 3.4.3 PMAxx™ and spiked stool

In Chapter 2 (**Table 2.10**), it was observed that some PMAxx™ was capable of adhering to the interior of microcentrifuge tubes (presumably via electrostatic interactions between the dye's positive charge and the plastic) and subsequently binding DNA from HK cell suspensions in PBS. In the stool context, some substances from the specimen will remain suspended in the liquid phase even after 15 mins of settling (see the yellow colour of the untreated liquid phase in **Figure 3.9**). The HK cell results (**Table 3.4**) suggest that a very small proportion of the dye may have also been able to associate with substances in the liquid phase and bind HK cell DNA. However, this effect was negligible when live cells were used, suggesting that the dye did not stay active long to affect live cells during subsequent DNA extraction.

Stool can contain a large amount of DNA (i.e., from the patient and their gut microbiome). It is possible that this may cause excess PMAxx™ to become inert quicker after photoactivation than was seen in cell suspensions in PBS (**Table 2.9**). Thus, it is possible that the tube transfer step implemented before DNA extraction in Chapter 2's viability RT-PCR protocol may not be needed in the stool context. In **3.3.3.2**, tube transfer was found to minorly help preserve the detection of live cells spiked into stool, but both conditions treated with PMAxx™ showed an increased Ct value compared to the untreated control. A transfer step was ultimately not included in the final DFS and RS protocols as a way of simplifying the procedures and ensuring that no STEC would be lost during tube transfer.

A STEC-free liquid stool was spiked with mixtures of live and HK cells to test the effectiveness of the final DFS and RS viability RT-PCR protocols. This was done to determine whether live cells could be selectively detected, and to predict how sensitive the assay would be when applied to clinical samples. The DFS (**Table 3.5**) and RS results mirror what was seen in the final viability RT-PCR protocol that was applied to pure culture (**2.3.9**). Although the dye is successful in eliminating the contaminating signal of HK cells, it can produce false negative results at low loads of live bacteria. Unlike in pure culture, the Ct increase associated with PMAxx™ treatment on low concentrations of live cells in the DFS and RS protocols was statistically significant ( $p < 0.05$ ). Based on the data here, it cannot be known exactly why false negative (i.e., increasing above the 32 Ct value cutoff because of treatment) results were generated when PMAxx™ (and DMSO) was applied to  $10^4$  live CFU/mL spiked in stool. Since the cells used in these experiments were freshly grown they should have had stable membrane integrity. This effect on live cells, then, may have occurred because a small proportion of PMAxx™ passively crossed intact membranes (which DMSO may have facilitated), or the dye associated with the cell membranes, tube interior, and substances in the liquid phase and then bound DNA during extraction.

### **3.4.4 Microbiological clearance testing methods: detection rate, sensitivity, and limitations**

#### **3.4.4.1 Post-enrichment (PE) RT-PCR**

At present, PE RT-PCR is used by ProvLab for microbiological clearance testing when the STEC strain infecting a patient is known to not grow successfully on CHROMagar™ STEC. This involves inoculating the specimen into trypticase soy broth (TSB), incubating overnight, then using an aliquot of the broth for *stx* testing.

PE RT-PCR was the most sensitive assay used in this study and detected all 24 STEC positive samples (**Table 3.14**). Across all of the patients it was the method that was positive the longest (or was on par with the other methods used), and in several instances it was the only positive assay. For Patients A, B, and C it was associated with at least a 6 Ct value decrease compared to the 10% suspensions. Crucially, it was successful for Patient B specimens, which could not grow on CHROMagar™ STEC. Further discussion of PE RT-PCR can be found in **Chapter 4**.

#### **3.4.4.2 Direct-from-stool viability RT-PCR**

For the microbiological clearance specimens, generally when the conventional RT-PCR Ct value was higher, then the viability RT-PCR was more likely to be negative. Using PE RT-PCR as a reference for positivity, there were several potential false negative viability RT-PCR results in the 10% (A: 2/5; B: 7/7; C: 2/2; D: 1/7) and 1% (A: 1/5; B: 4/7; C: 2/2; D: 0/7) suspensions. It is possible that the 10% and 1% suspensions reflected a sampling error. However, since these samples successfully grew in TSB it is more likely that PMAxx™ had a negative effect (i.e., inflated the Ct value) on the low number of live cells present as was seen in the spiked stools (**Table 3.5**).

A STEC-free liquid stool was chosen for the initial spiking experiments to help ensure a uniform dispersion of bacteria in the sample. However, microbiological clearance specimens are usually semi-solid to solid in texture because such patients are nearing the end of their STEC infection. Although RT-PCR inhibition was not suspected when the liquid spiked stool was used, inhibition may have been a factor when clinical specimens were analyzed. Rapid lysis buffer was initially deemed a sufficient DNA extraction method for this project based on the performance with the liquid stool, but lingering stool substances (that might have been removed more effectively by other DNA extraction methods) may have negatively affected detection. The variable detection

frequency between patients (**Table 3.14**) suggests that patient factors (e.g., diet habits and bile levels) may also impact viability RT-PCR.

Ultimately the DFS viability RT-PCR protocol's inconsistent performance across patients and potential for false-negative results at low loads of live STEC means that it is unsuitable for microbiological clearance testing. A more thorough discussion of this matter is presented in **Chapter 4**.

#### **3.4.4.3 CHROMagar™ STEC**

CHROMagar™ STEC is a major method used for microbiological clearance testing in Alberta. When inoculated onto the media, STEC are supposed to form mauve colonies whereas other Enterobacteriaceae form blue colonies. However, many non-O157 strains grow atypically (e.g., form grey colonies) or are not able to grow on the media at all (17). This is problematic given that recent estimates suggest that non-O157 strains contribute to half of all STEC infections (31). Several studies suggest that tellurite resistance—which is a feature thought to be common to most O157 and many “top 6” non-O157 strains—is one of the characteristics that the media's proprietary formulation selects for (17,32). It is likely that other selective features, bacterial load, and interactions with other bacteria further contribute to whether growth on CHROMagar™ STEC is successful.

The strains in this study showcase the possible outcomes associated with CHROMagar™ STEC. Patient D (O117:H7) samples consistently showed prototypical mauve growth (**Table 3.12**). Although some Patient A (O121:H19) and C (O157:H7) specimens produced mauve growth, at times this appeared as a smear or the colonies were a duller mauve that mimicked



other *stx*-negative colonies (**Table 3.13**). To overcome this issue it is important that when colony RT-PCR is conducted from a CHROMagar™ STEC plate, multiple colonies are tested (even if they appear the same) or a sweep of the colonies is used. None of the Patient B STEC strains (O88:H25, O75:H38, and O145:H undetermined) grew on the media. This is concerning given that the O145 serotype is among the top 6 most common non-O157 serotypes found in North America. Together these results emphasize the utility of screening patient samples for *stx* DNA or Stx protein via culture-independent methods, and the importance of including secondary culture methods (e.g., MacConkey agar) and PE RT-PCR in STEC testing protocols.

#### **3.4.4.4 SHIGA TOXIN QUIK CHEK™ (STQC)**

STQC is an enzyme immunoassay which qualitatively detects and differentiates Stx1 and Stx2 proteins. It has been documented to have a low sensitivity, especially for some toxin subtypes (33). For this reason, it is recommended that specimens be enriched (e.g., in TSB as done here) overnight before being analyzed by STQC (34). Although STQC is not used for microbiological clearance testing, it was included for comparison because it is approved (alongside culture and NAATs) by the CPHLN for STEC screening (34).

Only two patients in the study had samples with Stx expression detectable by STQC. Patient A STQC positive samples were consistently ~3 Ct values higher than Patient B STQC positive samples. Thus, the O121:H19 strain in Patient A samples likely expressed more of the toxin compared to the Stx2-expressing strain in Patient B samples.

In all, the relatively high Ct values observed in this study's microbiological clearance samples and the relatively low Ct value needed for STQC positivity reinforces that this assay is

unsuitable for the clearance context. Although active infections are more likely to have a higher bacterial load (and thus higher levels of toxin expression), false-negative STQC results could still be possible during initial diagnosis.

#### **3.4.4.5 Duration of microbiological clearance**

It is estimated that the median STEC microbiological clearance time (i.e., from symptom onset to negative stool) is around 17 days (35,36). Thus, STEC shedding can be categorized as “short carriage” (< 2.5 weeks) or “long carriage” ( $\geq$  2.5 weeks) (14). In rare cases, “long carriage” can last several months (14,36). Since this project did not include a chart review to identify when each patient’s symptoms started, clearance times only consider the time from the first microbiological clearance sample to the last positive submission. Patient A (O121:H19) and C (O157:H7) were “short” carriers because their clearance times were 8 and 7 days respectively. On the other hand, Patient B (O88:H25, O75:H38, and O145:HUN) and D (O117:H7) were “long” carriers with clearance times of 28 and  $\geq$  35 days respectively. It is likely that the strains infecting Patient B cleared at slightly different times, but this order cannot be determined because their specimens were consistently positive for both *stx*<sub>1</sub> and *stx*<sub>2</sub>.

Patient D stopped submitting specimens before they had fully cleared their infection. Although the exact reason is unknown, this occurrence emphasizes the adverse effects exclusion requirements can have on patients’ ability to maintain their income and business’ ability to operate. There continue to be discussions in the literature and amongst policy makers about how to reasonably balance protecting the public’s safety with supporting a patient’s return to work. For example, Norway’s 2016 guidelines differentiate between “low-virulent STEC” (e.g., adults with *stx*<sub>1</sub>) and “high-virulent STEC” (e.g., *stx*<sub>2a</sub>, *stx*<sub>2c</sub>, *stx*<sub>2d</sub>, or HUS-associated) infections

(38). Those with “high-virulent” infections must complete microbiological clearance testing similar to what is conducted in Alberta (submissions until negative), whereas those with “low-virulent” infections do not have to submit specimens and are only required to exclude themselves until 48 hours after their diarrhea ends. Under these rules Patient D would have been classified as a “low-virulent” STEC case and would have returned to work much sooner. Crucially, in the 3 years following the implementation of Norway’s new policy, no secondary infections were linked to “low-virulent” STEC index cases. The microbiological clearance landscape will likely evolve as more data emerges on this topic.

### **3.5 Conclusion**

Viability RT-PCR assays were developed for direct-from-stool and rectal swab applications, then the DFS protocol was tested using clinical microbiological clearance specimens. Both the DFS and RS approaches successfully eliminated the detection of heat-killed cells spiked into stool, but consistently produced false-negatives when live cells were spiked at  $10^5$  CFU/mL stool. A tube transfer before DNA extraction was not found to meaningfully reduce this effect. Since microbiological clearance specimens often have a low bacterial load, this issue translated into presumed false-negative results in several cases. For this reason the viability RT-PCR assay developed here should not be implemented for microbiological clearance testing.

Post-enrichment PCR is a more promising alternative because it was the most sensitive assay tested in this project and can be used for STEC strains that do not grow on CHROMagar™ STEC.

### 3.6 References

1. Gyles CL. Shiga toxin-producing *Escherichia coli*: An overview. *J Anim Sci*. 2007 Mar 1;85(suppl\_13):E45–62.
2. Awofisayo-Okuyelu A, Brainard J, Hall I, McCarthy N. Incubation Period of Shiga Toxin–Producing *Escherichia coli*. *Epidemiol Rev*. 2019 Oct 16;41(2):121–9.
3. Freedman SB, Eltorki M, Chui L, Xie J, Feng S, MacDonald J, et al. Province-Wide Review of Pediatric Shiga Toxin-Producing *Escherichia coli* Case Management. *J Pediatr*. 2017 Jan 1;180:184–90.
4. Johannes L, Römer W. Shiga toxins — from cell biology to biomedical applications. *Nat Rev Microbiol*. 2010 Feb;8(2):105–16.
5. Alberta Health Services - *E. coli* (STEC) Info for Health Care Providers [Internet]. [cited 2022 Nov 4]. Available from:  
<https://www.albertahealthservices.ca/assets/info/hp/diseases/if-hp-dis-ecoli-stec.pdf>
6. Bauwens A, Kunsmann L, Karch H, Mellmann A, Bielaszewska M. Antibiotic-Mediated Modulations of Outer Membrane Vesicles in Enterohemorrhagic *Escherichia coli* O104:H4 and O157:H7. *Antimicrob Agents Chemother*. 61(9):e00937-17.
7. Bielaszewska M, Idelevich EA, Zhang W, Bauwens A, Schaumburg F, Mellmann A, et al. Effects of Antibiotics on Shiga Toxin 2 Production and Bacteriophage Induction by Epidemic *Escherichia coli* O104:H4 Strain. *Antimicrob Agents Chemother*. 2012 Jun;56(6):3277–82.
8. Freedman SB, Xie J, Neufeld MS, Hamilton WL, Hartling L, Tarr PI, et al. Shiga Toxin-Producing *Escherichia coli* Infection, Antibiotics, and Risk of Developing Hemolytic Uremic Syndrome: A Meta-analysis. *Clin Infect Dis Off Publ Infect Dis Soc Am*. 2016 15;62(10):1251–8.
9. Hickey CA, Beattie TJ, Cowieson J, Miyashita Y, Strife CF, Frem JC, et al. Early Volume

- Expansion During Diarrhea and Relative Nephroprotection During Subsequent Hemolytic Uremic Syndrome. *Arch Pediatr Adolesc Med*. 2011 Oct;165(10):884–9.
10. Ardissino G, Tel F, Possenti I, Testa S, Consonni D, Paglialonga F, et al. Early Volume Expansion and Outcomes of Hemolytic Uremic Syndrome. *Pediatrics*. 2016 Jan;137(1).
  11. Baker CA, Rubinelli PM, Park SH, Carbonero F, Ricke SC. Shiga toxin-producing *Escherichia coli* in food: Incidence, ecology, and detection strategies. *Food Control*. 2016 Jan 1;59:407–19.
  12. Locking ME, Pollock KGJ, Allison LJ, Rae L, Hanson MF, Cowden JM. *Escherichia coli* O157 Infection and Secondary Spread, Scotland, 1999–2008. *Emerg Infect Dis*. 2011 Mar;17(3):524–7.
  13. Rangel JM, Sparling PH, Crowe C, Griffin PM, Swerdlow DL. Epidemiology of *Escherichia coli* O157:H7 Outbreaks, United States, 1982–2002. *Emerg Infect Dis*. 2005 Apr;11(4):603–9.
  14. Bai X, Mernelius S, Jernberg C, Einemo I, Monecke S, Ehricht R, et al. Shiga Toxin-Producing *Escherichia coli* Infection in Jönköping County, Sweden: Occurrence and Molecular Characteristics in Correlation With Clinical Symptoms and Duration of stx Shedding. *Front Cell Infect Microbiol*. 2018 May 1;8:125.
  15. Scavia G, Gianviti A, Labriola V, Chiani P, Maugliani A, Michelacci V, et al. A case of haemolytic uraemic syndrome (HUS) revealed an outbreak of Shiga toxin-2-producing *Escherichia coli* O26:H11 infection in a nursery, with long-lasting shedders and person-to-person transmission, Italy 2015. *J Med Microbiol*. 67(6):775–82.
  16. Alberta Health. Alberta Public Health Disease Management Guidelines - *Escherichia coli* Verotoxigenic Infections [Internet]. 2021. Available from: <https://open.alberta.ca/dataset/2b77e542-cfcb-4f93-b825-dca7d140e024/resource/b3c01b4a-8541-47fa-a19a-b7c3835a1cee/download/health-phdmg-escherichia-coli-verotoxigenic-infections-2021-11.pdf>

17. Fan R, Bai X, Fu S, Xu Y, Sun H, Wang H, et al. Tellurite resistance profiles and performance of different chromogenic agars for detection of non-O157 Shiga toxin-producing *Escherichia coli*. *Int J Food Microbiol*. 2018 Feb 2;266:295–300.
18. Hirvonen JJ, Siitonen A, Kaukoranta SS. Usability and Performance of CHROMagar STEC Medium in Detection of Shiga Toxin-Producing *Escherichia coli* Strains. *J Clin Microbiol*. 2012 Nov;50(11):3586–90.
19. Bording-Jorgensen M, Parsons BD, Tarr GA, Shah-Gandhi B, Lloyd C, Chui L. Association of Ct Values from Real-Time PCR with Culture in Microbiological Clearance Samples for Shiga Toxin-Producing *Escherichia coli* (STEC). *Microorganisms*. 2020;8(11):1801.
20. SHIGA TOXIN QUIK CHEK™ Package insert [Internet]. TechLab; 2021 [cited 2022 Nov 4]. Available from:  
[https://www.techlab.com/wp-content/uploads/2021/09/SHIGA-TOXIN-QUIK-CHEK-PI-91-625-01-TL\\_7-2021.pdf](https://www.techlab.com/wp-content/uploads/2021/09/SHIGA-TOXIN-QUIK-CHEK-PI-91-625-01-TL_7-2021.pdf)
21. Schrader C, Schielke A, Ellerbroek L, Johne R. PCR inhibitors – occurrence, properties and removal. *J Appl Microbiol*. 2012;113(5):1014–26.
22. Wagner AO, Praeg N, Reitschuler C, Illmer P. Effect of DNA extraction procedure, repeated extraction and ethidium monoazide (EMA)/propidium monoazide (PMA) treatment on overall DNA yield and impact on microbial fingerprints for bacteria, fungi and archaea in a reference soil. *Appl Soil Ecol*. 2015;93:56–64.
23. Zhuo R, Ding X, Freedman SB, Lee BE, Ali S, Luong J, et al. Molecular Epidemiology of Human Sapovirus among Children with Acute Gastroenteritis in Western Canada. *J Clin Microbiol*. 2021 Sep 20;59(10):e00986-21.
24. Elder RO, Keen JE, Siragusa GR, Barkocy-Gallagher GA, Koohmaraie M, Laegreid WW. Correlation of enterohemorrhagic *Escherichia coli* O157 prevalence in feces, hides, and carcasses of beef cattle during processing. *Proc Natl Acad Sci*. 2000 Mar

28;97(7):2999–3003.

25. Papanicolas LE, Wang Y, Choo JM, Gordon DL, Wesselingh SL, Rogers GB. Optimisation of a propidium monoazide based method to determine the viability of microbes in faecal slurries for transplantation. *J Microbiol Methods*. 2019 Jan 1;156:40–5.
26. Freedman SB, Xie J, Nettel-Aguirre A, Lee B, Chui L, Pang XL, et al. Enteropathogen detection in children with diarrhoea, or vomiting, or both, comparing rectal flocced swabs with stool specimens: an outpatient cohort study. *Lancet Gastroenterol Hepatol*. 2017 Sep;2(9):662–9.
27. Jean S, Yarbrough ML, Anderson NW, Burnham CAD. Culture of Rectal Swab Specimens for Enteric Bacterial Pathogens Decreases Time to Test Result While Preserving Assay Sensitivity Compared to Bulk Fecal Specimens. *J Clin Microbiol*. 2019 Jun;57(6):e02077-18.
28. Kabayiza JC, Andersson ME, Welinder-Olsson C, Bergström T, Muhirwa G, Lindh M. Comparison of rectal swabs and faeces for real-time PCR detection of enteric agents in Rwandan children with gastroenteritis. *BMC Infect Dis*. 2013 Sep 27;13(1):447.
29. Warnke P, Warning L, Podbielski A. Some Are More Equal - A Comparative Study on Swab Uptake and Release of Bacterial Suspensions. *PLoS ONE*. 2014 Jul 10;9(7):e102215.
30. Wine E. Rectal swabs: a diagnostic alternative in paediatric gastroenteritis? *Lancet Gastroenterol Hepatol*. 2017 Sep 1;2(9):623–4.
31. Zelyas N, Poon A, Patterson-Fortin L, Johnson RP, Lee W, Chui L. Assessment of commercial chromogenic solid media for the detection of non-O157 Shiga toxin-producing *Escherichia coli* (STEC). *Diagn Microbiol Infect Dis*. 2016 Jul 1;85(3):302–8.
32. Jenkins C, Perry NT, Godbole G, Gharbia S. Evaluation of chromogenic selective agar (CHROMagar STEC) for the direct detection of Shiga toxin-producing *Escherichia coli* from faecal specimens. *J Med Microbiol*. 2020 Mar;69(3):487–91.
33. Sánchez S, Llorente MT, Ramiro R, Herrera-León L, Herrera-León S. Evaluation of the

- SHIGA TOXIN QUIK CHEK after overnight enrichment as screening tool for Shiga toxin-producing *Escherichia coli* detection in human fecal samples. *Diagn Microbiol Infect Dis*. 2019 Jul 1;94(3):218–22.
34. Chui L, Christianson S, Alexander D, Arseneau V, Bekal S, Berenger B, et al. CPHLN recommendations for the laboratory detection of Shiga toxin-producing *Escherichia coli* (O157 and non-O157). *Can Commun Dis Rep*. 2018 Nov 1;44:304–7.
35. Mody RK, Griffin PM. Editorial Commentary: Fecal Shedding of Shiga Toxin-Producing *Escherichia coli*: What Should Be Done to Prevent Secondary Cases? *Clin Infect Dis*. 2013 Apr 15;56(8):1141–4.
36. Vonberg RP, Höhle M, Aepfelbacher M, Bange FC, Belmar Campos C, Claussen K, et al. Duration of fecal shedding of Shiga toxin-producing *Escherichia coli* O104:H4 in patients infected during the 2011 outbreak in Germany: a multicenter study. *Clin Infect Dis Off Publ Infect Dis Soc Am*. 2013 Apr;56(8):1132–40.
37. Matussek A, Jernberg C, Einemo I, Monecke S, Ehricht R, Engelmann I, et al. Genetic makeup of Shiga toxin-producing *Escherichia coli* in relation to clinical symptoms and duration of shedding: a microarray analysis of isolates from Swedish children. *Eur J Clin Microbiol Infect Dis*. 2017;36(8):1433–41.
38. Veneti L, Lange H, Brandal L, Danis K, Vold L. Mapping of control measures to prevent secondary transmission of STEC infections in Europe during 2016 and revision of the national guidelines in Norway. *Epidemiol Infect*. 2019 Jul 29;147(e267):1–10.



## Chapter 4: General Discussion

### 4.1 Significance

Viability RT-PCR is a burgeoning molecular biology technique undergoing optimization by the scientific community. In theory, it has the potential to be a useful viability-assessment tool for diagnostic microbiology laboratories as they further embrace culture-independent diagnostic testing. Although viability RT-PCR has been attempted using other complex sample types (1–4) and fecal transplant slurries (5,6), this study will be the first time it is applied directly to stool or rectal swabs for the detection of STEC. Further, this study's focus on microbiological clearance testing demonstrates a niche wherein viability RT-PCR could be especially useful given its fast indication of viability and potential sensitivity.

The first objective of this thesis (**Chapter 2**) was to determine the optimum conditions for viability RT-PCR to detect live STEC in PBS suspensions. The multiplexed *stx*<sub>1</sub> and *stx*<sub>2</sub> primer-probe sets (7) had a limit of detection of 10<sup>3</sup> CFU/mL, did not cross-react with DNA from other organisms, and detected all of the *stx* subtypes tested except for *stx*<sub>2f</sub> (**Table 2.3B**). These qualities suggest that this set of primers and probes is suitable for STEC detection. However, given the emergence of STEC cases with the Stx2f variant in Europe, further modifications are warranted to improve the suitability for diagnostics (8). The optimized viability RT-PCR protocol for cell suspensions in PBS (outlined in **Figure 2.5**) involved adding a final concentration of 100 µM PMAxx<sup>TM</sup> (a viability dye which irreversibly binds DNA when exposed to bright light) and 1% DMSO (a mild detergent). This was followed by a 15 min photoactivation and a transfer to a secondary tube for DNA extraction. A PMAxx<sup>TM</sup> concentration of 100 µM has been regularly used in other studies (1,9,10) as has the 15 min photoactivation (9–11) and addition of DMSO (11–13). This combination was able to successfully eliminate the detection of up to 10<sup>9</sup> CFU/mL HK cells in PBS (**Table 2.7**).

One of this study's novel findings is that a proportion of PMAxx™ can remain active beyond the photoactivation period, adhere to the inside of polystyrene tubes, and subsequently bind DNA (**Table 2.10**). Although the effect on Ct values is reduced compared to direct application of PMAxx™, this phenomenon may be relevant at low bacterial loads and sheds more light on how PMAxx™ functions. Our research group has recently corroborated this finding using *Salmonella* (14). Previous studies (15,16) have suggested using a tube transfer step to reduce false positive results (i.e., from HK cells adhering to the tube), but this study's tube transfer was done specifically to reduce the potential effect of PMAxx™ on live cells in PBS. However, a tube transfer did not improve live cell detection ( $\pm 1$  Ct value) when PMAxx™ treatment was applied to spiked stool (**3.3.3.2**). Although the reason for this difference is unclear, it is possible that the additional DNA (human and bacterial) and organic matter in the stool suspension plays a role.

When viability RT-PCR was applied to mixed cell suspensions ( $10^8$ ,  $10^6$ , or  $10^4$  live CFU/mL with  $10^8$  HK CFU/mL), the Ct values only reflected the amount of live cells present (**Tables 2.13A and 2.13B**). However, when applied to a low concentration of only live cells, the average Ct value inflated and false negatives occurred. Although this effect was not statistically significant in this study's PBS suspensions, it has been observed in another study using similar treatment conditions (17). PMAxx™ may passively penetrate some live cells resulting in cell death, as is seen to a greater extent with EMA, a predecessor to PMAxx™ (12). It is also possible that the addition of DMSO (a mild detergent which disrupts the cell membrane (18)) while beneficial for reducing HK cell detection (**Table 2.7**), may have exacerbated this issue.

The second objective of this thesis (**Chapter 3**) was to develop a viability RT-PCR for direct-from-stool (DFS) and rectal swab (RS) applications. As in the PBS suspension, when viability RT-PCR was applied to stool specimens spiked with cells ( $10^9$ ,  $10^7$ , or  $10^5$  live CFU/mL

stool with  $10^9$  HK CFU/mL stool), the Ct values only reflected the amount of live cells added to the sample (**Table 3.5**). However, the false-negative phenomenon above was observed to be statistically significant in the DFS and RS protocols when 100  $\mu$ M PMAxx™ and 1% DMSO was applied to liquid stool spiked with a low concentration of live STEC. Although the DFS and RS viability RT-PCR protocols did not have the desired sensitivity, the data in this study shows that PMAxx™ could be successfully photoactivated when added to a 10% stool suspension. This means that the turbidity of these samples was not prohibitive as has been seen in studies using environmental samples (19,20).

The microbiological clearance context was chosen to test the DFS viability RT-PCR protocol because it is important that such testing be sensitive while also only reflecting the presence of live bacteria. This is necessary to minimize the risk of patients transmitting their infection. Moreover, both methods currently used in Alberta for such testing (growth on CHROMagar™ STEC and post-enrichment RT-PCR) require an overnight growth period. However, the DFS viability RT-PCR assay developed here is ultimately unsuitable for microbiological clearance testing because of its sensitivity issues and inconsistent performance (**Table 3.14**). Further optimization could be conducted (as described below) to potentially produce a more successful protocol, however it is also possible that these issues are inherent qualities of the dye and procedure.

A previous study conducted in our laboratory (21) using microbiological clearance samples found that in most cases RT-PCR positivity persisted longer (up to a week) than positivity by CHROMagar™ STEC. The present study's findings suggest that this discordance was likely driven by CHROMagar™ STEC sensitivity issues (rather than the detection of dead STEC by RT-PCR). Patient A samples (**Table 3.7**) were positive by PE RT-PCR for three days longer than they were positive on CHROMagar™ STEC. Further, three of the six strains represented in this

study did not grow on the media (Patient B; **Table 3.9**). This included an O145 strain (from the “top-6” non-O157 STEC serotypes) which would typically be expected to grow.

Post-enrichment RT-PCR was found to be the best performing method used in this study. Across all four patients it was the method to be positive the longest. It was also successful in monitoring the clearance of strains which could not grow on CHROMagar™ STEC. Suggestions for further PE RT-PCR research are discussed below.

## **4.2 Limitations**

The basic design (**Figures 2.5** and **3.6**) used to test the final viability RT-PCR protocols had a few limitations. First, only one high concentration of HK cells ( $10^8$  CFU/mL) was combined with live cells. It is unclear how the protocols would perform with HK cells of lower concentrations or whether this combination is reflective of what would naturally occur in clinical samples. Second, the exact limit of detection of the viability RT-PCR assays could not be determined because the final protocols were tested using live cell concentrations that were 2-logs apart.

Although all steps involving PMAxx™ were conducted in dimly lit conditions, it is possible that the dye's binding capability was affected by this exposure to ambient light. The use of a stock solution over the course of a few weeks of experimentation may have further decreased the dyes effectiveness and led to variable performance.

A liquid stool was used for the optimization of the DFS and RS protocols because it was easier to evenly spike with STEC. However, it is possible that this stool did not sufficiently represent how the clinical microbiological clearance specimens would perform. For example, the bacteria in clinical samples might have been more attached to the stool particulate than was seen in the

spiked stool. If this were the case, then the liquid phase of clinical samples might not accurately reflect the total amount of bacteria found in the sample despite this being true for the spiked stool in **3.3.1.2**. Further, only four patients were included in Chapter 3. Since the stool consistency (and likely other factors like dietary habits) remained relatively the same throughout each sample series, it is difficult to make broader generalizations about the DFS viability RT-PCR assay's performance.

The use of an in-house rapid lysis buffer for the extraction of DNA from microbiological clearance samples likely contributed to several cases of RT-PCR inhibition. This method was selected as a fast and affordable option, and because the performance in the preliminary trials (with cell suspensions in PBS and spiked liquid stool) showed that it performed more effectively than the other extraction method tested (MagaZorb® DNA Mini-Prep Kit and KingFisher™ mL Purification System; **Table 3.2**). However, the analysis of solid and semi-solid clinical samples may have benefited from an extraction method capable of producing a purer DNA extract.

All of the microbiological clearance samples used in Chapter 3 were received from ProvLab in batches. As a consequence, some specimens were analyzed in this study several weeks after they were originally submitted by the patient. Thus, the results of the study might not accurately reflect how viability RT-PCR would perform were it to be directly implemented in the microbiological clearance testing workflow. The load of live bacteria may have decreased during transport and storage, which could have contributed to the issue of false-negatives seen in viability RT-PCR analysis. However, since the PE viability RT-PCR results concurred with ProvLab's results (which were generated immediately following submission), this confirmed that the specimens which were originally positive still contained some live organisms at the time they were tested. Since each clinical specimen was only tested once, sampling errors could not be recognized.

Finally, since the original stool specimen used for diagnosis in the frontline laboratory is not forwarded to ProvLab (and thus was unavailable for this study), the clearance times were calculated from the first microbiological clearance specimen submitted to ProvLab to the last positive submission. This means that in all cases the duration of clearance was underestimated to an unknown extent. The inability to determine exactly how long each patient was infected ultimately makes it challenging to directly compare the results of this study with that of other microbiological clearance studies (22–25) which calculate the duration from symptom onset.

#### **4.3 Future directions**

For most viability RT-PCR studies, eliminating the detection of dead cells is the first priority. However, this project illustrates that it is equally crucial to consider whether the detection of live cells is sufficiently preserved (i.e., to reduce false negatives). The mechanism by which false negatives might occur is also worthy of inquiry to see if further modifications could minimize the effect: does the dye penetrate live cells but not kill them? Is the DNA from live cells being bound during the extraction process? Does the amount of time the live cells spend in supernatant containing PMAxx™ have an impact? Since PMAxx™ is fluorescent, this could involve visually monitoring its penetration of cells and attachment to non-DNA molecules (e.g., to microcentrifuge tubes and particles).

Given that post-enrichment RT-PCR was the most sensitive method in this study, its optimization is worth investment. There continue to be studies that attempt to assess the suitability of different broths for STEC enrichment (26,27). To account for the diversity seen across STEC, it is important that such studies include a large number of both common and less common serotypes. Further, to assess the exact extent to which the specimen is enriched it would be valuable to conduct RT-PCR on an aliquot of broth immediately after inoculation (to

account for the original organisms and DNA in the sample) to serve as a comparison for the Ct value generated after enrichment. With the caveat of potential false-negatives in mind, a version of the viability RT-PCR assay developed here could also be applied to aliquots of broth at both time points to determine the relative load of live cells before and after enrichment. Finally using the above methods to analyze effectiveness, it would be valuable to assess other ways the enrichment process could be improved. For example, shaking the tube during incubation might encourage faster growth (28).

#### **4.4 Final conclusions**

In conclusion, all of the viability RT-PCR protocols developed in this thesis were successful at selectively detecting live cells at high bacterial loads when found alongside a high concentration of heat-killed STEC. This suggests that PMAxx<sup>TM</sup> was successfully activated in stool and bound DNA from heat-killed STEC. However the protocols were not successful at detecting live cells at low bacterial loads. Thus the hypothesis that viability RT-PCR would be as sensitive as conventional RT-PCR was not supported. This sensitivity issue means that this DFS viability RT-PCR assay is unsuitable for microbiological clearance testing because such specimens often have a low load of live bacteria. Instead, the results of this study endorse the use of post-enrichment RT-PCR as it was the most sensitive assay tested and was suitable for strains which did not grow on CHROMagar<sup>TM</sup> STEC.

## 4.5 References

1. Rey M de los Á, Cap M, Favre LC, Rodríguez Racca A, Dus Santos MJ, Vaudagna SR, et al. Evaluation of PMA-qPCR methodology to detect and quantify viable Shiga toxin-producing *Escherichia coli* in beef burgers. *J Food Process Preserv.* 2021;45(4):e15338.
2. Dinu LD, Bach S. Detection of viable but non-culturable *Escherichia coli* O157: H7 from vegetable samples using quantitative PCR with propidium monoazide and immunological assays. *Food Control.* 2013;31(2):268–73.
3. Elizaquível P, Aznar R, Sánchez G. Recent developments in the use of viability dyes and quantitative PCR in the food microbiology field. *J Appl Microbiol.* 2014;116(1):1–13.
4. Shekar A, Babu L, Ramlal S, Sripathy MH, Batra H. Selective and concurrent detection of viable *Salmonella* spp., *E. coli*, *Staphylococcus aureus*, *E. coli* O157:H7, and *Shigella* spp., in low moisture food products by PMA-mPCR assay with internal amplification control. *LWT.* 2017 Dec 1;86:586–93.
5. Papanicolas LE, Choo JM, Wang Y, Leong LE, Costello SP, Gordon DL, et al. Bacterial viability in faecal transplants: which bacteria survive? *EBioMedicine.* 2019;41:509–16.
6. Takahashi M, Ishikawa D, Sasaki T, Lu Y j., Kuwahara-Arai K, Kamei M, et al. Faecal freezing preservation period influences colonization ability for faecal microbiota transplantation. *J Appl Microbiol.* 2019;126(3):973–84.
7. Perelle S, Dilasser F, Grout J, Fach P. Detection by 5'-nuclease PCR of Shiga-toxin producing *Escherichia coli* O26, O55, O91, O103, O111, O113, O145 and O157:H7, associated with the world's most frequent clinical cases. *Mol Cell Probes.* 2004 Jun 1;18(3):185–92.
8. Friesema I, Zwaluw K van der, Schuurman T, Kooistra-Smid M, Franz E, Duynhoven Y van, et al. Emergence of *Escherichia coli* encoding Shiga toxin 2f in human Shiga toxin-producing *E. coli* (STEC) infections in the Netherlands, January 2008 to December 2011.



- Eurosurveillance. 2014 May 1;19(17):20787.
9. Rani A, Dike CC, Mantri N, Ball A. Point-of-Care Lateral Flow Detection of Viable *Escherichia coli* O157:H7 Using an Improved Propidium Monoazide-Recombinase Polymerase Amplification Method. *Foods*. 2022 Jan;11(20):3207.
  10. Van Holm W, Ghesquière J, Boon N, Verspecht T, Bernaerts K, Zayed N, et al. A Viability Quantitative PCR Dilemma: Are Longer Amplicons Better? *Appl Environ Microbiol*. 2021 Feb 12;87(5):e02653-20.
  11. Schnetzinger F, Pan Y, Nocker A. Use of propidium monoazide and increased amplicon length reduce false-positive signals in quantitative PCR for bioburden analysis. *Appl Microbiol Biotechnol*. 2013;97(5):2153–62.
  12. Nocker A, Cheung CY, Camper AK. Comparison of propidium monoazide with ethidium monoazide for differentiation of live vs. dead bacteria by selective removal of DNA from dead cells. *J Microbiol Methods*. 2006;67(2):310–20.
  13. Bonetta S, Pignata C, Bonetta S, Meucci L, Giacosa D, Marino E, et al. Viability of *Legionella pneumophila* in Water Samples: A Comparison of Propidium Monoazide (PMA) Treatment on Membrane Filters and in Liquid. *Int J Environ Res Public Health*. 2017 May;14(5):467.
  14. Thilakarathna SH, Stokowski T, Chui L. An Improved Real-Time Viability PCR Assay to Detect *Salmonella* in a Culture-Independent Era. *Int J Mol Sci*. 2022 Jan;23(23):14708.
  15. Codony F, Dinh-Thanh M, Agustí G. Key Factors for Removing Bias in Viability PCR-Based Methods: A Review. *Curr Microbiol*. 2020 Apr 1;77(4):682–7.
  16. Agustí G, Fittipaldi M, Codony F. False-Positive Viability PCR Results: An Association with Microtubes. *Curr Microbiol*. 2017 Mar;74(3):377–80.
  17. Seinige D, Krischek C, Klein G, Kehrenberg C. Comparative analysis and limitations of ethidium monoazide and propidium monoazide treatments for the differentiation of viable and nonviable *Campylobacter* cells. *Appl Environ Microbiol*. 2014;80(7):2186.

18. Gurtovenko AA, Anwar J. Modulating the structure and properties of cell membranes: the molecular mechanism of action of dimethyl sulfoxide. *J Phys Chem B*. 2007 Sep 6;111(35):10453–60.
19. Wagner AO, Malin C, Knapp BA, Illmer P. Removal of Free Extracellular DNA from Environmental Samples by Ethidium Monoazide and Propidium Monoazide. *Appl Environ Microbiol*. 2008 Apr;74(8):2537–9.
20. Luo JF, Lin WT, Guo Y. Method to detect only viable cells in microbial ecology. *Appl Microbiol Biotechnol*. 2010 Mar 1;86(1):377–84.
21. Bording-Jorgensen M, Parsons BD, Tarr GA, Shah-Gandhi B, Lloyd C, Chui L. Association of Ct Values from Real-Time PCR with Culture in Microbiological Clearance Samples for Shiga Toxin-Producing *Escherichia coli* (STEC). *Microorganisms*. 2020;8(11):1801.
22. Mody RK, Griffin PM. Editorial Commentary: Fecal Shedding of Shiga Toxin-Producing *Escherichia coli*: What Should Be Done to Prevent Secondary Cases? *Clin Infect Dis*. 2013 Apr 15;56(8):1141–4.
23. Vonberg RP, Höhle M, Aepfelbacher M, Bange FC, Belmar Campos C, Claussen K, et al. Duration of fecal shedding of Shiga toxin-producing *Escherichia coli* O104:H4 in patients infected during the 2011 outbreak in Germany: a multicenter study. *Clin Infect Dis Off Publ Infect Dis Soc Am*. 2013 Apr;56(8):1132–40.
24. Matussek A, Jernberg C, Einemo I, Monecke S, Ehricht R, Engelmann I, et al. Genetic makeup of Shiga toxin-producing *Escherichia coli* in relation to clinical symptoms and duration of shedding: a microarray analysis of isolates from Swedish children. *Eur J Clin Microbiol Infect Dis*. 2017;36(8):1433–41.
25. Veneti L, Lange H, Brandal L, Danis K, Vold L. Mapping of control measures to prevent secondary transmission of STEC infections in Europe during 2016 and revision of the national guidelines in Norway. *Epidemiol Infect*. 2019 Jul 29;147(e267):1–10.
26. Bording-Jorgensen M, Tyrrell H, Lloyd C, Chui L. Comparison of Common Enrichment

Broths Used in Diagnostic Laboratories for Shiga Toxin—Producing *Escherichia coli*.

*Microorganisms*. 2021 Mar;9(3):503.

27. Stromberg ZR, Lewis GL, Marx DB, Moxley RA. Comparison of Enrichment Broths for Supporting Growth of Shiga Toxin-Producing *Escherichia coli*. *Curr Microbiol*. 2015 Aug 1;71(2):214–9.

28. Juergensmeyer MA, Nelson ES, Juergensmeyer EA. Shaking alone, without concurrent aeration, affects the growth characteristics of *Escherichia coli*. *Lett Appl Microbiol*. 2007;45(2):179–83.

## Bibliography

Agustí G, Fittipaldi M, Codony F. False-Positive Viability PCR Results: An Association with Microtubes. *Curr Microbiol.* 2017 Mar;74(3):377–80.

Alberta Health Services - E. coli (STEC) Info for Health Care Providers [Internet]. [cited 2022 Nov 4]. Available from:  
<https://www.albertahealthservices.ca/assets/info/hp/diseases/if-hp-dis-ecoli-stec.pdf>

Alberta Health. Alberta Public Health Disease Management Guidelines - Escherichia coli Verotoxigenic Infections [Internet]. 2021. Available from:  
<https://open.alberta.ca/dataset/2b77e542-cfcb-4f93-b825-dca7d140e024/resource/b3c01b4a-8541-47fa-a19a-b7c3835a1cee/download/health-phdmg-escherichia-coli-verotoxigenic-infections-2021-11.pdf>

Àlvarez G, González M, Isabal S, Blanc V, León R. Method to quantify live and dead cells in multi-species oral biofilm by real-time PCR with propidium monoazide. *AMB Express.* 2013 Jan 4;3(1):1.

Anderson NW, Buchan BW, Ledebøer NA. Comparison of the BD MAX Enteric Bacterial Panel to Routine Culture Methods for Detection of *Campylobacter*, Enterohemorrhagic *Escherichia coli* (O157), *Salmonella*, and *Shigella* Isolates in Preserved Stool Specimens. *J Clin Microbiol.* 2014 Apr;52(4):1222–4.

Applied Biosystems 7500/7500 Fast Real-Time PCR Systems Manual [Internet]. Available from:  
<https://tools.thermofisher.com/content/sfs/manuals/4387777d.pdf>

- Ardissino G, Tel F, Possenti I, Testa S, Consonni D, Paglialonga F, et al. Early Volume Expansion and Outcomes of Hemolytic Uremic Syndrome. *Pediatrics*. 2016 Jan;137(1).
- Awofisayo-Okuyelu A, Brainard J, Hall I, McCarthy N. Incubation Period of Shiga Toxin–Producing *Escherichia coli*. *Epidemiol Rev*. 2019 Oct 16;41(2):121–9.
- Bai X, Mernelius S, Jernberg C, Einemo I, Monecke S, Ehricht R, et al. Shiga Toxin-Producing *Escherichia coli* Infection in Jönköping County, Sweden: Occurrence and Molecular Characteristics in Correlation With Clinical Symptoms and Duration of stx Shedding. *Front Cell Infect Microbiol*. 2018 May 1;8:125.
- Baker CA, Rubinelli PM, Park SH, Carbonero F, Ricke SC. Shiga toxin-producing *Escherichia coli* in food: Incidence, ecology, and detection strategies. *Food Control*. 2016 Jan 1;59:407–19.
- Bauwens A, Kunsmann L, Karch H, Mellmann A, Bielaszewska M. Antibiotic-Mediated Modulations of Outer Membrane Vesicles in Enterohemorrhagic *Escherichia coli* O104:H4 and O157:H7. *Antimicrob Agents Chemother*. 61(9):e00937-17.
- Berenger B, Chui L, Reimer A, Allen V, Alexander D, Domingo MC, et al. Canadian Public Health Laboratory Network position statement: Non-culture based diagnostics for gastroenteritis and implications for public health investigations. *Can Commun Dis Rep*. 2017 Dec 7;43(12):279–81.

Berenger BM, Ferrato C, Chui L. Viability of bacterial enteropathogens in fecal samples in the presence or absence of different types of transport media. *Diagn Microbiol Infect Dis*. 2019 Nov 1;95(3):114862.

Bhatta TR, Chamings A, Alexandersen S. Exploring the Cause of Diarrhoea and Poor Growth in 8–11-Week-Old Pigs from an Australian Pig Herd Using Metagenomic Sequencing. *Viruses*. 2021 Aug;13(8):1608.

Bonetta S, Pignata C, Bonetta S, Meucci L, Giacosa D, Marino E, et al. Viability of *Legionella pneumophila* in Water Samples: A Comparison of Propidium Monoazide (PMA) Treatment on Membrane Filters and in Liquid. *Int J Environ Res Public Health*. 2017 May;14(5):467.

Boone JT, Campbell DE, Dandro AS, Chen L, Herbein JF. A Rapid Immunoassay for Detection of Shiga Toxin-Producing *Escherichia coli* Directly from Human Fecal Samples and Its Performance in Detection of Toxin Subtypes. Tang YW, editor. *J Clin Microbiol*. 2016 Dec;54(12):3056–63.

Bording-Jorgensen M, Parsons BD, Tarr GA, Shah-Gandhi B, Lloyd C, Chui L. Association of Ct Values from Real-Time PCR with Culture in Microbiological Clearance Samples for Shiga Toxin-Producing *Escherichia coli* (STEC). *Microorganisms*. 2020;8(11):1801.

Bording-Jorgensen M, Tyrrell H, Lloyd C, Chui L. Comparison of Common Enrichment Broths Used in Diagnostic Laboratories for Shiga Toxin—Producing *Escherichia coli*. *Microorganisms*. 2021 Mar;9(3):503.

Burger R. EHEC O104: H4 in Germany 2011: Large outbreak of bloody diarrhea and haemolytic uraemic syndrome by Shiga toxin-producing *E. coli* via contaminated food. [Internet]. Improving Food Safety Through a One Health Approach: Workshop Summary. National Academies Press (US); 2012 [cited 2022 Apr 20]. Available from: <https://www.ncbi.nlm.nih.gov/books/NBK114499/>

Canadian Public Health Laboratory Network. Core Functions of Canadian Public Health Laboratories [Internet]. 2011 [cited 2022 Nov 4]. Available from: <https://nccid.ca/wp-content/uploads/sites/2/2020/03/CPHLN-Core-Functions.pdf>

Chan YS, Ng TB. Shiga toxins: from structure and mechanism to applications. *Appl Microbiol Biotechnol.* 2016 Feb 1;100(4):1597–610.

Chekabab SM, Paquin-Veillette J, Dozois CM, Harel J. The ecological habitat and transmission of *Escherichia coli* O157:H7. *FEMS Microbiol Lett.* 2013 Apr 1;341(1):1–12.

Chui L, Christianson S, Alexander D, Arseneau V, Bekal S, Berenger B, et al. CPHLN recommendations for the laboratory detection of Shiga toxin-producing *Escherichia coli* (O157 and non-O157). *Can Commun Dis Rep.* 2018 Nov 1;44:304–7.

Chui L, Patterson-Fortin L, Kuo J, Li V, Boras V. Evaluation of Enzyme Immunoassays and Real-Time PCR for Detecting Shiga Toxin-Producing *Escherichia coli* in Southern Alberta, Canada. Munson E, editor. *J Clin Microbiol.* 2015 Mar;53(3):1019–23.

Church DL, Emshey D, Semeniuk H, Lloyd T, Pitout JD. Evaluation of BBL CHROMagar O157 versus Sorbitol-MacConkey Medium for Routine Detection of Escherichia coli O157 in a Centralized Regional Clinical Microbiology Laboratory. *J Clin Microbiol.* 2007 Sep;45(9):3098–100.

Codony F, Dinh-Thanh M, Agustí G. Key Factors for Removing Bias in Viability PCR-Based Methods: A Review. *Curr Microbiol.* 2020 Apr 1;77(4):682–7.

Conrad C, Stanford K, McAllister T, Thomas J, Reuter T. Shiga toxin-producing Escherichia coli and current trends in diagnostics. *Anim Front.* 2016 Apr 1;6(2):37–43.

Cronquist AB, Mody RK, Atkinson R, Besser J, D'Angelo MT, Hurd S, et al. Impacts of Culture-Independent Diagnostic Practices on Public Health Surveillance for Bacterial Enteric Pathogens. *Clin Infect Dis.* 2012 Jun 1;54(suppl\_5):S432–9.

Croxen MA, Law RJ, Scholz R, Keeney KM, Wlodarska M, Finlay BB. Recent Advances in Understanding Enteric Pathogenic Escherichia coli. *Clin Microbiol Rev.* 2013 Oct;26(4):822–80.

Currie A, Honish L, Cutler J, Locas A, Lavoie MC, Gaulin C, et al. Outbreak of Escherichia coli O157:H7 Infections Linked to Mechanically Tenderized Beef and the Largest Beef Recall in Canada, 2012. *J Food Prot.* 2019 Sep 1;82(9):1532–8.

De Rauw K, Breyneart J, Piérard D. Evaluation of the Alere SHIGA TOXIN QUIK CHEK™ in comparison to multiplex Shiga toxin PCR. *Diagn Microbiol Infect Dis.* 2016



Sep;86(1):35–9.

DeBurger B, Hanna S, Powell EA, Ventrola C, Mortensen JE. Utilizing BD MAX™ Enteric Bacterial Panel to Detect Stool Pathogens from Rectal Swabs. *BMC Clin Pathol*. 2017 Apr 8;17(1):7.

Dinu LD, Bach S. Detection of viable but non-culturable *Escherichia coli* O157: H7 from vegetable samples using quantitative PCR with propidium monoazide and immunological assays. *Food Control*. 2013;31(2):268–73.

Dinu LD, Bach S. Induction of Viable but Nonculturable *Escherichia coli* O157:H7 in the Phyllosphere of Lettuce: a Food Safety Risk Factor. *Appl Environ Microbiol*. 2011 Dec;77(23):8295–302.

Elder RO, Keen JE, Siragusa GR, Barkocy-Gallagher GA, Koohmaraie M, Laegreid WW. Correlation of enterohemorrhagic *Escherichia coli* O157 prevalence in feces, hides, and carcasses of beef cattle during processing. *Proc Natl Acad Sci*. 2000 Mar 28;97(7):2999–3003.

Elizaquível P, Aznar R, Sánchez G. Recent developments in the use of viability dyes and quantitative PCR in the food microbiology field. *J Appl Microbiol*. 2014;116(1):1–13.

Elizaquível P, Sánchez G, Aznar R. Quantitative detection of viable foodborne *E. coli* O157:H7, *Listeria monocytogenes* and *Salmonella* in fresh-cut vegetables combining propidium monoazide and real-time PCR. *Food Control*. 2012 Jun 1;25(2):704–8.

Epand RM, Walker C, Epand RF, Magarvey NA. Molecular mechanisms of membrane targeting antibiotics. *Biochim Biophys Acta BBA - Biomembr.* 2016 May 1;1858(5):980–7.

Ethidium bromide monoazide [Internet]. ottokemi.com. [cited 2022 Nov 4]. Available from:  
<https://www.ottokemi.com/product/ethidium-bromide-monoazide-95-hplc-e-3676.aspx>

Fan R, Bai X, Fu S, Xu Y, Sun H, Wang H, et al. Tellurite resistance profiles and performance of different chromogenic agars for detection of non-O157 Shiga toxin-producing *Escherichia coli*. *Int J Food Microbiol.* 2018 Feb 2;266:295–300.

Feng P, Weagant SD, Jinneman K. Bacteriological Analytical Manual Chapter 4A: Diarrheagenic *Escherichia coli* [Internet]. FDA; 2020 [cited 2022 Mar 22]. Available from:  
<https://www.fda.gov/food/laboratory-methods-food/bam-chapter-4a-diarrheagenic-escherichia-coli>

Feng P. Identification of *Escherichia coli* serotype O157:H7 by DNA probe specific for an allele of uid A gene. *Mol Cell Probes.* 1993 Apr;7(2):151–4.

Fratamico PM, DebRoy C, Liu Y, Needleman DS, Baranzoni GM, Feng P. Advances in Molecular Serotyping and Subtyping of *Escherichia coli*. *Front Microbiol.* 2016;7:644.

Freedman SB, Eltorki M, Chui L, Xie J, Feng S, MacDonald J, et al. Province-Wide Review of Pediatric Shiga Toxin-Producing *Escherichia coli* Case Management. *J Pediatr.* 2017 Jan 1;180:184–90.

Freedman SB, Xie J, Nettel-Aguirre A, Lee B, Chui L, Pang XL, et al. Enteropathogen detection in children with diarrhoea, or vomiting, or both, comparing rectal flocced swabs with stool specimens: an outpatient cohort study. *Lancet Gastroenterol Hepatol*. 2017 Sep;2(9):662–9.

Freedman SB, Xie J, Neufeld MS, Hamilton WL, Hartling L, Tarr PI, et al. Shiga Toxin-Producing *Escherichia coli* Infection, Antibiotics, and Risk of Developing Hemolytic Uremic Syndrome: A Meta-analysis. *Clin Infect Dis Off Publ Infect Dis Soc Am*. 2016 15;62(10):1251–8.

Friesema I, Zwaluw K van der, Schuurman T, Kooistra-Smid M, Franz E, Duynhoven Y van, et al. Emergence of *Escherichia coli* encoding Shiga toxin 2f in human Shiga toxin-producing *E. coli* (STEC) infections in the Netherlands, January 2008 to December 2011. *Eurosurveillance*. 2014 May 1;19(17):20787.

Fu Y, Ye Z, Jia Y, Fan J, Hashmi MZ, Shen C. An Optimized Method to Assess Viable *Escherichia coli* O157:H7 in Agricultural Soil Using Combined Propidium Monoazide Staining and Quantitative PCR. *Front Microbiol*. 2020;11:1809.

Gerner-Smidt P, Kincaid J, Kubota K, Hise K, Hunter SB, Fair MA, et al. Molecular Surveillance of Shiga Toxigenic *Escherichia coli* O157 by PulseNet USA. *J Food Prot*. 2005 Sep 1;68(9):1926–31.

Gill A, editor. Review of the State of Knowledge on Verotoxigenic *Escherichia coli* and the Role of Whole Genome Sequencing as an Emerging Technology Supporting Regulatory Food Safety in Canada [Internet]. Innovation, Science and Economic Development Canada; 2020 [cited 2022 Nov 4]. Available from:  
<https://science.gc.ca/site/science/en/blogs/cultivating-science/review-state-knowledge-verotoxigenic-escherichia-coli-and-role-whole-genome-sequencing-emerging>

Glassman H, Ferrato C, Chui L. Epidemiology of Non-O157 Shiga Toxin-Producing *Escherichia coli* in the Province of Alberta, Canada, from 2018 to 2021. *Microorganisms*. 2022 Apr;10(4):814.

Government of Canada. VTEC Illness Monitoring In Canada [Internet]. Innovation, Science and Economic Development Canada; [cited 2022 Jun 9]. Available from:  
[https://www.ic.gc.ca/eic/site/063.nsf/eng/h\\_98071.html#nesp](https://www.ic.gc.ca/eic/site/063.nsf/eng/h_98071.html#nesp)

Gurtovenko AA, Anwar J. Modulating the structure and properties of cell membranes: the molecular mechanism of action of dimethyl sulfoxide. *J Phys Chem B*. 2007 Sep 6;111(35):10453–60.

Gyles CL. Shiga toxin-producing *Escherichia coli*: An overview. *J Anim Sci*. 2007 Mar 1;85(suppl\_13):E45–62.

Harrington SM, Buchan BW, Doern C, Fader R, Ferraro MJ, Pillai DR, et al. Multicenter Evaluation of the BD Max Enteric Bacterial Panel PCR Assay for Rapid Detection of

- Salmonella spp., Shigella spp., Campylobacter spp. (*C. jejuni* and *C. coli*), and Shiga Toxin 1 and 2 Genes. *J Clin Microbiol.* 2015 May;53(5):1639–47.
- Haugum K, Johansen J, Gabrielsen C, Brandal LT, Bergh K, Ussery DW, et al. Comparative Genomics to Delineate Pathogenic Potential in Non-O157 Shiga Toxin-Producing *Escherichia coli* (STEC) from Patients with and without Haemolytic Uremic Syndrome (HUS) in Norway. *PLOS ONE.* 2014 Oct 31;9(10):e111788.
- Hirvonen JJ, Siitonen A, Kaukoranta SS. Usability and Performance of CHROMagar STEC Medium in Detection of Shiga Toxin-Producing *Escherichia coli* Strains. *J Clin Microbiol.* 2012 Nov;50(11):3586–90.
- Hughes JM, Wilson ME, Johnson KE, Thorpe CM, Sears CL. The Emerging Clinical Importance of Non-O157 Shiga Toxin—Producing *Escherichia coli*. *Clin Infect Dis.* 2006 Dec 15;43(12):1587–95.
- Imdad A, Retzer F, Thomas LS, McMillian M, Garman K, Rebeiro PF, et al. Impact of Culture-Independent Diagnostic Testing on Recovery of Enteric Bacterial Infections. *Clin Infect Dis.* 2018 Jun 1;66(12):1892–8.
- Irvin RT, MacAlister TJ, Costerton JW. Tris(hydroxymethyl)aminomethane buffer modification of *Escherichia coli* outer membrane permeability. *J Bacteriol.* 1981 Mar;145(3):1397–403.
- Jean S, Yarbrough ML, Anderson NW, Burnham CAD. Culture of Rectal Swab Specimens for Enteric Bacterial Pathogens Decreases Time to Test Result While Preserving Assay Sensitivity Compared to Bulk Fecal Specimens. *J Clin Microbiol.* 2019 Jun;57(6):e02077-18.

Jenkins C, Perry NT, Godbole G, Gharbia S. Evaluation of chromogenic selective agar (CHROMagar STEC) for the direct detection of Shiga toxin-producing *Escherichia coli* from faecal specimens. *J Med Microbiol.* 2020 Mar;69(3):487–91.

Jenssen GR, Veneti L, Lange H, Vold L, Naseer U, Brandal LT. Implementation of multiplex PCR diagnostics for gastrointestinal pathogens linked to increase of notified Shiga toxin-producing *Escherichia coli* cases in Norway, 2007–2017. *Eur J Clin Microbiol Infect Dis.* 2019 Apr 1;38(4):801–9.

Johannes L, Römer W. Shiga toxins — from cell biology to biomedical applications. *Nat Rev Microbiol.* 2010 Feb;8(2):105–16.

Joseph A, Cointe A, Mariani Kurkdjian P, Rafat C, Hertig A. Shiga Toxin-Associated Hemolytic Uremic Syndrome: A Narrative Review. *Toxins.* 2020 Jan 21;12(2):67.

Juergensmeyer MA, Nelson ES, Juergensmeyer EA. Shaking alone, without concurrent aeration, affects the growth characteristics of *Escherichia coli*. *Lett Appl Microbiol.* 2007;45(2):179–83.

Kabayiza JC, Andersson ME, Welinder-Olsson C, Bergström T, Muhirwa G, Lindh M. Comparison of rectal swabs and faeces for real-time PCR detection of enteric agents in Rwandan children with gastroenteritis. *BMC Infect Dis.* 2013 Sep 27;13(1):447.

Large TM, Walk ST, Whittam TS. Variation in Acid Resistance among Shiga Toxin-Producing

Clones of Pathogenic *Escherichia coli*. *Appl Environ Microbiol*. 2005  
May;71(5):2493–500.

Lee AS, Lamanna OK, Ishida K, Hill E, Nguyen A, Hsieh MH. A Novel Propidium  
Monoazide-Based PCR Assay Can Measure Viable Uropathogenic *E. coli* In Vitro and In  
Vivo. *Front Cell Infect Microbiol*. 2022;12:40.

Lee JE, Reed J, Shields MS, Spiegel KM, Farrell LD, Sheridan PP. Phylogenetic analysis of  
Shiga toxin 1 and Shiga toxin 2 genes associated with disease outbreaks. *BMC  
Microbiol*. 2007 Dec 4;7(1):109.

Li D, Tong T, Zeng S, Lin Y, Wu S, He M. Quantification of viable bacteria in wastewater  
treatment plants by using propidium monoazide combined with quantitative PCR  
(PMA-qPCR). *J Environ Sci*. 2014;26(2):299–306.

Lienemann T, Salo E, Rimhanen-Finne R, Rönholm K, Taimisto M, Hirvonen JJ, et al. Shiga  
Toxin-producing *Escherichia coli* Serotype O78:H– in Family, Finland, 2009. *Emerg  
Infect Dis*. 2012 Apr;18(4):577–81.

Lisboa LF, Szelewicki J, Lin A, Latonas S, Li V, Zhi S, et al. Epidemiology of Shiga  
Toxin-Producing *Escherichia coli* O157 in the Province of Alberta, Canada, 2009–2016.  
*Toxins*. 2019 Oct 22;11(10):613.

Liu Y, Wang C, Tyrrell G, Li XF. Production of Shiga-like toxins in viable but nonculturable  
*Escherichia coli* O157:H7. *Water Res*. 2010 Feb 1;44(3):711–8.

- Louise CB, Obrug TG. Specific interaction of Escherichia coli O157:H7-derived Shiga-like toxin II with human renal endothelial cells. *J Infect Dis.* 1995 Nov;172(5):1397–401.
- Luo JF, Lin WT, Guo Y. Method to detect only viable cells in microbial ecology. *Appl Microbiol Biotechnol.* 2010 Mar 1;86(1):377–84.
- Macori G, McCarthy SC, Burgess CM, Fanning S, Duffy G. Investigation of the causes of shigatoxigenic Escherichia coli PCR positive and culture negative samples. *Microorganisms.* 2020;8(4):587.
- March SB, Ratnam S. Sorbitol-MacConkey medium for detection of Escherichia coli O157:H7 associated with hemorrhagic colitis. *J Clin Microbiol.* 1986 May;23(5):869–72.
- Marder EP, Cieslak PR, Cronquist AB, Dunn J, Lathrop S, Rabatsky-Ehr T, et al. Incidence and Trends of Infections with Pathogens Transmitted Commonly Through Food and the Effect of Increasing Use of Culture-Independent Diagnostic Tests on Surveillance — Foodborne Diseases Active Surveillance Network, 10 U.S. Sites, 2013–2016. *MMWR Morb Mortal Wkly Rep.* 2017 Apr 21;66(15):397–403.
- Margot H, Cernela N, Iversen C, Zweifel C, Stephan R. Evaluation of Seven Different Commercially Available Real-Time PCR Assays for Detection of Shiga Toxin 1 and 2 Gene Subtypes. *J Food Prot.* 2013 May 1;76(5):871–3.
- Matussek A, Jernberg C, Einemo I, Monecke S, Ehricht R, Engelmann I, et al. Genetic makeup of Shiga toxin-producing Escherichia coli in relation to clinical symptoms and duration of shedding: a microarray analysis of isolates from Swedish children. *Eur J Clin Microbiol Infect Dis.* 2017;36(8):1433–41.



McIngvale SC, Elhanafi D, Drake MA. Optimization of Reverse Transcriptase PCR To Detect Viable Shiga-Toxin-Producing *Escherichia coli*. *Appl Environ Microbiol*. 2002 Feb;68(2):799–806.

Melton-Celsa AR. Shiga Toxin (Stx) Classification, Structure, and Function. *Microbiol Spectr*. 2014;4(2):2–4.

Mody RK, Griffin PM. Editorial Commentary: Fecal Shedding of Shiga Toxin–Producing *Escherichia coli*: What Should Be Done to Prevent Secondary Cases? *Clin Infect Dis*. 2013 Apr 15;56(8):1141–4.

Muniesa M, Hammerl JA, Hertwig S, Appel B, Brüssow H. Shiga Toxin-Producing *Escherichia coli* O104:H4: a New Challenge for Microbiology. *Appl Environ Microbiol*. 2012 Jun 15;78(12):4065–73.

Murinda SE, Nguyen LT, Landers TL, Draughon FA, Mathew AG, Hogan JS, et al. Comparison of *Escherichia coli* Isolates from Humans, Food, and Farm and Companion Animals for Presence of Shiga Toxin–Producing *E. coli* Virulence Markers. *Foodborne Pathog Dis*. 2004 Sep;1(3):178–84.

Nocker A, Camper AK. Novel approaches toward preferential detection of viable cells using nucleic acid amplification techniques. *FEMS Microbiol Lett*. 2009 Feb 1;291(2):137–42.

Nocker A, Cheung CY, Camper AK. Comparison of propidium monoazide with ethidium

monoazide for differentiation of live vs. dead bacteria by selective removal of DNA from dead cells. *J Microbiol Methods*. 2006;67(2):310–20.

Notman R, Noro M, O'Malley B, Anwar J. Molecular Basis for Dimethylsulfoxide (DMSO) Action on Lipid Membranes. *J Am Chem Soc*. 2006 Nov 1;128(43):13982–3.

Papanicolas LE, Choo JM, Wang Y, Leong LE, Costello SP, Gordon DL, et al. Bacterial viability in faecal transplants: which bacteria survive? *EBioMedicine*. 2019;41:509–16.

Perelle S, Dilasser F, Grout J, Fach P. Detection by 5'-nuclease PCR of Shiga-toxin producing *Escherichia coli* O26, O55, O91, O103, O111, O113, O145 and O157:H7, associated with the world's most frequent clinical cases. *Mol Cell Probes*. 2004 Jun 1;18(3):185–92.

Persson S, Olsen KEP, Ethelberg S, Scheutz F. Subtyping Method for *Escherichia coli* Shiga Toxin (Verocytotoxin) 2 Variants and Correlations to Clinical Manifestations. *J Clin Microbiol*. 2007 Jun;45(6):2020–4.

PMAXx™ Dye, 20 mM in H<sub>2</sub>O [Internet]. Biotium. [cited 2022 Nov 8]. Available from: <https://biotium.com/product/pmaxx-20-mm-in-h2o/>

Probst A, Mahnert A, Weber C, Haberer K, Moissl-Eichinger C. Detecting inactivated endospores in fluorescence microscopy using propidium monoazide. *Int J Astrobiol*. 2012 Apr;11(2):117–23.

Propidium monoazide. In: Wikipedia [Internet]. 2022 [cited 2022 Nov 4]. Available from: [https://en.wikipedia.org/w/index.php?title=Propidium\\_monoazide&oldid=1117032474](https://en.wikipedia.org/w/index.php?title=Propidium_monoazide&oldid=1117032474)

Rani A, Dike CC, Mantri N, Ball A. Point-of-Care Lateral Flow Detection of Viable *Escherichia coli* O157:H7 Using an Improved Propidium Monoazide-Recombinase Polymerase Amplification Method. *Foods*. 2022 Jan;11(20):3207.

Reischl U, Youssef MT, Kilwinski J, Lehn N, Zhang WL, Karch H, et al. Real-Time Fluorescence PCR Assays for Detection and Characterization of Shiga Toxin, Intimin, and Enterohemolysin Genes from Shiga Toxin-Producing *Escherichia coli*. *J Clin Microbiol*. 2002 Jul;40(7):2555–65.

Rey M de los Á, Cap M, Favre LC, Rodríguez Racca A, Dus Santos MJ, Vaudagna SR, et al. Evaluation of PMA-qPCR methodology to detect and quantify viable Shiga toxin-producing *Escherichia coli* in beef burgers. *J Food Process Preserv*. 2021;45(4):e15338.

Sánchez S, Llorente MT, Ramiro R, Herrera-León L, Herrera-León S. Evaluation of the SHIGA TOXIN QUIK CHEK after overnight enrichment as screening tool for Shiga toxin-producing *Escherichia coli* detection in human fecal samples. *Diagn Microbiol Infect Dis*. 2019 Jul 1;94(3):218–22.

Scavia G, Gianviti A, Labriola V, Chiani P, Maugliani A, Michelacci V, et al. A case of haemolytic uraemic syndrome (HUS) revealed an outbreak of Shiga toxin-2-producing *Escherichia coli* O26:H11 infection in a nursery, with long-lasting shedders and person-to-person transmission, Italy 2015. *J Med Microbiol*. 67(6):775–82.

Schnetzing F, Pan Y, Nocker A. Use of propidium monoazide and increased amplicon length reduce false-positive signals in quantitative PCR for bioburden analysis. *Appl Microbiol Biotechnol.* 2013;97(5):2153–62.

Schrader C, Schielke A, Ellerbroek L, John R. PCR inhibitors – occurrence, properties and removal. *J Appl Microbiol.* 2012;113(5):1014–26.

Seinige D, Krischek C, Klein G, Kehrenberg C. Comparative analysis and limitations of ethidium monoazide and propidium monoazide treatments for the differentiation of viable and nonviable *Campylobacter* cells. *Appl Environ Microbiol.* 2014;80(7):2186.

Shekar A, Babu L, Ramlal S, Sripathy MH, Batra H. Selective and concurrent detection of viable *Salmonella* spp., *E. coli*, *Staphylococcus aureus*, *E. coli* O157:H7, and *Shigella* spp., in low moisture food products by PMA-mPCR assay with internal amplification control. *LWT.* 2017 Dec 1;86:586–93.

SHIGA TOXIN QUIK CHEK™ Package insert [Internet]. TechLab; 2021 [cited 2022 Nov 4].

Available from:

[https://www.techlab.com/wp-content/uploads/2021/09/SHIGA-TOXIN-QUIK-CHEK-PI-91-625-01-TL\\_7-2021.pdf](https://www.techlab.com/wp-content/uploads/2021/09/SHIGA-TOXIN-QUIK-CHEK-PI-91-625-01-TL_7-2021.pdf)

Takahashi M, Ishikawa D, Sasaki T, Lu Y j., Kuwahara-Arai K, Kamei M, et al. Faecal freezing preservation period influences colonization ability for faecal microbiota transplantation. *J Appl Microbiol.* 2019;126(3):973–84.

TaqMan. In: Wikipedia [Internet]. 2022 [cited 2022 Nov 4]. Available from:

<https://en.wikipedia.org/w/index.php?title=TaqMan&oldid=1109226283>

Tarr GAM, Stokowski T, Shringi S, Tarr PI, Freedman SB, Oltean HN, et al. Contribution and Interaction of Shiga Toxin Genes to Escherichia coli O157:H7 Virulence. *Toxins*. 2019 Oct;11(10):607.

Thanh MD, Agustí G, Mader A, Appel B, Codony F. Improved sample treatment protocol for accurate detection of live Salmonella spp. in food samples by viability PCR. *PLOS ONE*. 2017 Dec 12;12(12):e0189302.

Trachtman H, Austin C, Lewinski M, Stahl RAK. Renal and neurological involvement in typical Shiga toxin-associated HUS. *Nat Rev Nephrol*. 2012 Nov;8(11):658–69.

Unkmeir A, Schmidt H. Structural Analysis of Phage-Borne stx Genes and Their Flanking Sequences in Shiga Toxin-Producing Escherichia coli and Shigella dysenteriae Type 1 Strains. *Infect Immun*. 2000 Sep;68(9):4856–64.

van Frankenhuyzen JK, Trevors JT, Lee H, Flemming CA, Habash MB. Molecular pathogen detection in biosolids with a focus on quantitative PCR using propidium monoazide for viable cell enumeration. *J Microbiol Methods*. 2011 Dec 1;87(3):263–72.

Van Holm W, Ghesquière J, Boon N, Verspecht T, Bernaerts K, Zayed N, et al. A Viability Quantitative PCR Dilemma: Are Longer Amplicons Better? *Appl Environ Microbiol*. 2021

Feb 12;87(5):e02653-20.

Varma M, Field R, Stinson M, Rukovets B, Wymer L, Haugland R. Quantitative real-time PCR analysis of total and propidium monoazide-resistant fecal indicator bacteria in wastewater. *Water Res.* 2009;43(19):4790–801.

Veneti L, Lange H, Brandal L, Danis K, Vold L. Mapping of control measures to prevent secondary transmission of STEC infections in Europe during 2016 and revision of the national guidelines in Norway. *Epidemiol Infect.* 2019 Jul 29;147(e267):1–10.

Vonberg RP, Höhle M, Aepfelbacher M, Bange FC, Belmar Campos C, Claussen K, et al. Duration of fecal shedding of Shiga toxin-producing *Escherichia coli* O104:H4 in patients infected during the 2011 outbreak in Germany: a multicenter study. *Clin Infect Dis Off Publ Infect Dis Soc Am.* 2013 Apr;56(8):1132–40.

Wagner AO, Malin C, Knapp BA, Illmer P. Removal of Free Extracellular DNA from Environmental Samples by Ethidium Monoazide and Propidium Monoazide. *Appl Environ Microbiol.* 2008 Apr;74(8):2537–9.

Wagner AO, Praeg N, Reitschuler C, Illmer P. Effect of DNA extraction procedure, repeated extraction and ethidium monoazide (EMA)/propidium monoazide (PMA) treatment on overall DNA yield and impact on microbial fingerprints for bacteria, fungi and archaea in a reference soil. *Appl Soil Ecol.* 2015;93:56–64.

Warnke P, Warning L, Podbielski A. Some Are More Equal - A Comparative Study on Swab Uptake and Release of Bacterial Suspensions. *PLoS ONE.* 2014 Jul 10;9(7):e102215.

- Wine E. Rectal swabs: a diagnostic alternative in paediatric gastroenteritis? *Lancet Gastroenterol Hepatol*. 2017 Sep 1;2(9):623–4.
- Wylie JL, Van Caesele P, Gilmour MW, Sitter D, Guttek C, Giercke S. Evaluation of a New Chromogenic Agar Medium for Detection of Shiga Toxin-Producing *Escherichia coli* (STEC) and Relative Prevalences of O157 and Non-O157 STEC in Manitoba, Canada. *J Clin Microbiol*. 2013 Feb;51(2):466–71.
- Yalamanchili H, Dandachi D, Okhuysen PC. Use and Interpretation of Enteropathogen Multiplex Nucleic Acid Amplification Tests in Patients With Suspected Infectious Diarrhea. *Gastroenterol Hepatol*. 2018 Nov;14(11):646–52.
- Yamasaki E, Watahiki M, Isobe J, Sata T, Nair GB, Kurazono H. Quantitative Detection of Shiga Toxins Directly from Stool Specimens of Patients Associated with an Outbreak of Enterohemorrhagic *Escherichia coli* in Japan—Quantitative Shiga toxin detection from stool during EHEC outbreak. *Toxins*. 2015 Oct;7(10):4381–9.
- Zelyas N, Poon A, Patterson-Fortin L, Johnson RP, Lee W, Chui L. Assessment of commercial chromogenic solid media for the detection of non-O157 Shiga toxin-producing *Escherichia coli* (STEC). *Diagn Microbiol Infect Dis*. 2016 Jul 1;85(3):302–8.
- Zhuo R, Ding X, Freedman SB, Lee BE, Ali S, Luong J, et al. Molecular Epidemiology of Human Sapovirus among Children with Acute Gastroenteritis in Western Canada. *J Clin Microbiol*. 2021 Sep 20;59(10):e00986-21.

## Appendix A: Chapter 2 supplementary data

### Nomenclature:

$$\Delta Ct = Ct_{\text{sample}} - Ct_{\text{reference (control)}}$$

UND = no Ct value within 40 cycles

$\Delta Ct_{\text{UND}} \geq 40$  – control; where “ $\geq$ ” indicates the value is theoretical.

**Table A.1. Effect of increasing concentrations of PMAxx™ treatment on *stx*<sub>1</sub>  $\Delta Ct$  values for heat-killed cells.**

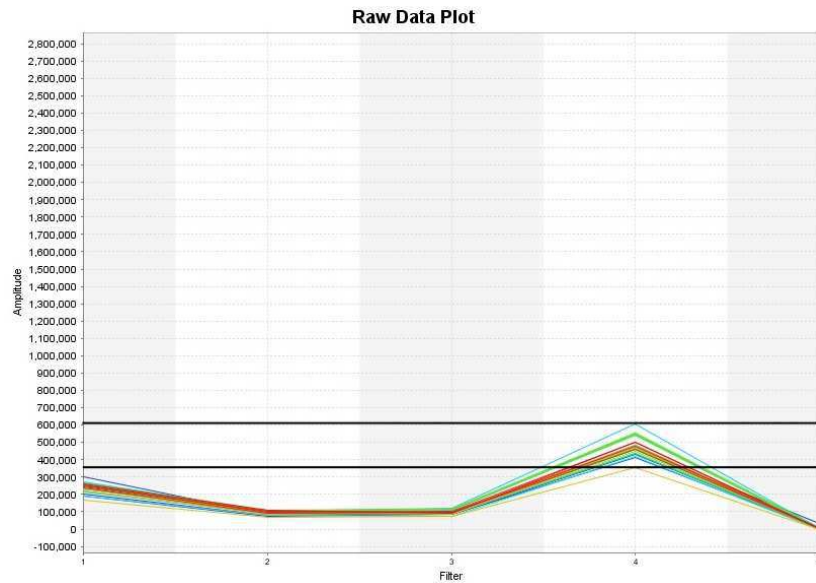
HK cells (Log CFU/mL)	PMAxx™ treatment ( <i>stx</i> <sub>1</sub> Ct value)						
	A. No treatment	B. 50 $\mu\text{M}$		C. 75 $\mu\text{M}$		D. 100 $\mu\text{M}$	
	Mean $\pm$ SD	Mean $\pm$ SD	$\Delta Ct$ (B - A)	Mean $\pm$ SD	$\Delta Ct$ (C - A)	Mean $\pm$ SD	$\Delta Ct$ (D - A)
8	12.9 $\pm$ 0.5	28.3 $\pm$ 0.7	+ 15.3	29.5 $\pm$ 4.8	+ 16.6	33.4 $\pm$ 3.6	+ 20.5
7	16.5 $\pm$ 0.2	29.9 $\pm$ 0.9	+ 13.3	35.5 $\pm$ 4.6	+ 19.0	38.7 $\pm$ 2.7	+ 22.2
6	19.8 $\pm$ 0.4	30.5 $\pm$ 0.7	+ 10.8	36.4 $\pm$ 3.7	+ 16.7	38.0 $\pm$ 1.0	+ 18.2
5	23.5 $\pm$ 0.1	34.2 $\pm$ 1.1	+ 10.7	39.3 $\pm$ 4.5	+ 15.8	UND	$\geq 16.5^*$
4	26.7 $\pm$ 0.1	36.9 $\pm$ 0.7	+ 10.2	38.7 $\pm$ 4.2	+ 12.0	UND	$\geq 13.3^*$
3	29.5 $\pm$ 0.4	35.5 $\pm$ 2.6	+ 6.0	UND	$\geq 10.5^*$	UND	$\geq 10.5^*$
2	33.7 $\pm$ 0.5	UND	$\geq 6.3^*$	UND	$\geq 6.3^*$	UND	$\geq 6.3^*$
Mean $\Delta Ct^*$	-	-	11.1 $\pm$ 3.1	-	16.0 $\pm$ 2.5	-	20.3 $\pm$ 2.0

*stx*<sub>1</sub> Ct values represent 3 replicates

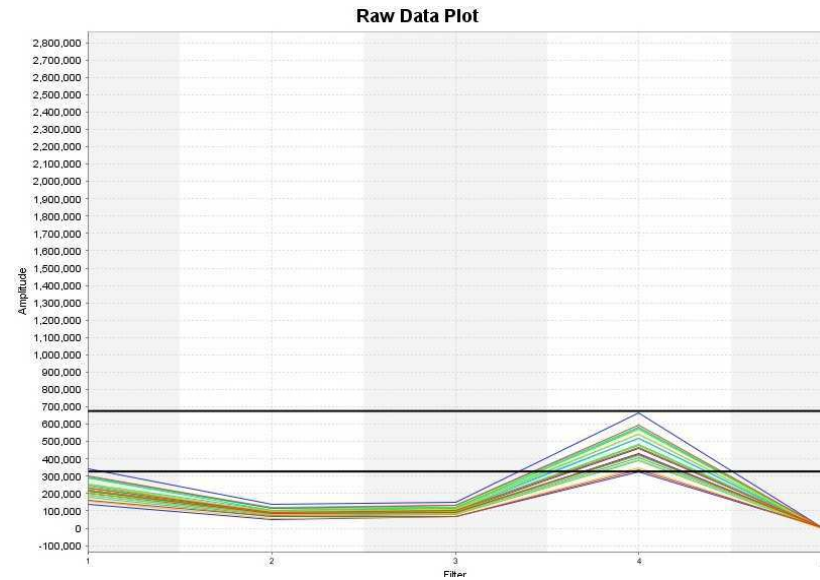
\*Theoretical  $\Delta Ct$  values not included in mean  $\Delta Ct$  calculation



### No Treatment

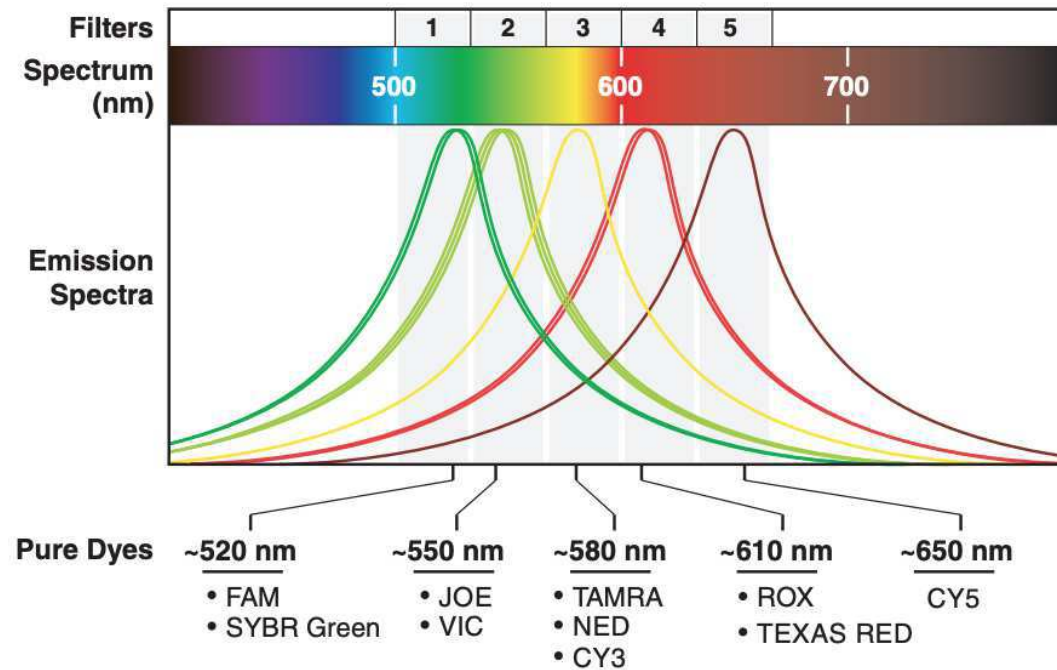


### 100 $\mu$ M PMAxx™



**Figure A.1. Raw data plot from Applied Biosystems™ 7500 Fast Real-Time PCR instrument**

Initial fluorescence (cycle 1) of a series of untreated and previously treated (100  $\mu$ M PMAxx™) samples as detected by Filters 1 - 5 of an Applied Biosystems™ 7500 Fast Real-Time PCR instrument. ROX™ (the passive reference dye in the PrimeTime® Gene Expression Master Mix used in this study) and PMAxx™ both have emission spectra of  $\sim$ 610 nm, which is detected by Filter 4. Horizontal bars added to highlight fluorescence amplitude range



**Figure A.2. Emission wavelengths detected by each filter of the The Applied Biosystems™ 7500 Fast Real-Time PCR instrument.**

Applied Biosystems 7500/7500 Fast Real-Time PCR Systems Manual [Internet]. Available from: <https://tools.thermofisher.com/content/sfs/manuals/4387777d.pdf>

**Table A.2. Effect of treatment with 1% DMSO, 100  $\mu$ M PMAxx<sup>TM</sup>, and 100  $\mu$ M PMAxx<sup>TM</sup> + 1% DMSO on *stx*<sub>1</sub>  $\Delta$ Ct value for heat-killed cells.**

HK cells (Log CFU/mL)	Experimental condition ( <i>stx</i> <sub>1</sub> Ct value)							
	A. No treatment		B. 1% DMSO		C. 100 $\mu$ M PMAxx <sup>TM</sup>		D. 100 $\mu$ M PMAxx <sup>TM</sup> + 1% DMSO	
	Mean $\pm$ SD	Mean $\pm$ SD	$\Delta$ Ct (B - A)	Mean $\pm$ SD	$\Delta$ Ct (C - A)	Mean $\pm$ SD	$\Delta$ Ct (D - A)	
9	12.6 $\pm$ 0.2	12.4 $\pm$ 0.1	- 0.2	31.3 $\pm$ 2.8	+ 18.7	UND	$\geq$ 27.4	
8	16.9 $\pm$ 0.2	17.5 $\pm$ 0.3	+ 0.6	UND	+ 14.9	UND	$\geq$ 23.1	
7	20.8 $\pm$ 0.1	21.2 $\pm$ 0.1	+ 0.4	UND	+ 15.6	UND	$\geq$ 19.2	

*stx*<sub>1</sub> Ct values represent 3 independent runs

**Table A.3. Effect of resuspension in fresh PBS versus remaining in the original supernatant (with or without 100  $\mu$ M PMAxx<sup>TM</sup> + 1% DMSO) during boiling on *stx*<sub>7</sub>  $\Delta$ Ct value for live cells.**

Live cells (Log CFU/mL)	Treatment before boiling ( <i>stx</i> <sub>7</sub> Ct value)						
	No treatment			100 $\mu$ M PMAxx <sup>TM</sup> + 1% DMSO			
	A. Original	B. Resuspended		C. Original		D. Resuspended	
	Mean $\pm$ SD	Mean $\pm$ SD	$\Delta$ Ct (B - A)	Mean $\pm$ SD	$\Delta$ Ct (C - A)	Mean $\pm$ SD	$\Delta$ Ct (D - A)
8	13.7 $\pm$ 0.6	14.7 $\pm$ 0.6	+ 1.0	UND	$\geq$ 26.3	15.4 $\pm$ 1.1	+ 1.7
7	18.8 $\pm$ 0.9	18.8 $\pm$ 0.5	$\pm$ 0.0	UND	$\geq$ 21.2	19.5 $\pm$ 0.8	+ 0.7
6	22.2 $\pm$ 0.8	20.7 $\pm$ 0.7	- 1.5	UND	$\geq$ 17.8	23.5 $\pm$ 1.6	+ 1.3
5	26.1 $\pm$ 1.1	24.3 $\pm$ 0.9	- 1.8	UND	$\geq$ 13.9	26.8 $\pm$ 1.4	+ 0.7
4	28.1 $\pm$ 0.9	27.6 $\pm$ 0.9	- 0.5	UND	$\geq$ 11.9	30.1 $\pm$ 1.8	+ 2.0
3	31.4 $\pm$ 1.2	30.1 $\pm$ 0.6	- 1.3	UND	$\geq$ 8.6	34.3 $\pm$ 2.1	+ 2.9

*stx*<sub>7</sub> Ct values represent 3 independent runs

Original = boiled in original supernatant

Resuspended = pelleted, supernatant removed, cells resuspended in fresh PBS, then boiled

**Table A.4. Effect of 100  $\mu$ M PMAxx<sup>TM</sup> + 1% DMSO residue on the *stx*<sub>1</sub> cycle threshold value of heat-killed cells.**

HK cells added (Log CFU/mL)	Microcentrifuge tube condition ( <i>stx</i> <sub>1</sub> Ct value)				
	A. No exposure	Exposure to 100 $\mu$ M PMAxx <sup>TM</sup> + 1% DMSO			C. Wash
		B. No wash	$\Delta$ Ct (B - A)	Mean $\pm$ SD	
5	Mean $\pm$ SD 24.5 $\pm$ 0.5	Mean $\pm$ SD 26.9 $\pm$ 1.5	+ 2.3	Mean $\pm$ SD 28.5 $\pm$ 1.0	+ 4.0
4	Mean $\pm$ SD 28.9 $\pm$ 0.6	Mean $\pm$ SD 33.1 $\pm$ 0.5	+ 4.2	Mean $\pm$ SD 33.3 $\pm$ 0.6	+ 4.3
3	Mean $\pm$ SD 32.6 $\pm$ 0.7	Mean $\pm$ SD 37.7 $\pm$ 1.8	+ 5.2	Mean $\pm$ SD 38.1 $\pm$ 1.7	+ 5.5

*stx*<sub>1</sub> Ct values represent 3 independent runs

Exposure = PMAxx<sup>TM</sup> treatment simulated in PBS, supernatant removed, then HK cells added.

Wash = 1 mL wash with PBS introduced after supernatant removed, then HK cells added.

**Table A.5. Effect of “pre-photoactivation” (dye photoactivated prior to being added to samples) compared to standard photoactivation (dye photoactivated after being added to samples) on the cycle threshold value of heat-killed cells treated with 100 µM PMAxx™ + 1% DMSO.**

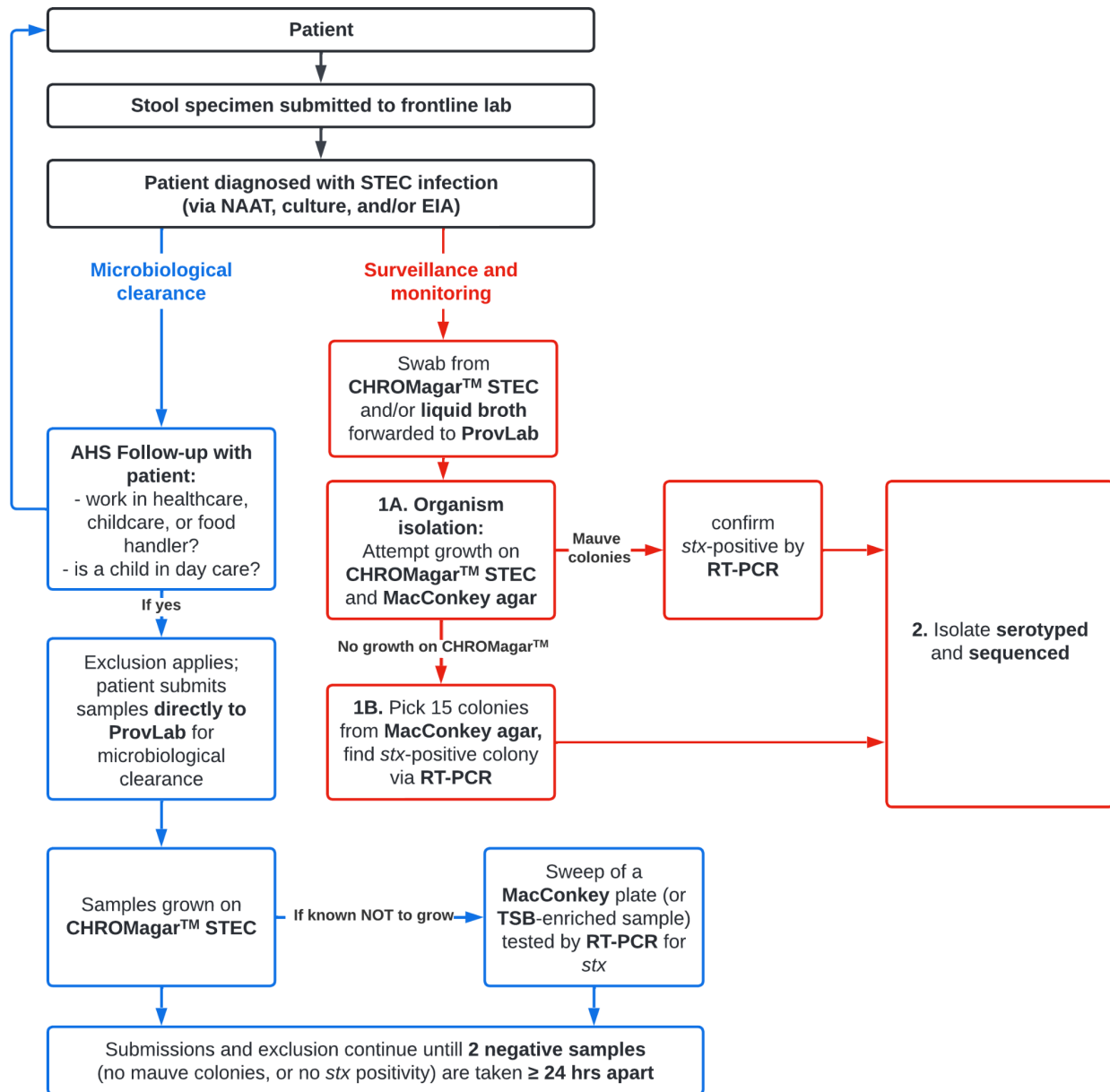
HK cells added (Log CFU/mL)	Experimental condition ( <i>stx</i> <sub>1</sub> Ct value)				
	100 µM PMAxx™ + 1% DMSO				
	A. No Treatment	B. Standard photoactivation		C. Pre-photoactivation	
	Mean ± SD	Mean ± SD	ΔCt (B - A)	Mean ± SD	ΔCt (C - A)
8	12.8 ± 0.3	33.1 ± 3.5	+ 20.3	14.6 ± 0.5	+ 1.8
7	15.9 ± 0.6	UND	≥ 24.1	18.4 ± 0.4	+ 2.5
6	19.5 ± 0.5	UND	≥ 16.9	22.7 ± 0.6	+ 3.2
5	23.3 ± 0.1	UND	≥ 16.0	29.5 ± 0.3	+ 6.3
4	27.0 ± 0.3	UND	≥ 13.0	33.2 ± 1.2	+ 6.6
3	30.8 ± 0.5	UND	≥ 9.2	UND	≥ 9.2

*stx*<sub>1</sub> Ct values represent 3 independent runs

Standard photoactivation: dye photoactivated after being added to samples

Pre-photoactivation: dye photoactivated prior to being added to samples

## Appendix B: Chapter 3 reference images



**Figure B.1. Albertan laboratory workflow for STEC detection, surveillance, and microbiological clearance.**



**Figure B.2. Bristol Stool Form Scale.** Reproduced under CC BY-SA 3.0.

Bristol stool scale. In: Wikipedia [Internet]. 2022 [cited 2022 Nov 4]. Available from: [https://en.wikipedia.org/w/index.php?title=Bristol\\_stool\\_scale&oldid=1114842788](https://en.wikipedia.org/w/index.php?title=Bristol_stool_scale&oldid=1114842788)



Appendix C: Chapter 3 supplementary data

Table C.1. Shiga toxin assay results for Patient A stool submissions.

Days since first clearance submission	Bristol stool type	10% Stool		1% stool		TSB-enriched stool	
		<i>stx</i> <sub>2</sub> Ct		<i>stx</i> <sub>2</sub> Ct		<i>stx</i> <sub>2</sub> Ct	Stx
		RT-PCR	Viability RT-PCR	RT-PCR	Viability RT-PCR	PE RT-PCR	STQC EIA
0	4	22.3	23.6	23.3	25.8	15.4	Stx2+
2	4	26.1	UND	25.2	29.5	15.4	Stx2+
3	3	25.1	28.6	25.1	31.6	17.4	Stx2+
5	4	26.7	27.5	25.5	29.4	15.5	Stx2+
8	4	31.4	UND	29.8	33.2	22.1	–
11	5	UND	UND	UND	UND	32.0	–
17	3	UND	UND	UND	UND	UND	–

Patient A isolate: O121:H19 (*stx*<sub>2</sub><sup>+</sup>)

PE: Post-enrichment

STQC EIA: SHIGA TOXIN QUIK CHEK™ enzyme immunoassay

UND: undetermined Ct value

“----” Specimens below the dashed line were determined to be negative by ProvLab

**Table C.2. Shiga toxin-1 assay results for Patient B stool submissions.**

Days since first clearance submission	Bristol stool type	10% Stool		1% stool		TSB-enriched stool	
		<i>stx</i> <sub>1</sub> Ct		<i>stx</i> <sub>1</sub> Ct		<i>stx</i> <sub>1</sub> Ct	Stx
		RT-PCR	Viability RT-PCR	RT-PCR	Viability RT-PCR	PE RT-PCR	STQC EIA
0	6	26.7	UND	27.9	37.2	31.4	–
5	6	30.1	UND	32.1	UND	13.4	–
10	6	31.2	UND	33.4	UND	13.6	–
12	6	27.7	UND	30.1	34.6	14.5	–
17	6	23.4	UND	25.4	26.1	12.3	–
19	6	26.9	UND	28.9	UND	19.4	–
21	6	23.1	UND	23.9	26.1	12	–
24	6	UND	UND	23.3	24.6	12.1	–
26	6	32.1	UND	33.1	33.7	16.2	–
28	6	UND	UND	35.1	35	16	–
33	6	UND	UND	UND	UND	UND	–
38	6	UND	UND	UND	UND	UND	–

Patient B isolates: O88:H25 (*stx*<sub>1</sub><sup>+</sup> and *stx*<sub>2</sub><sup>+</sup>), O75:H38 (*stx*<sub>1</sub><sup>+</sup>), and O145:H undetermined (*stx*<sub>2</sub><sup>+</sup>)

PE: Post-enrichment

STQC EIA: SHIGA TOXIN QUIK CHEK™ enzyme immunoassay

“----” Specimens below the dashed line were determined to be negative by ProvLab

**Table C.3. Shiga toxin-2 assay results for Patient B stool submissions.**

Days since first clearance submission	Bristol stool type	10% Stool		1% stool		TSB-enriched stool	
		<i>stx</i> <sub>2</sub> Ct		<i>stx</i> <sub>2</sub> Ct		<i>stx</i> <sub>2</sub> Ct	Stx
		RT-PCR	Viability RT-PCR	RT-PCR	Viability RT-PCR	PE RT-PCR	STQC EIA
0	6	27.6	UND	28.7	28.7	28.5	–
5	6	30.6	UND	31.5	31.5	14.1	–
10	6	31.9	UND	34.7	34.7	14.3	–
12	6	27.9	UND	30.6	30.6	15.2	–
17	6	23.7	UND	26	26	12.8	Stx2+
19	6	27.1	UND	29.7	29.7	20.1	–
21	6	24.4	UND	24.6	24.6	12.6	Stx2+
24	6	UND	UND	24.2	24.2	13.3	Stx2+
26	6	32.9	UND	34.1	34.1	16.3	–
28	6	UND	UND	35	35	16.3	–
33	6	UND	UND	UND	UND	UND	–
38	6	UND	UND	UND	UND	UND	–

Patient B isolates: O88:H25 (*stx*<sub>1</sub><sup>+</sup> and *stx*<sub>2</sub><sup>+</sup>), O75:H38 (*stx*<sub>1</sub><sup>+</sup>), and O145:H undetermined (*stx*<sub>2</sub><sup>+</sup>)

PE: Post-enrichment

STQC EIA: SHIGA TOXIN QUIK CHEK™ enzyme immunoassay

UND: undetermined Ct value

“----” Specimens below the dashed line were determined to be negative by ProvLab



**Figure C.1. Colony RT-PCR results of a blue colony typical of Patient B specimens.** The plate shown is the enriched day 28 sample; the circled colony was negative for both *stx*<sub>1</sub> and *stx*<sub>2</sub>.

**Table C.4. Shiga toxin assay results for Patient C stool submissions.**

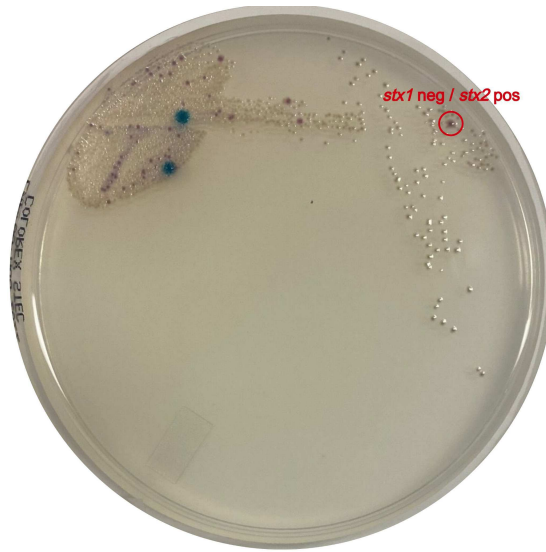
Days since first clearance submission	Bristol stool type	10% Stool		1% stool		TSB-enriched stool	
		<i>stx</i> <sub>2</sub> Ct		<i>stx</i> <sub>2</sub> Ct		<i>stx</i> <sub>2</sub> Ct	Stx
		RT-PCR	Viability RT-PCR	RT-PCR	Viability RT-PCR	PE RT-PCR	STQC EIA
0	5	27.9	34.7	29.6	32.5	21.5	–
7	4	36.2	UND	UND	35.2	26.9	–
11	3	UND	UND	UND	UND	UND	–
12	4	UND	UND	UND	UND	UND	–

Patient C isolate: O157:H7 (*stx*<sub>2</sub><sup>+</sup>)

PE: Post-enrichment

STQC EIA: SHIGA TOXIN QUIK CHEK™ enzyme immunoassay

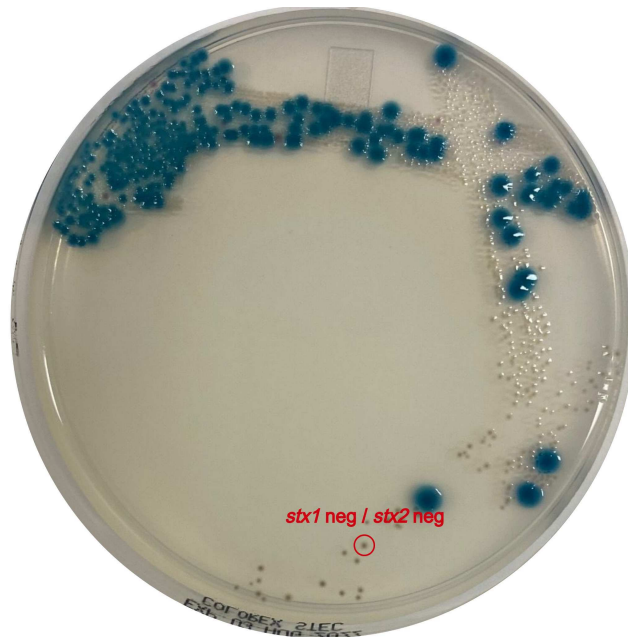
“----” Specimens below the dashed line were determined to be negative by ProvLab



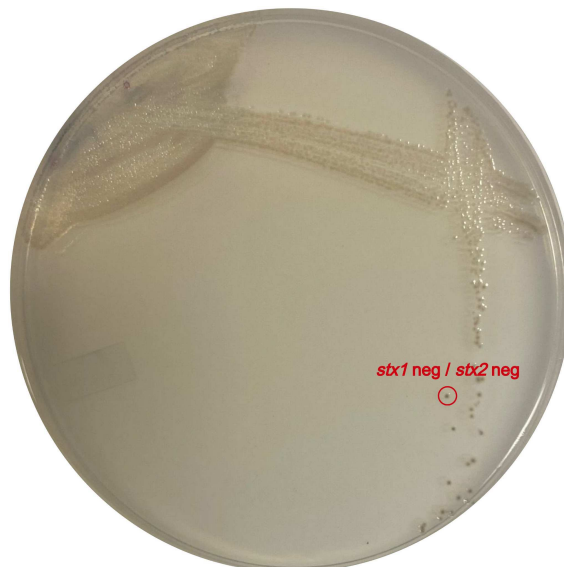
**Figure C.2. Colony RT-PCR results of mauve colony from Patient C day 0, 10% stool suspension.** The circled colony was negative for *stx*<sub>1</sub>, but positive for *stx*<sub>2</sub>.



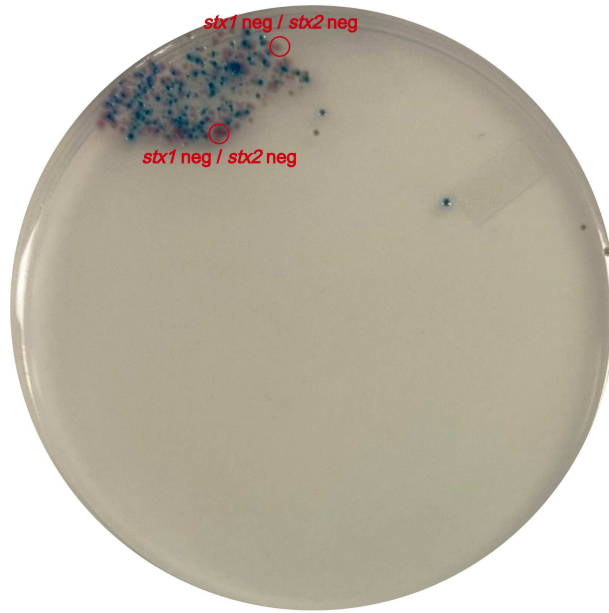
**Figure C.3. Colony RT-PCR results of mauve colony from Patient C day 7, 10% stool suspension.** The circled colony was *stx*<sub>1</sub> negative, *stx*<sub>2</sub> positive.



**Figure C.4. Colony RT-PCR results of a grey colony from Patient C enriched day 7 specimen.** The circled colony was negative for both *stx*<sub>1</sub> and *stx*<sub>2</sub>.



**Figure C.5. Colony RT-PCR results of a grey colony from Patient C enriched day 11 specimen.** The circled colony was negative for both *stx*<sub>1</sub> and *stx*<sub>2</sub>.



**Figure C.6. Colony RT-PCR results of mauve colonies from Patient C enriched day 12 specimen.** Both of the circled colonies were negative for *stx*<sub>1</sub> and *stx*<sub>2</sub>.



**Table C.5. Shiga toxin assay results for Patient D stool submissions.**

Days since first clearance submission	Bristol stool type	10% Stool		1% stool		TSB-enriched stool	
		<i>stx</i> <sub>1</sub> Ct		<i>stx</i> <sub>1</sub> Ct		<i>stx</i> <sub>1</sub> Ct	Stx
		RT-PCR	Viability RT-PCR	RT-PCR	Viability RT-PCR	PE RT-PCR	STQC EIA
0	4	21.1	28.9	26.7	31.3	21.8	–
3	3	24.8	UND	25.7	30.1	22.8	–
12	3	23.3	25.7	26.0	29.5	20.6	–
16	2	22.0	24.8	26.2	29.5	20.0	–
21	2	20.4	22.8	23.9	27.4	15.8	–
27	2	25.1	28.0	28.9	31.0	22.6	–
35	2	24.8	26.9	28.1	29.7	23.2	–

Patient D isolate: O117:H7 (*stx*<sub>1</sub><sup>+</sup>)

PE: Post-enrichment

STQC EIA: SHIGA TOXIN QUIK CHEK™ enzyme immunoassay

UND: undetermined Ct value